1999 Hurricane Field Program Plan

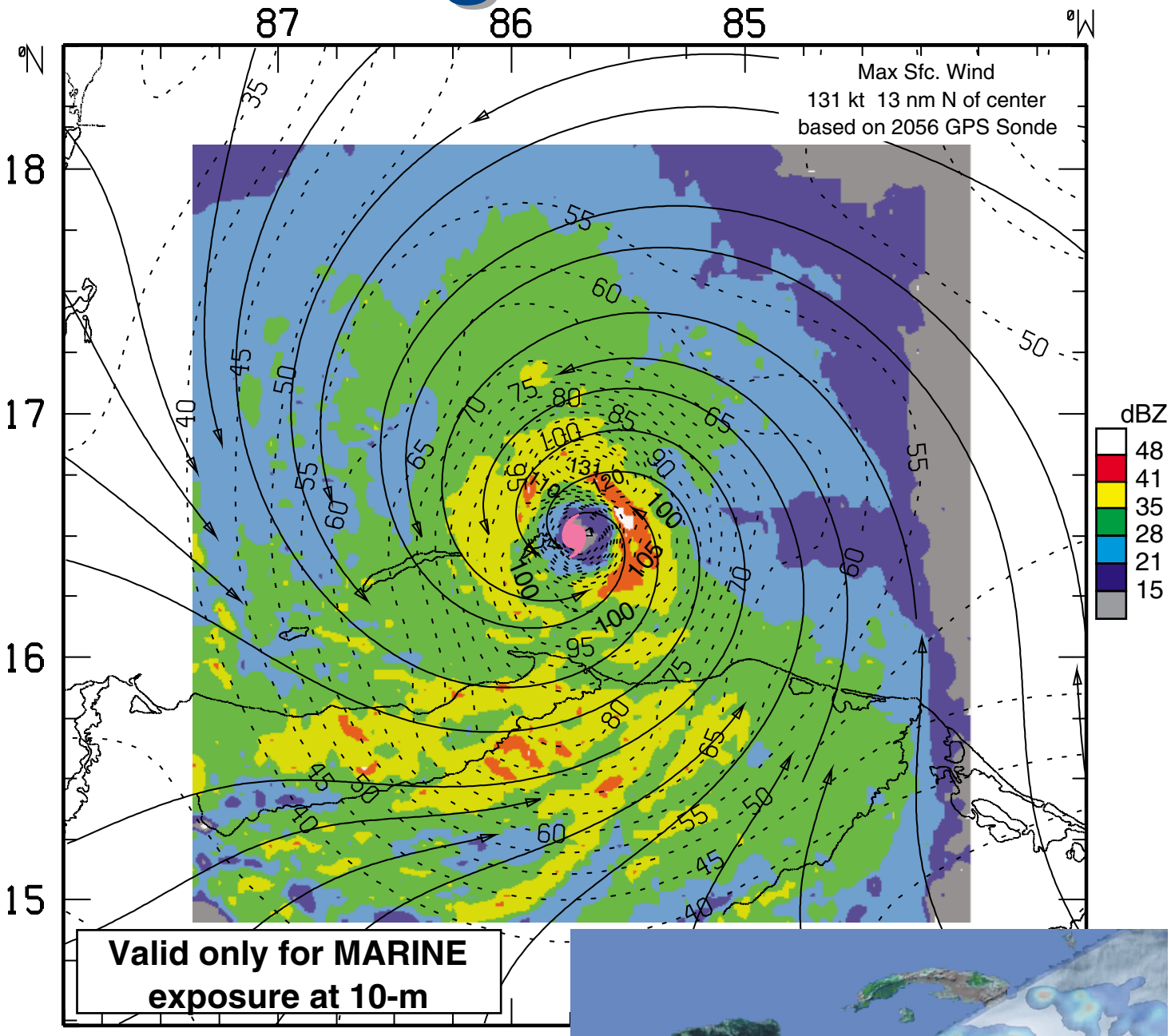

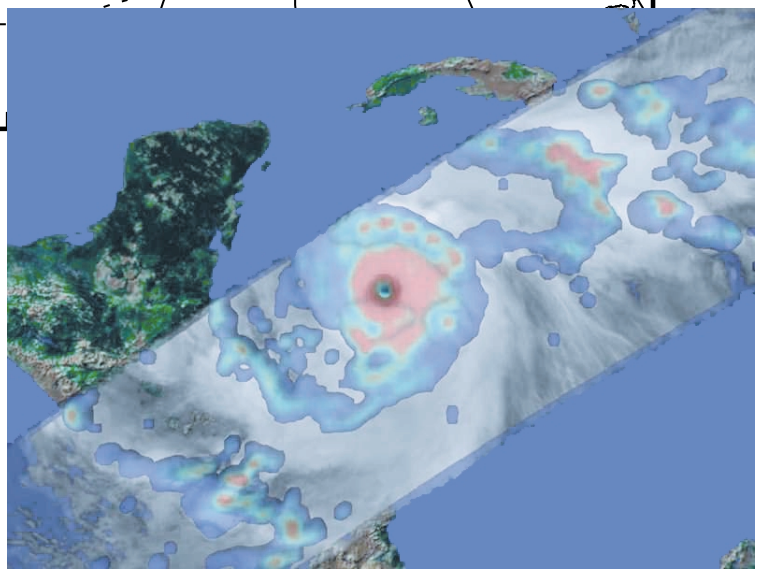

Atlantic Oceanographic and Meteorological Laboratory
Hurricane Research Division
Miami, FL

1999 Hurricane Field Program Plan

NATIONAL OCEANIC AND ATMOSPHERIC ADMINISTRATION
ATLANTIC OCEANOGRAPHIC AND METEOROLOGICAL LABORATORY
4301 RICKENBACKER CAUSEWAY
MIAMI, FL 33149

PREPARED BY:
FRANK D. MARKS, JR. AND HOWARD A. FRIEDMAN
HURRICANE RESEARCH DIVISION

Hugh E. Willoughby
Director, Hurricane Research Division

28JUN99
Date

Cover: Top: Real-time surface wind field analysis superimposed on radar reflectivities for Hurricane Mitch at 0130 UTC on 28 October 1998. The surface wind field, represented by isotachs (contour interval of 5 kt [2.5 m s^{-1}]) and streamlines, is for an ocean exposure. The radar reflectivities (dBZ) are a composite from the NOAA WP-3D lower fuselage radar for the period 2339 UTC, 27 October to 0014 UTC, 28 October 1998, produced in real-time onboard the aircraft and transmitted to TPC/NHC via a satellite data link. The combined wind field and radar analyses was generated in real-time by HRD scientists and sent to the hurricane specialist on duty. Bottom: Hurricane Mitch as viewed by the Tropical Rain Measurement Mission (TRMM) satellite at 0116 UTC, 27 October 1998 (orbit 5254). Colors represent rain rate and the gray shades clouds as viewed from the infrared (IR) sensor.

CONTENTS

1999 HURRICANE FIELD PROGRAM PLAN

National Oceanic and Atmospheric Administration
Atlantic Oceanographic and Meteorological Laboratory
Hurricane Research Division

INTRODUCTION

The objective of the National Oceanic and Atmospheric Administration (NOAA) hurricane research field program is the collection of descriptive data that are required to support analytical and theoretical hurricane studies. These studies are designed to improve the understanding of the structure and behavior of hurricanes. The ultimate purpose is to develop improved methods for hurricane prediction.

Ten major experiments have been planned, by principal investigators at the Hurricane Research Division (HRD)/Atlantic Oceanographic and Meteorological Laboratory (AOML) of NOAA for the 1999 Hurricane Field Program. These experiments will be conducted with the NOAA/Aircraft Operations Center (AOC) WP-3D and Gulfstream IV-SP aircraft.

(1) Hurricane Synoptic-Flow Experiment: With the arrival of the new NOAA Gulfstream IV-SP high-altitude jet (G-IV), the Hurricane Synoptic Flow Experiment makes the transition from a research program to operations. Beginning in 1997, the G-IV started conducting routine "hurricane surveillance" missions that are essentially HRD Synoptic Flow experiments. When coordinated with these operational G-IV flights, the HRD Synoptic Flow experiment now becomes a *single-option, multi-aircraft* experiment. As in previous years, the experiment seeks to obtain accurate, high-density wind and thermodynamic data sets from the environment and vortex regions of tropical cyclones (TC) that are within 72 h of potential landfall. The availability of the G-IV, however, greatly increases the amount of environment sampled. GPS-based dropwindsondes (GPS-sondes) deployed from the G-IV and the two NOAA/AOC WP-3D aircraft provide these data over the normally data-void oceanic regions at distances up to 810 nmi (1500 km) from the TC center. Mandatory and significant level GPS-sonde data, transmitted in real time, are used to prepare official forecasts at the Tropical Prediction Center/National Hurricane Center (TPC/NHC). These data are also incorporated into objective statistical and dynamical TC prediction models at TPC/NHC and the National Centers for Environmental Prediction (NCEP). In a research mode, these data help improve short and medium term (24-72 h) TC track predictions, study the influence of synoptic-scale fields on vortex track and intensity, and assess methods for obtaining satellite soundings.

(2) Extended Cyclone Dynamics Experiment: This is a *multi-option, multi-aircraft* experiment which uses in–situ and radar data from the WP-3Ds flying at 500 mb, the G-IV at 200 mb, to monitor the structure and evolution of a TC on a spatial scales ranging from the convective and mesoscale in the vortex core (10-100 nmi [18-185 km] radius) to the synoptic-scale (1,000 nmi [1,850 km] radius) in the surrounding large-scale environment over a nominal period of 48 h. The WP-3D and G-IV data will be augmented by flight–level data from Air Force WC-130s flying reconnaissance at 700 mb within 110 nmi (200 km) of the center The experiment goal is a better understanding of how lateral interactions between the vortex and the synoptic–scale environment control TC intensity and motion.

(3) Vortex Motion and Evolution Experiment: This experiment is a *single-option*, *multi-aircraft* experiment designed to observe the structure and evolution of the inner core wind field of developing or mature TCs. True dual-Doppler data are obtained within 45 nmi (75 km) of the center with a horizontal grid spacing of 0.5 nmi (1 km). Three such data sets over 7 h, 2.3 h apart, are obtained during the mission, along with 9 pseudo-dual-Doppler data sets, to examine the evolution of the inner vortex. These data are supplemented by five rings of 8 or more GPS-sondes, from 50-160 nmi (95-300 km). This dropwindsonde coverage will provide azimuthal wave number 0 and 1 outside the inner core of the vortex, thus specifying the overall strength of the vortex and its three-dimensional "steering" asymmetry. Satellite information from NCEP and the University of Wisconsin will supplement the sonde coverage above flight level.

(4) Tropical Cyclogenesis Experiment: This *multi-option, multi-aircraft* experiment is designed to study one of the most important unanswered questions in tropical meteorology is: How does a tropical disturbance become a tropical depression with a closed surface circulation? This experiment seeks to answer the question through multilevel aircraft penetrations using dropwindsondes, flight-level data, and

radar observations on the synoptic, meso, and convective spatial scales. It will focus particularly on both thermodynamic transformations in the mid-troposphere and lateral interactions between the disturbance and its synoptic-scale environment. The possible addition of the G-IV this season will allow sampling of the upper tropospheric structure using flight-level and GPS-sondes in these developing disturbances.

(5) Tropical Cyclone Wind Fields Near Landfall: This experiment is a *multi-option*, *multi-aircraft* experiment designed to study the changes in TC near surface wind structure near and after landfall. An accurate description of the TC surface wind field near and after landfall in real-time is important for warning, preparedness, and recovery efforts. HRD is developing a real-time surface wind analysis system to aid the TPC/NHC in the preparation of warnings and advisories in TCs. The analyses could reduce uncertainties in the size of hurricane warning areas. Flight-level and Doppler wind data collected by a NOAA WP-3D will be transmitted to TPC/NHC where they could result in improved real-time and post-storm analyses. Doppler data collected near a WSR-88D would yield a time series of three-dimensional wind analyses showing the evolution of the inner core of TCs near and after landfall.

(6) Tropical Cyclone Air-Sea Interaction Experiment: This experiment is a *multi-option*, *multi-aircraft* experiment designed to determine the contribution of pre-existing and storm-induced ocean features to changes in TC intensity and surface wind field structure. This experiment seeks to address this issue through single-level aircraft penetrations using GPS-sondes, flight-level data, air-deployed drifting buoys, AXBTs, AXCPs, AXCTDs, Surface Contour Radar (SCR), C-band scatterometer (C-SCAT)/profiler, stepped frequency microwave radiometer (SFMR) and airborne Doppler radar observations on the synoptic, meso, and convective scales. It will focus particularly on both thermodynamic and wind field transformations in the boundary and lateral interactions between the TC and its synoptic-scale environment.

(7) Rainband Structure Experiment: This experiment is a *multi-option*, *multi-aircraft* experiment that will lead to a better understanding of the structure of TC rainbands and should provide valuable insight on the possible influence of rainbands on the overall intensity of a storm. It is designed to investigate the kinematic and thermodynamic structure of TC rainbands and the environment in which they are embedded. Many previous studies have explored the nature of TC eyewalls, yet few have actively examined the three-dimensional wind field and thermodynamics associated with rainbands. Doppler radar and flight level data will be gathered inside and outside of rainbands, including those that may form a convective ring around the eyewall, and GPS-sondes will be utilized to gain mid-tropospheric and boundary layer information. There are *two* formal options included in this experiment. The first is designed to study 'principal' rainbands, and the second will be used to investigate concentric eyewalls. Two stand-alone single aircraft modules which can be flown with other experiments: (1) the Rainband Module (lasting 30-60 min); and (2) the Rainband Thermodynamics Module (lasting 1-1.5 h) are also included.

(8) Electrification of Tropical Cyclone Convection Experiment: This experiment is a *multi-option*, *multi-aircraft* experiment designed to seek out the electrically active convection in TCs for in-depth study. The first option uses the Desert Research Institute (DRI) electric field mills and the DRI induction ring, to obtain both the electric field strength and the charge carried on the hydrometeors within the TC eyewall and convective rainbands. The information will help to determine why some TC convection is electrically active while other, similar, TC convection is not. A second option will investigate the relationship between cloud physics, vertical velocity, and the occurrence and location of cloud-to-ground (CG) lightning within ~325 nmi (600 km) range of the NLDN. Together, these data sources and techniques should lead to a better understanding of the characteristics of the convective processes that lead to lightning in TCs and, possibly, to intensity changes of the storms.

(9) Structure of Eyewall Convection Experiment: This experiment is a *single-option*, *multi-aircraft* experiment designed to map the three-dimensional spatial structure of the TC eyewall up- and downdrafts and to use dual-Doppler analysis to relate the vertical motion structure to the effects of environmental shear through the eyewall. It utilizes both NOAA WP-3D aircraft flying highly coordinated flight patterns to map the three-dimensional structure of eyewall vertical motions. The target storm must have an eyewall (or a developing one) with significant areas of deep convection.

(10) Clouds and Climate: This experiment is a *single-option*, *single-aircraft* experiment that uses the airborne Doppler radar and microphysics instrumentation to accumulate a data base of cloud precipitation properties over a wide range of environments. This study emphasizes the exploitation of

airborne in-situ microphysics and remote sensing (radar), together with satellite observations of clouds. It will provide a data base for studies of clouds and precipitation mechanisms, their effect on climate, and provide ground truth for satellite techniques, particularly the NASA Tropical Rain Measurement Mission (TRMM).

CONCEPT OF OPERATIONS

1. Location

The primary base of operations for the NOAA aircraft will be Miami, Florida, with provision for deployments to Bermuda, Barbados, Puerto Rico, and St. Croix for storms in the Atlantic basin (including the Atlantic Ocean and the Caribbean Sea).

Deployments of the NOAA aircraft may be implemented to U.S. coastal locations in the western Gulf of Mexico for suitable Gulf storms and to western Mexico for eastern Pacific storms. Occasionally, post mission recovery may be accomplished elsewhere.

2. Field Program Duration

The hurricane field research program will be conducted from 6 August through 31 October 1999.

3. Research Mission Operations

The decision and notification process used for hurricane research missions is illustrated, in flow chart form, by Fig. A-1 (Appendix A). The names of those persons who are to receive primary notification at each decision/notification point shown in Fig. A-1 are in Tables A-1 and A-2 (Appendix A). In addition, contacts are maintained each weekday among the directors of HRD/AOML, TPC/NHC, and AOC to discuss the "storm outlook."

Research operations must consider that the research aircraft are required to be placed in the National Hurricane Operations "Plan of the Day" (POD) 24 h before a mission. If operational "fix" requirements are accepted, the research aircraft must follow the operational constraints described in section 7.

4. Task Force Configuration

Two NOAA/AOC WP-3D aircraft (N42RF and N43RF), equipped as shown in Table B (Appendix B), will be available for research operations throughout the 1999 Hurricane Field Program (on or about 6 August through 31 October). When possible, the G-IV jet aircraft will be used with the WP-3Ds during the Synoptic-Flow or Genesis Experiment.

5. Field Operations

5.1 Scientific Leadership Responsibilities

The implementation of HRD's 1999 Hurricane Field Program Plan is the responsibility of the field program director, who is, in turn, responsible to the HRD director. The field program director will be assisted by the field program ground team manager. In the event of deployment, the field program ground team manager shall be prepared to assume overall responsibility for essential ground support logistics, site communications, and HRD site personnel who are not actively engaged in flight. Designated lead project scientists are responsible to the field program director or designated assistants. While in flight, lead project scientists are in charge of the scientific aspects of the mission being flown.

5.2 Aircraft Scientific Crews

Tables C-2.1 through C-2.10 (Appendix C) list the NOAA scientific crew members needed to conduct the 1999 hurricane field experiments. Actual named assignments may be adjusted on a case-by-case basis. Operations in 1999 will include completion of detailed records by each scientific member while on the aircraft. General checklists of NOAA science-related functions are included in E.2 through E.6 (Appendix E).

5.3 Principal Duties of the Scientific Personnel

A list of primary duties for each NOAA scientific personnel position is given in D.1 through D.12 (Appendix-D).

5.4 HRD Communications

The HRD/Miami Ground Operations Center (MGOC) will operate from offices at AOML on Virginia Key (4301 Rickenbacker Causeway, Miami, Florida) or from TPC/NHC (11691 S.W. 17th Street, Miami, Florida). TRDIS operations will also be conducted at TPC/NHC.

During actual operations, the senior team leader of the MGOC, or his designee, can be reached by commercial telephone at (305) 221-4381 (HRD/TPC/NHC) or at (305) 361-4400 (HRD/AOML). At other times, an updated, automated telephone answering machine [(305) 221-3679] will be available at the MGOC. Also, MGOC team leaders and the field program director can be contacted by calling their respective telepager phone number (available at a later date).

MGOC, operating from AOML or TPC/NHC, will serve as "communications central" for information and will provide interface with AOC, TPC/NHC, and CARCAH (Chief, Aerial Reconnaissance Coordinator, All Hurricanes). In the event of a deployment of aircraft and personnel for operations outside Miami, HRD's field program ground team manager will provide up-to-date crew and storm status and schedules through the field program director or the named experiment lead project scientist. HRD personnel who have completed a flight will provide information to MGOC, as required.

6. Data Management

All requests for NOAA data gathered during the 1999 Hurricane Field Program should be forwarded to: Director, Hurricane Research Division/AOML, 4301 Rickenbacker Causeway, Miami, Florida 33149.

7. Operational Constraints

Hurricane research missions are routinely coordinated with hurricane reconnaissance operations. As each research mission is entered into the planned operation, a block of time is reserved for that mission and operational reconnaissance requirements are assigned. A mission, once assigned, *must be flown in the time period allotted and the tasked operational fixes met.* Flight departure times are critical. Scientific equipment or personnel not properly prepared for flight at the designated pre-take-off or "show" time will remain inoperative or be left behind to insure meeting scheduled operational fix requirements.

8. Calibration of Aircraft Systems

Calibration of aircraft systems is described in Appendix C (en-route calibration). True airspeed (TAS) calibrations are required for each NOAA flight, both to and from station and should be performed as early and as late into each flight as possible (Fig. C-1).

EXPERIMENTS

9. Hurricane Synoptic-Flow Experiment

Program Significance: Accurate numerical TC forecasts require the representation of meteorological fields on a variety of scales, and the assimilation of the data into realistic models. Omega dropwindsonde (ODW) observations from WP-3D aircraft obtained between 1982 and 1996 during the Hurricane Synoptic Flow Experiment produced significant improvement in the guidance for official track forecasts. Since 1997, twenty-five operational “Synoptic Surveillance” missions have been flown with the NOAA G-IV jet in the environments of TCs threatening the United States coastline; almost half of these have been supplemented with dropwindsonde observations from one or two WP-3D aircraft during Hurricane Synoptic Flow Experiments. An improved dropwindsonde based on the Global Positioning System has been developed by the National Center for Atmospheric Research and has replaced the ODW. With further operational use of the G-IV aircraft, and as other mobile observing platforms become available, optimal sampling and utilization techniques must be devised to provide the greatest possible improvement in initial condition specification.

Since the exact atmospheric state can never be measured, all model initial conditions contain errors whose magnitudes can only be estimated. Therefore, an ensemble of initial conditions consistent with the observations at a given synoptic time can be used to initialize numerical models. Many operational forecast centers, therefore, now employ ensemble forecasting to quantify the uncertainty in the evolution of the atmospheric system. In most systems, perturbations to a best "control" state are designed to mimic the fastest growing modes in the model so as to encompass the probability distribution of the forecast. Therefore, large perturbation locate areas where analysis differences will most impact the forecast, allowing ensemble forecasts to be used to target observations.

Objectives: The goal of the HRD synoptic flow experiment is to improve landfall predictions of TCs by releasing dropwindsondes at approximately the resolution of the North American Rawinsonde Network in all directions from the TC center. These data will be used by TPC/NHC and NCEP to prepare real-time analyses and official forecasts through their incorporation in operational prediction models. Because the atmosphere is known to be chaotic, very small perturbations to initial conditions in some locations can amplify with time. However, in other locations, perturbations may result in only small differences in subsequent forecasts. Therefore, targeting locations in which the initial conditions have errors that grow most rapidly may lead to the largest possible forecast improvements. Locating these regions that impact the particular forecast is necessary.

A number of methods to find targets have been investigated, mainly in the wintertime extratropics. Potential vorticity diagnosis can help to find the cause of forecast failure. Singular vectors of the linearized equations of motion can estimate the growth of small perturbations in the model. This method is relatively expensive, and full implementation in the Tropics where adiabatic processes dominate has proven difficult, and the linear assumption tends to break down at the 72 h forecast time necessary for the posting of hurricane watches and warnings. Related strategies involve the sensitivity vector, and quasi-inverse linear method. All these methods may depend on the accuracy of the initial conditions determined without the supplemental data.

A fully nonlinear technique uses the breeding method, the operational NCEP perturbation technique in which initially random perturbations are repeatedly evolved and rescaled over a relatively short cycling time. These vectors are related to local Lyapunov vectors and, therefore, define the fastest growing modes of the system. Changes to initial conditions due to dropwindsonde data obtained from operational synoptic surveillance missions during the 1997 and 1998 hurricane seasons grow (decay) in regions of large (small) perturbation in the operational NCEP Ensemble Forecasting System. Therefore, these bred-modes provide a good estimate of the locations in which supplemental observations are likely to have the most impact. However, though the breeding method can find locations of probable error growth in the model globally, it does not distinguish those locations which impact the particular forecast from those which do not.

A more generalized method which can use any dynamical ensemble forecast system is the ensemble transform. This method transforms an ensemble of forecasts appropriate for one observational network into one appropriate for other observational networks. Ensemble forecasts corresponding to adaptations

of the standard observational network are computed, and the expected prediction error variance at the observation time is computed for each potential network. The prediction error variance is calculated using the distances between the forecast tracks from all ensemble members and the ensemble mean. This method has shown promise during previous synoptic flow experiments.

Mission Description: To assess targeting strategies a relatively uniform distribution of GPS-sonde soundings will be collected over a minimum period of time by both NOAA/AOC WP-3D aircraft operating *simultaneously within and surrounding the TC, and in coordination with operational surveillance missions of the G-IV.* Specific flight tracks will vary depending on such factors as the location of the storm, relative both to potential bases of operation and to particular environmental meteorological features of interest, and the operational pattern being flown by the G-IV.

A sample mission is shown in Fig. 1. The two WP-3D aircraft and the G-IV will begin their missions at the same time. Subject to safety and operational constraints, each WP-3D will climb to the 500-mb level (about FL 180) or above, then proceed, step-climbing, along the routes assigned during preflight. *It is particularly important that both aircraft climb to and maintain the highest possible altitude as early into the mission as aircraft performance and circumstances allow, and attain additional altitude whenever possible during the mission.*

GPS-sondes are released in one of two modes. Beyond 40 nmi (75 km) from the storm center, drops are made at pre-assigned locations, generally every 25 min or 120 nmi (222 km). These drop locations are provided with the particular mission flight tracks 2 h before blockout. Within 40 nmi (75 km) of the TC's center, drop locations are specified relative to the center's position (e.g., 40 nmi (75 km) north of the eye). During in-storm portions of the mission, drops will be made with possible spacing <8 min or 40 nmi (75 km). Dropwindsondes should generally be released *after the turn is complete*.

At least one aircraft will fly through the TC center and execute a figure-4 pattern. This aircraft's Doppler radar should be set to scan perpendicular to the aircraft track. *"Hard" center fixes are not desirable*. On the downwind leg of the figure-4, the Doppler should be set to record forward and aft (F/AST) continuously. If both aircraft penetrate the storm, the figure-4 pattern will generally be executed by the *second* aircraft through the storm, and the first aircraft through will collect vertical incidence Doppler data. Coordination with potential USAF reconnaissance is necessary to ensure adequate aircraft separation. The in-storm portion of the missions is shown schematically in Fig. 2, although the actual orientation of these tracks may be rotated.

Of paramount importance is the transmission of the GPS-sonde data to NCEP and TPC/NHC for timely incorporation into operational analyses, models, forecasts, and warnings. Operational constraints dictate an 0600 or 1800 UTC blockout time, so that the GPS-sonde data will be included in the 1200 or 0000 UTC analysis cycle. Further, limiting the total block time to 9 h allows adequate preparation time for aircraft and crews to repeat the mission at 24-h intervals. These considerations will ensure a fixed, daily real-time data collection sequence that is synchronized with NCEP and TPC/NHC's analysis and forecasting schedules.

HURRICANE SYNOPTIC FLOW EXPERIMENT

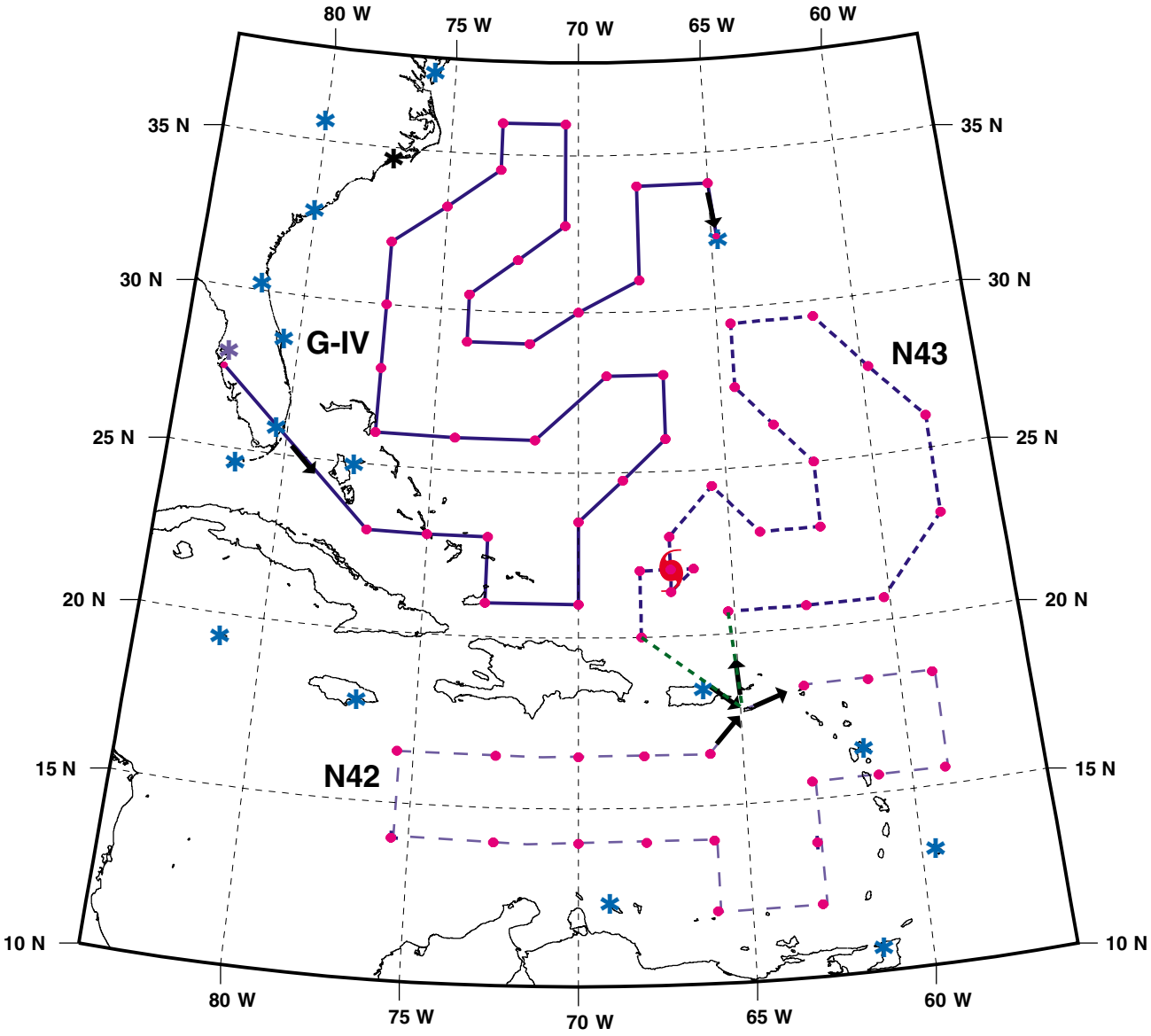

Fig. 1. Sample Environmental Patterns

• Note 1.	During the ferry to the **IP**, the WP-3D aircraft will climb to the 500 mb level (about FL 180). The 400 mb level (about FL 250) should be reached as soon as possible and maintained throughout the remainder of the pattern, unless icing or electrical conditions require a lower altitude.
• Note 2.	During the ferry to the **IP**, The G-IV should climb to the 41,000 ft (200 mb) as soon as possible and climb as feasible to maintain the highest altitude for the duration of the pattern.

HURRICANE SYNOPTIC FLOW EXPERIMENT

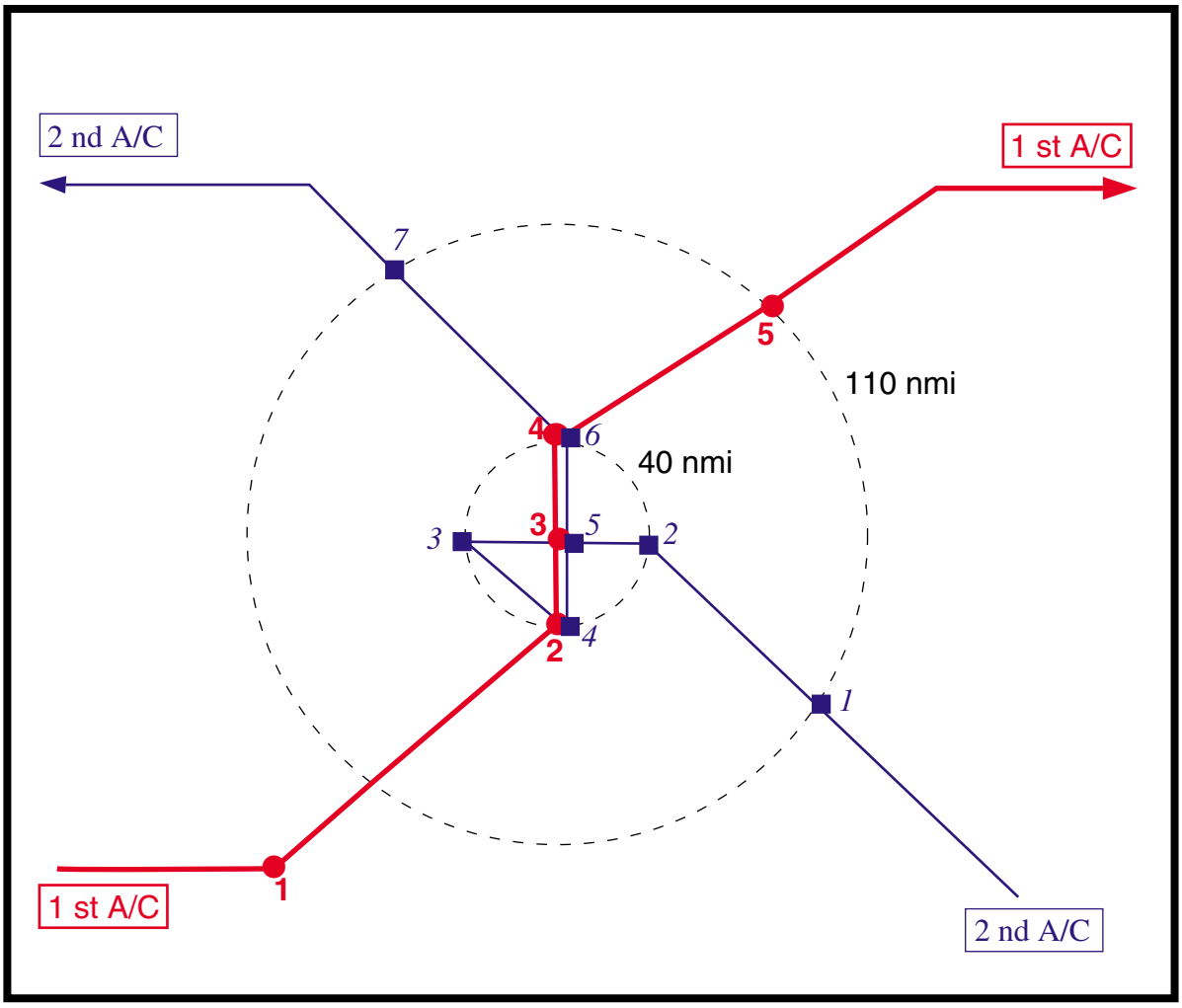

Fig. 2 In-Storm Patterns

• Note 1.	Within the 40 nmi (75 km) range ring, all legs are on cardinal tracks.
• Note 2.	The second aircraft through the storm will execute the Doppler "figure-4" pattern. The Doppler radar should be set to continuously scan perpendicular to the track during radial penetrations and to F/AST on the downwind leg.
• Note 3.	Numbered symbols (◆, ■) reflect scheduled drops for each aircraft.
• Note 4.	Drop #5 in the "figure-4" pattern occurs on the second pass through the eye.
• Note 5.	A/C 1 should collect vertical incidence Doppler data during storm penetration.
• Note 6.	If missions are not repeated, then block times may exceed 9 h. In addition to the GPS-sonde data, *3-4 RECCO's h^{-1} should be transmitted during each mission.*

Special Notes: Missions similar to the Synoptic Flow missions may be flown in non-hurricane conditions to collect GPS-sonde data sets for satellite sounding evaluations. These missions differ from the normal experiment as follows:

- Block times are 10 h, and the experiment is not repeated on the following day.
- In-storm portion of the pattern (Fig. 2) is omitted and no Doppler data are collected.
- The G-IV does not participate in the mission

10. Extended Cyclone Dynamics Experiment (XCDX)

Program significance: Starting in the early 1980s, the Vortex Dynamics Experiment was the focus of observational studies of the evolution of the TC's inner core. It accumulated an archive of more than 3000 radial passes in 50 different Atlantic and Eastern Pacific TCs. The main scientific result was formulation of an observationally based model in which TC intensity and structure change were explained in terms of convective rings, circles of convection coincident with maxima of the swirling wind that intensify and propagate inward. Remaining unanswered questions were the dynamics of the rings' formation and factors that control timing and amount of intensity changes.

Since 1991, HRD has received the flight–level observations from routine reconnaissance flights by the IWRS-equipped WC-130Hs of the 53rd Weather Squadron. Although these observations have proven to be of excellent quality, their value is compromised by a lack of vertical velocity, microphysics, or radar reflectivity data. The USAF aircraft typically remain on station for 4–6 h, flying figure-four (ALFA) patterns at 850 or 700 mb (5,000 or 10,000 ft (1.5 or 3.0 km) altitude) with 150 nmi (278 km) legs oriented along the cardinal directions. Between sorties, there is usually a gap of 6–7 h during which no aircraft is in the TC, except near landfall when the interval between fixes decreases to 3 h. Experience with USAF observations from the 1991 through 1998 seasons shows that they document the evolution of the TC core well, but that they are even more valuable when augmented by occasional sorties of the NOAA WP-3Ds. The advent of the G-IV and introduction of GPS–based dropwindsondes present a long–awaited opportunity to study vortex interaction with vertical shear of the environmental wind and with upper tropospheric waves that are hypothesized to control TC intensification through eddy influxes of angular momentum.

The conventional reason offered for shear's negative effect on intensification has been that it ventilates the vortex by blowing warm air out of the core aloft to raise the hydrostatic surface pressure. Recent theoretical work suggests that the asymmetric stability and distribution of convection associated with shear–induced tilt of the vortex may be more significant. The net result of eddy momentum import is not a direct spin up of the swirling wind but outflow near the tropopause, which destabilizes the tropospheric column and strengthens the convection. Rapid intensification, apparently triggered by this mechanism, is a one of the most challenging problems that forecasters face. Jet airplanes and the new dropwindsondes are ideal tools to address this problem.

Objective: This experiment is designed to study the mechanisms by which environmental shear and eddy fluxes control TC intensity changes. A secondary objective is to obtain a time series of eye soundings to study the thermodynamics of intensity change.

Mission Description: The Vortex Option uses Air Force flight-level data to monitor the vortex core and frequent dropwindsondes and Radar data from the WP-3Ds or G-IV to monitor interactions with the environment. If only the WP-3Ds are available, they fly successive star patterns out to 200–300 km at 600–500 mb {15,000-18,000 ft [5-6 km)}. If jet aircraft are available, they will fly at or near their ceiling dispensing dropwindsondes through nearly the whole tropospheric column, either in a pattern similar to the WP–3Ds or in a circumnavigation. Thus, the combined flights can observe both the near–field environmental forcing and the vortex response.

The ideal target is a northward moving TC that has a fairly small Central Dense Overcast (CDO) and is expected to interact with vertical shear, an approaching mid-latitude trough, or a upper-level low.

The WP-3Ds will fly at 500–600 mb isobaric level {15,000-18,000 ft [5-6 km)} in a pattern of three equilateral triangles with common vertices at the TC's center (Fig. 3). Altitude will be the highest attainable that avoids too much aircraft icing and electrical charging. It is crucial to the analysis that a fixed pressure altitude is maintained throughout. The nominal leg length will be 250-300 nmi (460-550 km), but the size of the pattern will be adjusted to make the legs as long as possible given the available aircraft range. The WP-3D will deploy dropwindsondes in a symmetrical pattern to map the vertical structure of the secondary circulation below flight level. On each passage through the center it will deploy a pair of sondes as close to the axis of vortex rotation as possible to study the thermodynamic transformations of the eye. The basic XCDX is three maximum-endurance sorties in 42 h or four in 56 h, with alternating aircraft and crews. Nominal flight duration will be 10 h with 4 h gaps between flights. The second aircraft will take off 14 h after the first. The third sortie, the second flight by the first aircraft, will depart 14 h after the second sortie or 18

h after the first sortie landed. Thus, take-off times by the same aircraft and crew will shift 4 h later in the next day on subsequent flights. The aircraft may, depending upon altitude, spend a third or a quarter of its time in icing conditions under the CDO, which may compromise range. A variation of the XCDX is one or more sorties at the same altitude with shorter legs and more frequent drops in the eye to focus on eye thermodynamics.

The G–IV, if available, will fly a hexagonal circumnavigation of the storm at 600 nmi (1,110 km) radius, dispensing up to five dropwindsondes on each of the six sides of the pattern (Fig. 4). The aircraft will dispense dropwindsondes frequently along track. Since the purpose of the pattern will be to observe asymmetric structure and compute eddy correlations, the turn points will need to move with the TC, placing a premium on accurate navigation.

XCDX EXPERIMENT

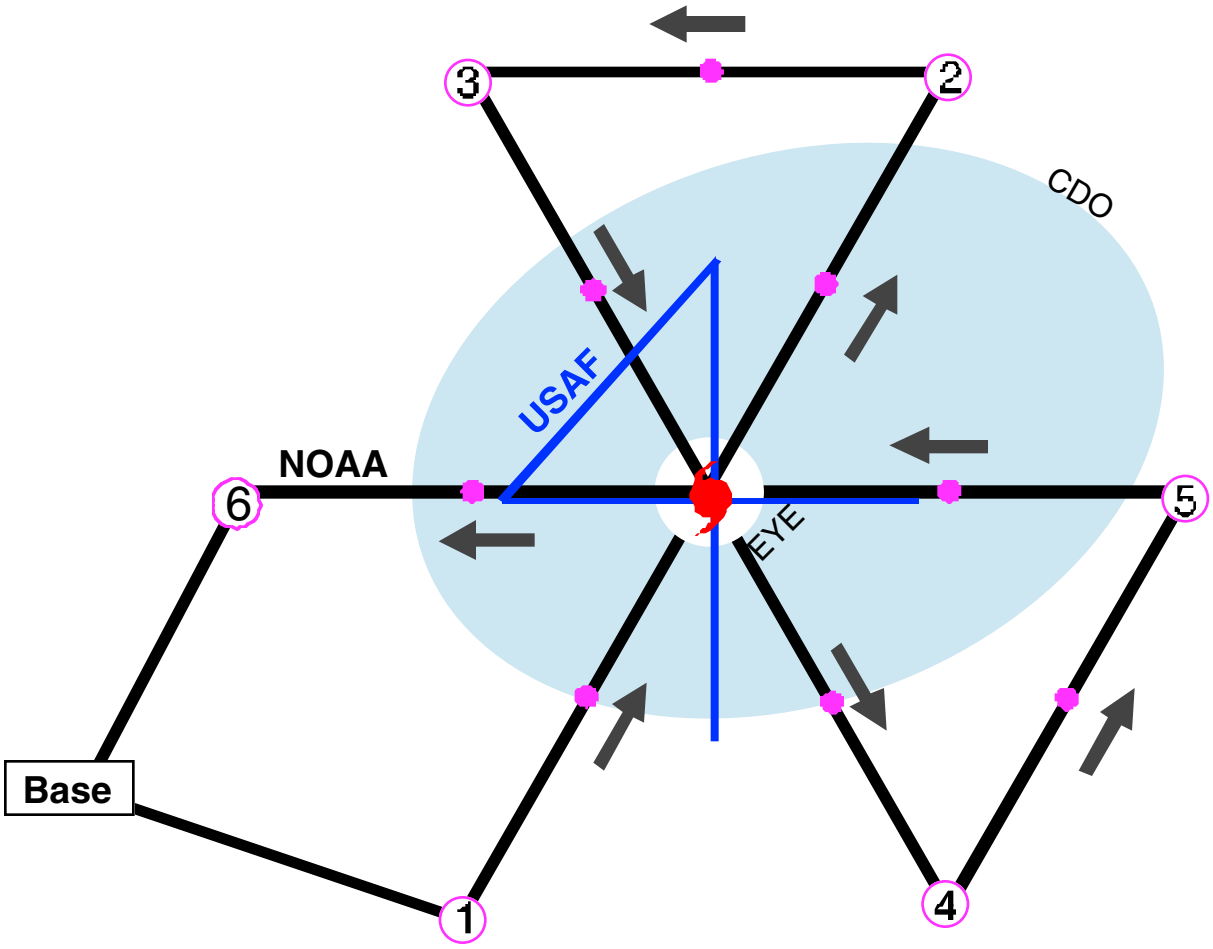

Fig. 3. WP-3D pattern

• Note 1.	WP-3Ds fly **1–§–2–3–§–4–5–§–6** at 500 mb pressure altitude if the CDO is small, or at 15,000 ft (4.5 km) radar altitude to avoid icing if it is large. The leg length is the longest possible given aircraft range and ferry distance to the storm.
• Note 2.	Dropwindsonde observations occur at the midpoints of the legs, after turns, and in pairs as close to the axis of rotation as possible on each passage through the eye.
• Note 3.	Each WP-3D sortie will take off is 19 h after the previous one.
• Note 4.	Airborne Doppler radar scans perpendicular to the aircraft track within 50 nmi (95 km) of the center on penetration and exit, and on F/AST elsewhere.

XCDX EXPERIMENT

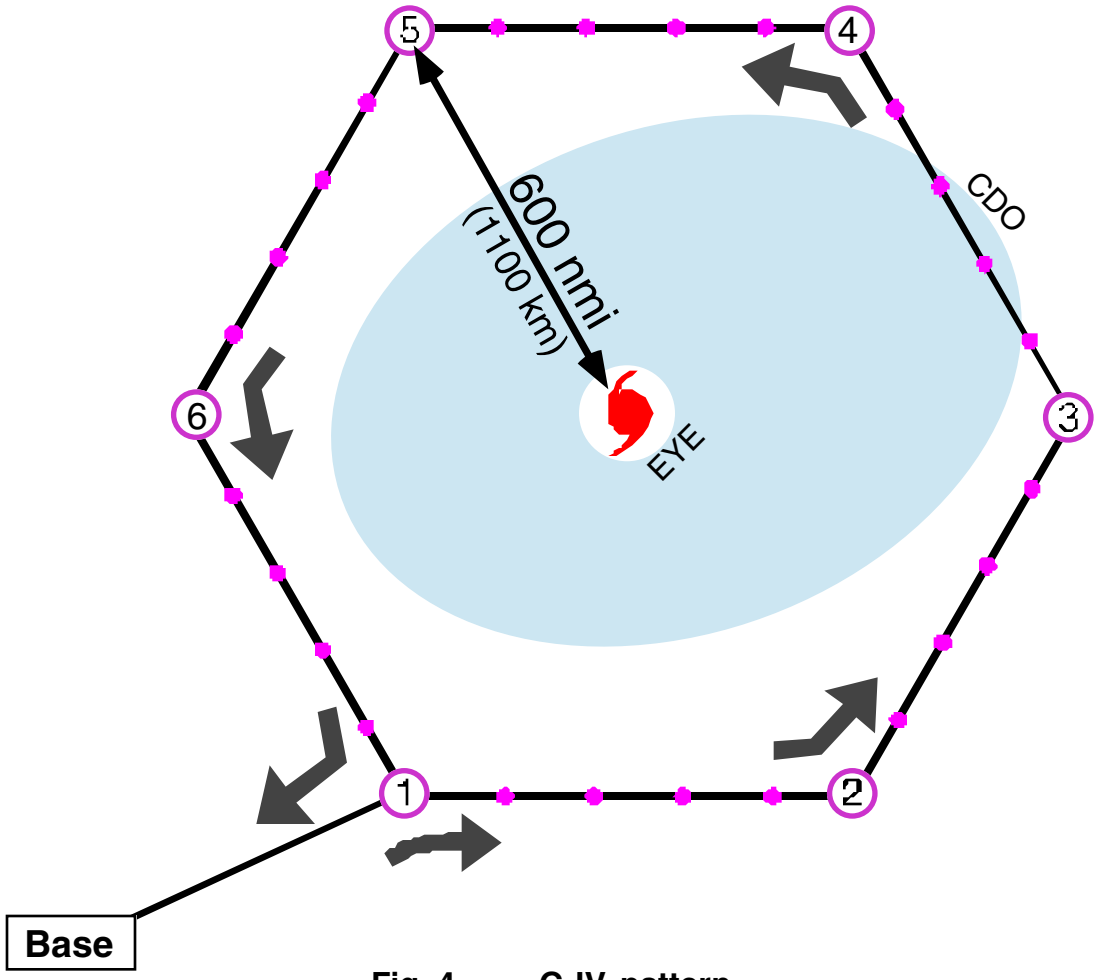

Fig. 4. G-IV pattern

• Note 1.	The G–IV flies 1–2–3–4–5–6. The entire pattern is at 200 mb pressure altitude with turn points positioned relative to the moving TC center point. Leg length (pattern radius) will be adjusted to use the available range.
• Note 2.	Four or five GPS-sondes will be deployed on each leg.

11. Vortex Motion and Evolution (VME) Experiment

Program Significance: Recent research suggests that important environmental controls on TC motion are active in the region surrounding the cyclone's inner core, within about 160 nmi (300 km) of the center. Studies of Hurricane Gloria from Doppler radar and ODW data suggest that the environmental influence on vortex motion was maximized in an envelope near 35 nmi (65 km) radius from the center. The region from 35-160 nmi has been poorly sampled during other experiments, which have either emphasized the vortex core or the more distant environment. A primary goal of the VME experiment is to improve our understanding of how the environmental steering flow is communicated to the vortex.

Analyses of the core regions of TCs based on the pseudo-dual Doppler approach have increased our understanding of TC structure and evolution. However, recent studies using true dual-Doppler data collected from simultaneous passes by two aircraft through the center of TCs, have shown that significant changes in storm intensity and structure can take place over periods of 30 min or less. This implies that the pseudo-dual-Doppler analyses obtained from a single aircraft's "figure-4" pattern may be subject to significant aliasing. Additional true dual-Doppler data sets are required to properly document the evolution of the vortex core region over periods of several hours.

In 1995, two successful VME experiments were conducted in Hurricanes Iris and Luis, using the previous (ODW) generation of dropwindsonde. In 1997 and 1998, VME missions were also flown in Hurricanes Guillermo and Danielle, respectively. The latter two missions employed the new GPS-sondes, doubling the horizontal sounding resolution in the radial direction to 25 nmi (46 km). In the inner core, improvements over dual-Doppler data sets can be obtained by altering the antenna scanning mode to yield multiple-Doppler wind fields.

The G-IV synoptic surveillance mission results suggest that dropwindsonde data are not optimally assimilated into the models. Aliasing of data into regions on the edges of flight patterns can lead to forecast degradation despite the inclusion of quality data. Further, synthetic vortex representations in global and regional models frequently introduce errors into the initial conditions. Current data assimilation techniques generally allow for the data to impact the analyses equally in all directions from the location of the observation. However, in the TC core, this can cause large initial condition errors. An ensemble or ensemble transform Kalman filter can limit this problem by providing flow dependent data analysis increments. The relatively even coverage of dropwindsonde data within the inner regions of the TC in the vortex motion and evolution experiment provides an excellent data set for the testing of sophisticated data assimilation techniques to limit aliasing and provide better initial condition vortices in the numerical models.

Objectives: The immediate goal of the experiment is to document the three-dimensional wind and thermodynamic fields within 160 nm of TCs. Data sets obtained from the experiment will be used to relate asymmetries in the wind field to short and long-term vortex motion. The data sets will also be used to determine the utility of the pseudo- and true-dual-Doppler approach, and in further studies of the role of inner core asymmetries in TC motion, structure and evolution.

Doppler radar and GPS-sondes will be used to document the three-dimensional wind field within 160 nmi of TCs. True dual-Doppler data are obtained within 45 nmi (83 km) of the center with a horizontal grid spacing of 0.6 nmi (1 km). Three such data sets over 7 hours, 2.3 hours apart, are obtained during the mission, supplemented by pseudo-dual-Doppler data sets that span the intervals between the true-dual-Doppler sets, to examine the evolution of the inner vortex. These data are supplemented by five rings of 6 or more GPS-sondes, at 50, 75, 100, 130, and 160 nmi (93, 139, 185, 241, and 300 km). This GPS-sonde coverage will provide azimuthal wave numbers 0 and 1 at these radii, to specify the overall strength of the vortex and its basic steering asymmetry. Satellite information from NCEP and the University of Wisconsin will supplement the GPS-sonde coverage above flight level.

Mission Description: The experiment involves both WP-3D aircraft flying simultaneous, predetermined and coordinated patterns. One aircraft will fly at maximum altitude and release dropwindsondes in the pattern shown in Fig. 5; the second aircraft will fly at a lower, fixed altitude, and drop sondes in the eye and eye wall. Care should be taken to provide an azimuthally even distribution of eyewall sondes. Both aircraft will collect Doppler-radar and cloud-physics data. The upper aircraft will also measure the atmospheric electric field on an opportunity basis for other investigators. The experiment

requires a strong tropical storm or TC, with unsheared convection near the center to provide Doppler targets. The length of the flight patterns requires that the cyclone be within about 540 nmi (1,000 km) of the base of operations, and it must be far enough from land to allow drops 160 nmi from the center. The experiment requires only one day of flying, but may be repeated on subsequent days if desired.

Subject to safety and operation constraints, takeoff time will be 1800 UTC, to coordinate with the NCEP analysis cycle at 0000 UTC. The flight pattern for the dropwindsonde (upper) aircraft is shown in Fig. 5. During the ferry to the initial position (IP), the aircraft will climb to the 500-mb level (about FL 180) or above. The 400 mb level (about FL 250) should be reached as soon as possible and maintained throughout the pattern, unless icing conditions dictate a lower level for safety. GPS-sondes will be released at the indicated locations in Fig. 5, and true-dual Doppler data will be collected during the three “figure-4" portions of the pattern. If there is active convection in the outer triangle portions of the pattern, Doppler data should be collected there as well. All drop and turn points in the pattern are relative to the moving center of the storm. Mandatory and significant level information from selected GPS-sondes will be transmitted in real time back to NCEP and TPC/NHC.

The flight pattern for the lower aircraft is given in Fig. 6 Subject to safety and operational constraints, the lower aircraft should take off first. Flight level for the lower aircraft will be FL100. *In order to ensure that the most simultaneous true-dual-Doppler data are obtained, communication and coordination between the two aircraft are essential. Both aircraft must begin their patterns at their respective IP’s simultaneously. Once the patterns are underway, all coordination maneuvers should be performed by the lower aircraft; except for changes in air-speed, the upper aircraft will fly its pattern as drawn. In addition to the IP’s, the start of each inbound Doppler leg should be coordinated.*

VME Coordination Points	
Upper Aircraft Nav Point	**Lower Aircraft Nav Point**
1 (IP)	1 (IP)
2	2
4	4
8	10
10	12
14	18
16	20

The lower aircraft is responsible for delaying to ensure that the CP’s are reached simultaneously by both aircraft. The patterns are designed so that the lower aircraft will reach the CP’s shortly before the upper aircraft; however, if necessary, the lower aircraft may cut the corners at points **9** and **17** in order to reach points **10** and **18** on time.

At times the lower aircraft may fly an optional circle pattern just outside the eyewall (Fig. 6). This would occur just after the coordinated figure-4 pattern (i.e., immediately following navigation points **5**, **13**, or **21** (Fig. 6). The aircraft flies a nearly circular pattern (actually numerous short straight-line segments) just outside the eyewall while the tail radar scans in a fore/aft sequence. The circle must be as small as possible, since no data are obtained from the inner 40% (by radius) of the circle. The lower aircraft would be re-coordinated with the upper aircraft at navigation points **10** or **18** (Fig. 6).

Special Note: The VME pattern can be coordinated with the Hurricane Surveillance Mission flown by the G-IV. The VME pattern is unchanged while the G-IV drops sondes in the TC’s large-scale environment.

VORTEX MOTION AND EVOLUTION EXPERIMENT

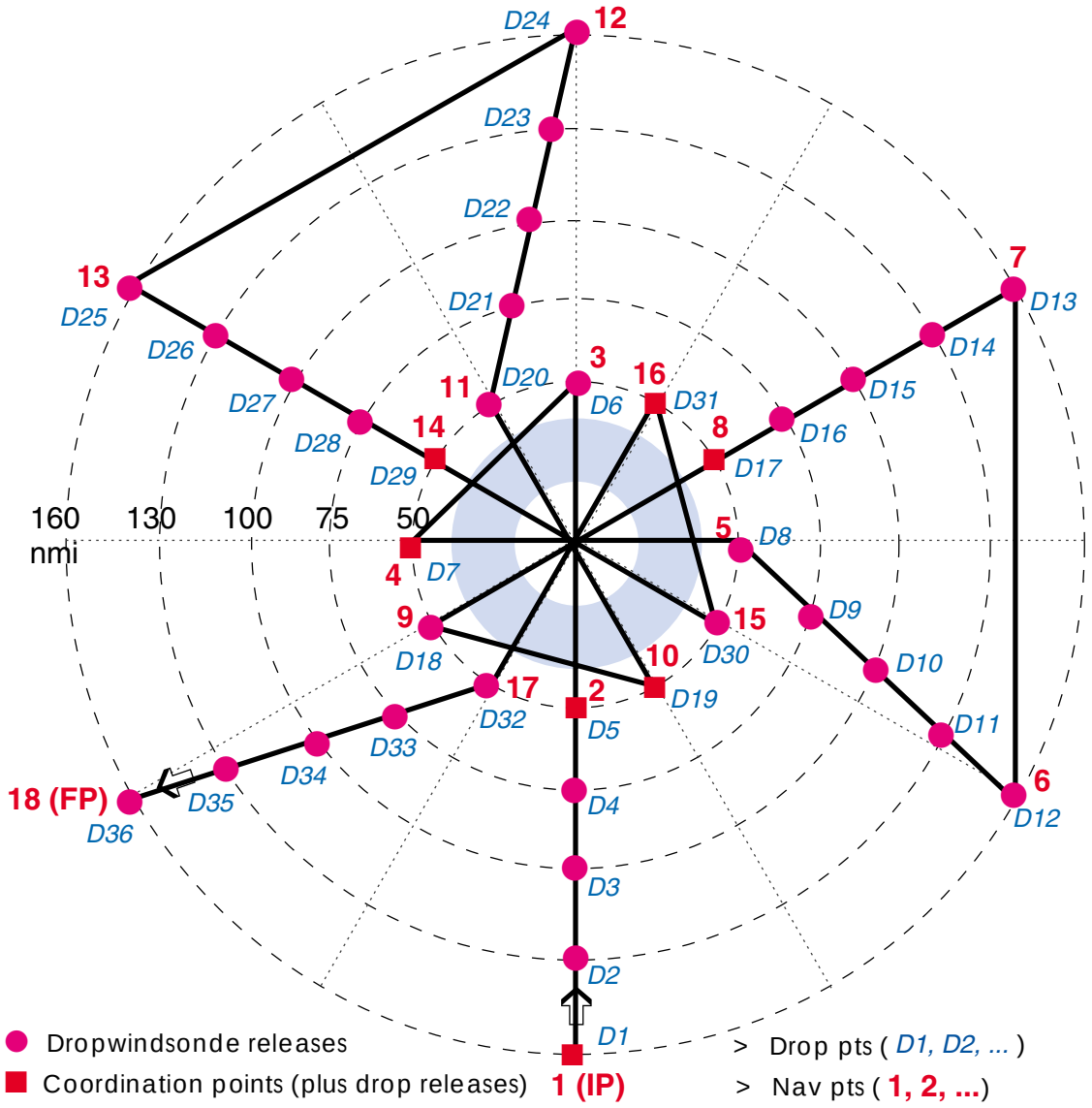

Fig. 5. Sample Upper Aircraft Flight Pattern

• Note 1.	True airspeed calibration is required.
• Note 2.	During the ferry to the **IP**, aircraft will climb to the 500 mb level (about FL 180). The 400 mb level (about FL 250) should be reached as soon as possible and maintained throughout the remainder of the pattern, unless icing or electrical conditions require a lower altitude.
• Note 3.	The pattern may be entered along any compass heading. The **IP** and coordinating points (**CP**) must be reached simultaneously with the lower aircraft. The lower aircraft is responsible for ensuring that these points are reached simultaneously.
• Note 4.	There are **no** scheduled drops in the eye. It may be desirable to make a drop during the second pass of each figure-4, assuming clearance from the lower aircraft and USAF reconnaissance aircraft. GPS-sonde frequencies should be coordinated with USAF aircraft. All drops are to be made after turns.
• Note 5.	Airborne Doppler radar scans in F/AST mode throughout the mission.
• Note 6.	Aircraft should not deviate from the pattern to find the wind center in the eye.

VORTEX MOTION AND EVOLUTION EXPERIMENT

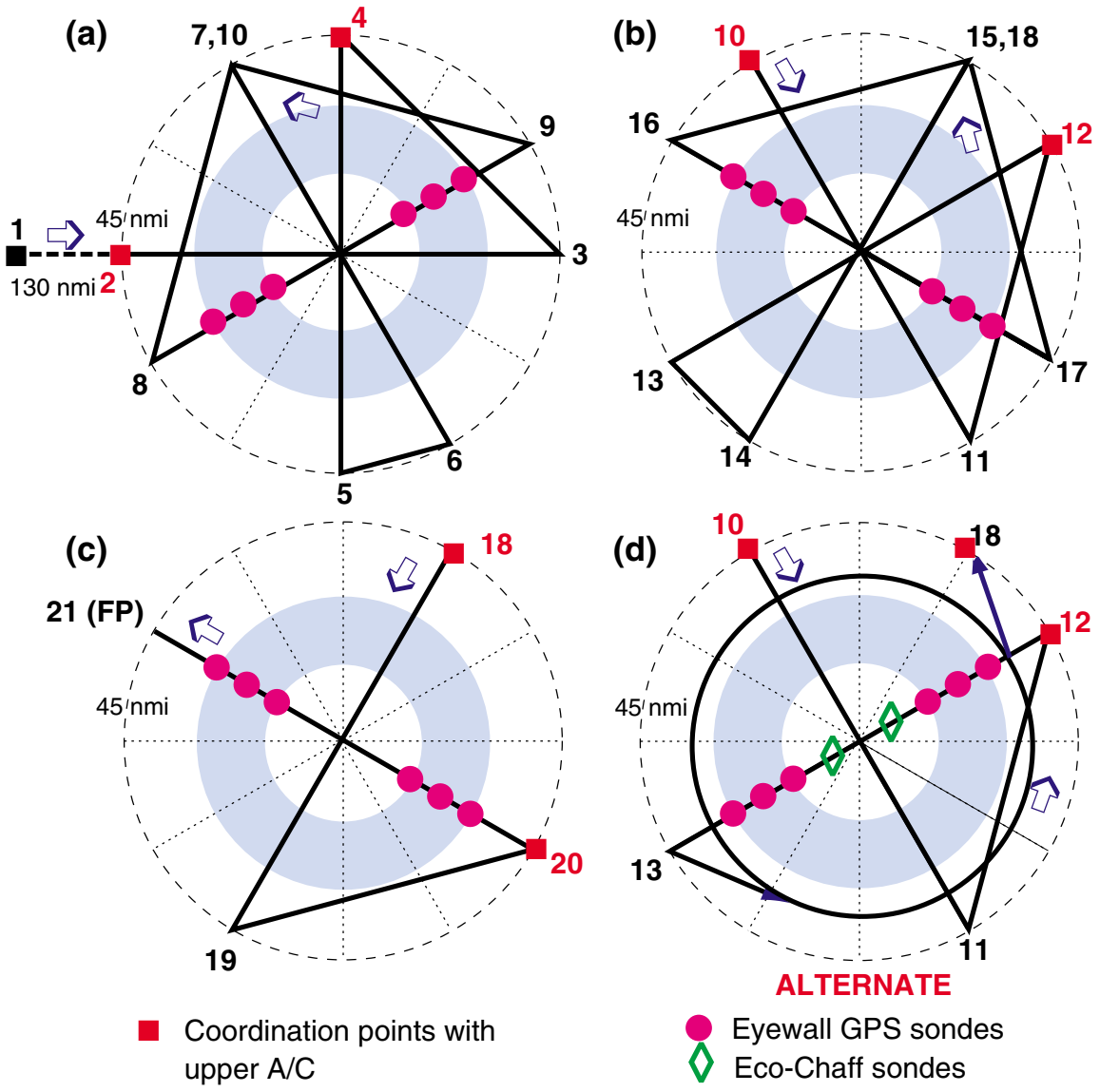

Fig. 6. Sample Lower Aircraft Flight Pattern

• Note 1.	True airspeed calibration is required.
• Note 2.	Unless there is a conflict with the USAF aircraft, the lower NOAA aircraft will operate at FL 100 (10,000 ft or 3 km). Eyewall drops may be required at the discretion of the lead mission scientist. As many as 3 drops per penetration, with spacing of 10-30 km, may be requested. Care should be taken to provide an azimuthally even distribution of eyewall sondes
• Note 3.	The **IP** is at 130 nmi (240 km) radius from the storm center. The pattern may be entered at any compass heading, but will always be 90° upwind of the entry point of the upper aircraft. Radial legs are 45 nmi (83 km) long.
• Note 4.	The **IP** and coordinating points (**CP**) must be reached simultaneously with the lower aircraft. The lower aircraft is responsible for ensuring that these points are reached simultaneously.
• Note 5.	Airborne Doppler radar scans continuously perpendicular to the track on radial penetrations at radii<50 nmi (95 km) , and F/AST during the rest of the pattern.
• Note 6.	Aircraft should not deviate from the pattern to find the wind center in the eye.

12. Tropical Cyclogenesis Experiment

Program Significance: Tropical cyclogenesis can be viewed as a rapid increase of low- and mid-level mesoscale cyclonic vorticity within a region of positive synoptic-scale relative vorticity. Numerous theories have been advanced in the literature to explain how this vorticity develops and amplifies. The purpose of the proposed experiment is to identify the important processes that contribute to low and mid-level vortex amplification and, ultimately, to tropical cyclogenesis.

Many researchers have demonstrated the importance of multiscale processes during tropical cyclogenesis. Large-scale environments favorable for genesis or lysis in the Atlantic Ocean have been revealed by composites of operational analyses and case studies of genesis (e.g., Dolly of 1996) and lysis events (e.g., Tropical Depression #5 of 1997). Western and eastern Atlantic composites created using archived NHC ATOLL/200 mb analyses and best track data for 1975-1993 have shown the dynamical importance of ascent forced through cyclonic vorticity advection (CVA) by the thermal wind in the incipient storm environment. Over the eastern Atlantic, this CVA and forced ascent is generally found equatorward of a 200 mb zonally-oriented ridge axis in association with an upper-level easterly jet, while over the western Atlantic the CVA occurs downstream (upstream) of a 200 mb trough (ridge). In both composites the ATOLL disturbance is located beneath an area of CVA and near a minimum in vertical wind shear (200 mb-ATOLL). Flow decomposition techniques reveal the importance of large-scale deformation processes at both the 200 mb and ATOLL levels and indicate that both developing disturbances are found downstream of a low-level ($\geq$700 mb) southeasterly jet along the equatorward side of a ridge axis. Together, results from the flow decomposition diagnostics and compositing techniques depict a large-scale environment favorable for persistent deep, moist convection over the ATOLL-level disturbance. The conditions important in the Atlantic basin are similar to those found to be important in other basins, where conditions of weak vertical shear, low-level positive vorticity, and the repeated development of convective bursts are all necessary conditions for tropical cyclogenesis.

Recent observations from genesis cases have also identified important processes on the mesoscale that contribute to tropical cyclogenesis. For example, results obtained from a WP-3D aircraft investigation of Dolly (1996) indicate its genesis was strongly influenced by persistent, deep convection, in the form of mesoscale convective systems (MCSs), that developed in association with an easterly wave over the Caribbean. Within this deep convection an eye-like feature formed, after which time the system was declared a depression. Similar observations have been made in the western Pacific, where discrete maxima in convective activity coincide with disturbance-to-tropical depression and tropical depression-to-tropical storm transitions.

Crucial to understanding the formation of this eye-like feature is a determination of the sources of low level cyclonic vorticity. The flow decomposition and compositing techniques discussed above, in addition to numerous other observational and modeling studies, indicate that an environment favorable to the onset of deep, moist convection is vital in initiating and sustaining the tropical cyclogenesis process. What is not as well understood is precisely how this convection leads to an increase in the low-level cyclonic vorticity. Detailed observations of the upper and lower-level thermal, moisture, and flow fields within a developing disturbance, with high spatial resolution over an extended time period, are necessary to understand how this low- and mid-level cyclonic vorticity develops and amplifies.

Since both tropical cyclogenesis and TC intensity change can be defined by changes in low- and mid-level vorticity, knowledge of the processes that play a significant role in genesis might also advance our understanding of intensity change. A better understanding of the processes that lead to an increase in low- and mid-level cyclonic vorticity will also allow NHC to better monitor and forecast tropical cyclogenesis and intensity change, improvements that would be especially valuable for those events that threaten coastal areas. Data obtained by aircraft investigating potential genesis events will positively impact operations and research in other ways as well. The ingestion of this data into the NCEP model analysis and initialization schemes should permit an improvement in NCEP model forecast performance based upon a better representation of the mesoscale and synoptic-scale structure in the vicinity of the incipient disturbance. In addition to improving the understanding and forecasting of tropical cyclogenesis and intensity change, the proposed experiment should yield useful insight into the structure, growth and ultimately the predictability of the systems responsible for almost all of the weather-related destruction in the tropical Atlantic. Investigation of systems that fail to complete the genesis process should also result in a better understanding and prediction of easterly disturbances in general so that distinction can be better made between developing and non-developing tropical disturbances.

Objectives:

- Determine how low-level vortices associated with organized mesoscale convective systems are produced.
- Determine what distinguishes developing from non-developing low-level vortices.
- Determine the dynamical linkage between synoptic-scale forcing and processes that lead to spin-up of the low-level mesoscale vortex.
- Determine the role of the onset and impulsiveness of deep moist convection in the upward growth of low-level vortices and the downward growth of mid-level vortices.
- Determine how preexisting mid- and low-level mesoscale vortices interact during genesis.
- Determine the dynamical and thermodynamical linkage between low-level mesoscale vortex spin-up and the larger scale environmental relative humidity.
- Determine the relative importance of external influences and internal processes during genesis.

Mission Description: This experiment may be executed with aircraft from NOAA alone, or NOAA in cooperation with the USAF flying into pre-genesis and incipient tropical disturbances over the Atlantic Ocean, Caribbean Sea, Gulf of Mexico, and tropical eastern North Pacific Ocean. The primary mission will require two WP-3Ds flying back-to-back with the G-IV aircraft flying a coordinated pattern. The two WP-3Ds will fly low- and mid-level mesoscale patterns in close proximity to any suspected low-level vortices while the G-IV simultaneously flies at upper levels (200-300 mb) and collects observations to a distance of ~1500 km from the center of the disturbance. If available, the USAF WC-130 aircraft can be used to significantly enhance observations at all levels.

The staggered WP-3D missions are designed to commence on station at 3 AM local and again on station at 3 PM local. The G-IV mission would occur coincident with the afternoon flight and consistent with synoptic missions centered on the 0000 UTC synoptic time.

The main aircraft for the low- and mid-level flights will be the two WP-3Ds. Doppler radar observations, GPS-sondes, scatterometer, and flight level observations obtained during these flights will help locate low- and mid-level vortices and help document their structures and life cycles. Crucial to a complete understanding of the genesis process is the collection of observations with high temporal and spatial resolution. A primary aspect of this experiment will be to observe the complete life cycle and interaction of low- and mid-level vortices and understand how these vortices are influenced by the diurnal cycle of convection. Staggered missions with the two WP-3D aircraft will begin with the first aircraft flying a figure-4 pattern at 700-500 mb (10,000-18,000 ft or 3.0-5.5 km; Fig. 7). Persistent areas of deep convection and/or low-level rotation identified with satellite imagery will be used to center the flight plan. Leg lengths will be 325-430 nmi (600-800 km), and the pattern will be centered approximately on the deep convection, if convection is occurring at the time, or the incipient vortex, if convection has recently subsided. The primary purpose of these aircraft missions will be to collect F/AST Doppler radar and GPS-sonde data in the area of deep convection in order to map the evolution of the three-dimensional wind and thermodynamic structure of the deep convection and incipient vortex. Once a low-level vortex is identified flight legs will be significantly reduced in length [100-135 nmi (180-250 km)] to allow for the collection of data with high temporal and spatial resolution in the vicinity of the vortex (Fig. 8). If no low-level vortex is apparent the low-level grid pattern (Fig. 9) should be employed.

In addition to observing the evolution of the thermal and wind fields associated with the deep convection and incipient vortex, observations of the low-level inflow environment of the deep convection will be taken, if possible. Sampling the inflow environment will involve dropping a high density of GPS sondes within and immediately upstream of the deep convection. The GPS sondes will provide observations of the mechanisms operating on the mesoscale that trigger the deep convection and lead to the horizontal and vertical distributions of diabatic heating.

If available, the G-IV will be most beneficial flying a synoptic-scale pattern. It will fly at maximum altitude observing the upper and lower troposphere with GPS-sondes in the pre-genesis and incipient tropical disturbance environment. A potential genesis event occurring in conjunction with primarily an upper tropospheric anticyclone will require a flight pattern similar to that given in Fig. 10a. The aircraft will dispense 20-25 GPS-sondes mostly on the poleward side of the incipient disturbance during the flight to

help define wind, temperature and moisture patterns near the ridge axis. Should a potential genesis event occur in association with an upper-tropospheric trough-ridge couplet a flight pattern similar to that shown in Fig. 10b will be required. This flight pattern will collect observations in the vicinity of both the trough and ridge with upwards of 20-25 GPS-sondes. These flight patterns are designed to define those regions where large-scale forcing for ascent exists and persistent deep convection is favored.

An enhancement of the data collected during genesis by the three NOAA aircraft may be accomplished by adding observations from investigative USAF WC-130 aircraft. Should a USAF WC-130 aircraft be available it would be requested to fly at maximum altitude dispensing GPS-sondes in the southern and eastern quadrants of the incipient disturbance. This aircraft would be requested to fly a saw-tooth pattern centered on asymptotes of confluence, convective inflow bands, and/or thermal boundaries within ~300 nmi (500 km) of the incipient disturbance.

In addition to using aircraft, collaboration with the scientists at CIRA will provide a wealth of satellite-based information that will be useful in identifying the flow fields and thermal structures of an incipient disturbance. CIRA has access to the capabilities of the new generation of GOES satellites, particularly the super rapid scan operations (SRSO) and the sounding unit. The SRSO observations during the daylight hours would provide data from which very high-density cloud track winds would be obtained. These winds would be used in conjunction with the Doppler radar, GPS sondes, scatterometer, and flight-level observations to document the structure and evolution of low- and mid-level vortices associated with bursts of convection within an easterly wave. The time period during which the SRSO observations would be available is 1300-1500 UTC. The request for SRSO will be made 24 h prior to the flight, with an alert 48 h ahead.

Since the time of the SRSO observations is after the typical nocturnal convective maximum in the tropics, it would enable an easier identification of flow features as the anvil debris from the convective bursts would have dissipated by then. The temperature sounding unit aboard the GOES satellite and the AMSU instrument aboard the polar-orbiting NOAA-15 satellite will provide a picture of the mid- and upper-level thermodynamic environment both within the disturbance and in the synoptic environment. These observations will yield important information about the response of the vortex's thermal structure to the convective bursts that will complement well the GPS sondes dropped from the aircraft. SSM/I imagery, available from the world wide web, will also be used to infer the intensity of incipient disturbances during times when the aircraft are not flying.

The possible availability of multiple aircraft during this experiment leads to several different scenarios. A summary of the potential combinations of aircraft during genesis experiments follows:

- Option 1 (lesser experiment):

  The two core NOAA WP-3D aircraft alone will fly staggered figure-4 or grid patterns (Figs. 7-9) centered on the area of persistent deep convection and/or any low level vortex over a 2-4 day period.

- Option 2 (primary experiment):

  Option 1 augmented with large-scale upper- and lower-tropospheric observations obtained by the G-IV aircraft flying patterns similar to those given in Figs. 10.

- Option 3 (optimal experiments):

A) Option 2 with USAF WC-130 flying a standard reconnaissance mission.

B) Option 2 with USAF WC-130 flying a targeted mission to sample asymptotes of confluence, convective inflow bands, and/or thermal boundaries within ~300 nmi (500 km) of the incipient disturbance.

C) Option 2 with the G-IV aircraft to collect quasi-continuous observations in the upper and lower troposphere within ~900 nmi (1500 km) of the disturbance.

D) Option 3B with the G-IV aircraft to collect quasi-continuous observations in the upper and lower troposphere within ~900 nmi (1500 km) of the disturbance.

TROPICAL CYCLOGENESIS EXPERIMENT

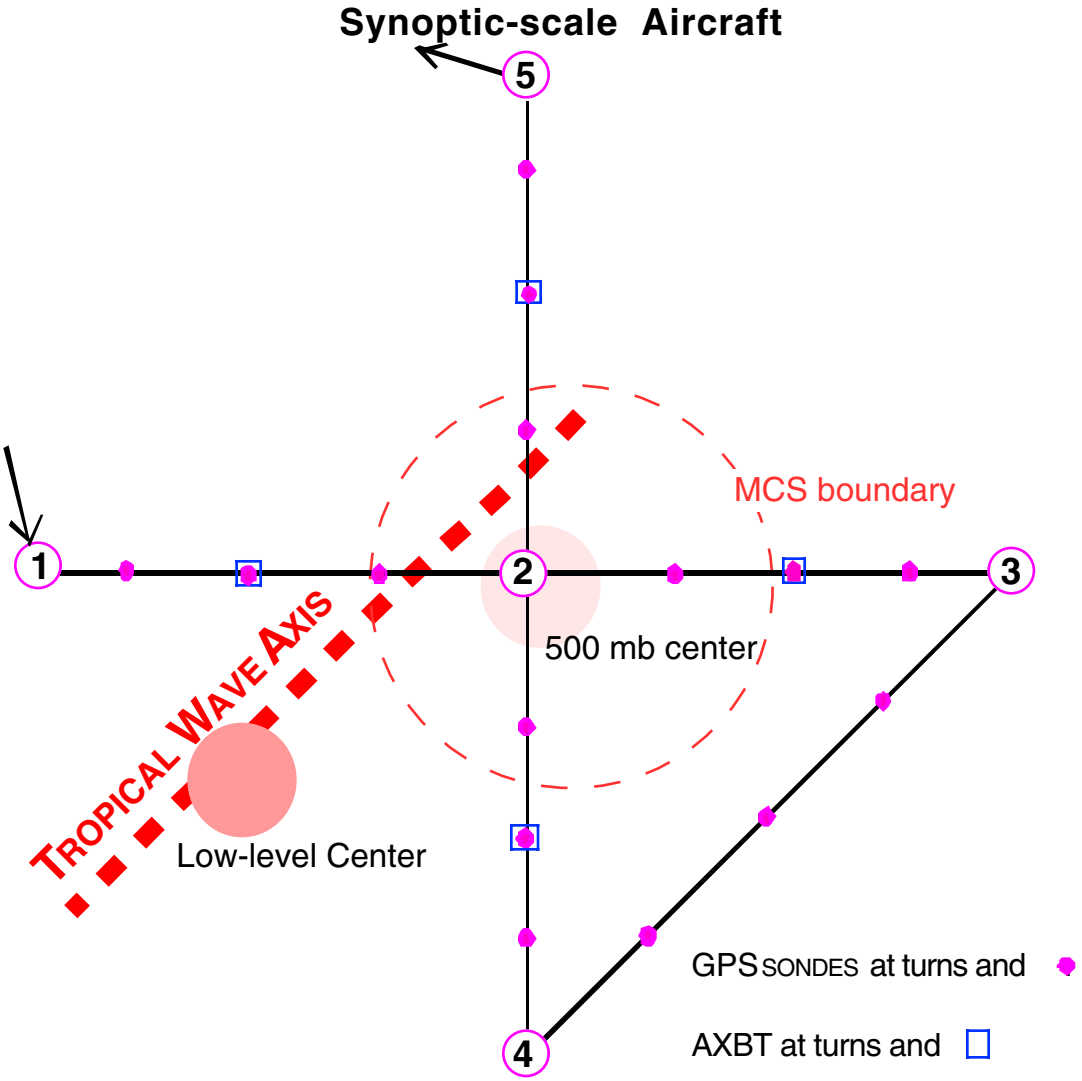

Fig. 7. Synoptic-scale Aircraft Flight Track

• Note 1.	True airspeed calibration is required.
• Note 2.	The pattern may be entered along any compass heading.
• Note 3.	Fly **1—2—3—4—2—5** at 18,000 ft (5.5 km or ~500 mb), 325–430 nmi (600-800 km) leg length, depending on ferry distance.
• Note 4.	Point 2 is near the moving apex of the trough axis.
• Note 5.	Set airborne Doppler radar to continuously scan perpendicular to the track on radial penetrations, and F/AST on downwind legs.

TROPICAL CYCLOGENESIS EXPERIMENT

Mesoscale Aircraft

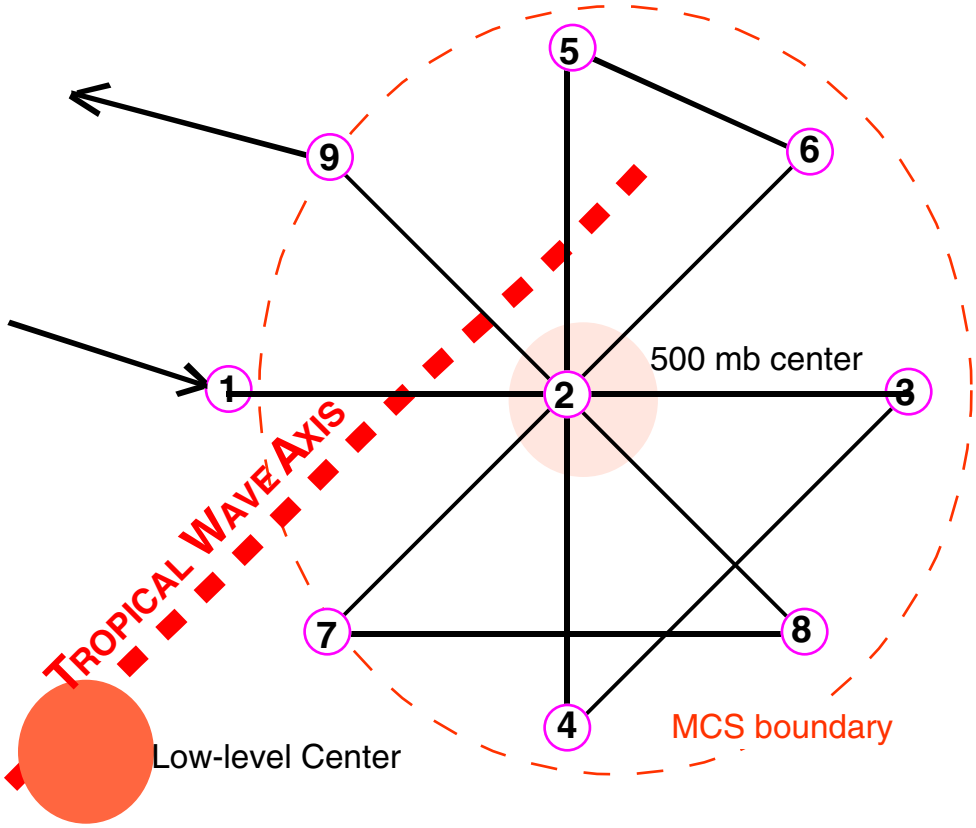

Fig. 8. Mesoscale Aircraft Flight Track

• Note 1.	True airspeed calibration is required.
• Note 2.	The pattern may be entered along any compass heading.
• Note 3.	Fly **1—2—3—4—2—5—6—2—7—8—2—9** at 600 or 700 mb (PA), 100–135 nmi (185-250 km) leg length.
• Note 4.	Point **2** is near the moving apex of the trough axis.
• Note 5.	Set airborne Doppler radar to continuously scan perpendicular to the track on radial penetrations, and F/AST on downwind legs.

TROPICAL CYCLOGENESIS EXPERIMENT

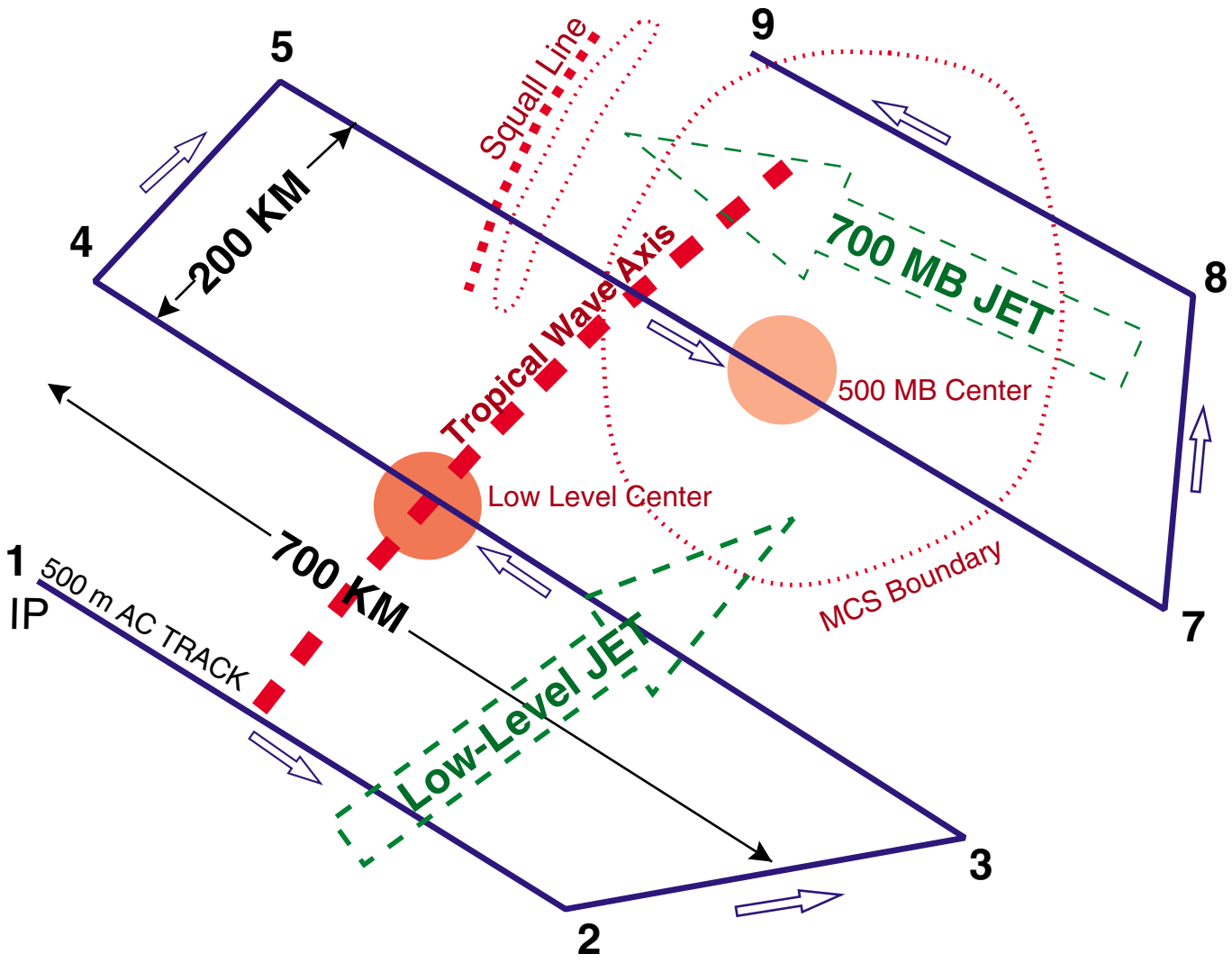

Fig. 9. Low-level Grid Flight Track

• Note 1.	True airspeed calibration is required.
• Note 2.	The pattern is flown with respect to the wave axis, typically inclined at 30°–40° from N, or relative to circulation or vorticity centers.
• Note 3.	Fly **1—2—3—4—5—6—7—8—9** at 1,000 ft (300 m) or 10,000 ft (3.0 km) altitude, passing through the low–level jet, low–level circulation center (if it exists), MCS and associated mid–level center, or across mid–level jet.
• Note 4.	Set airborne Doppler radar to F/AST on all legs.

TROPICAL CYCLOGENESIS EXPERIMENT

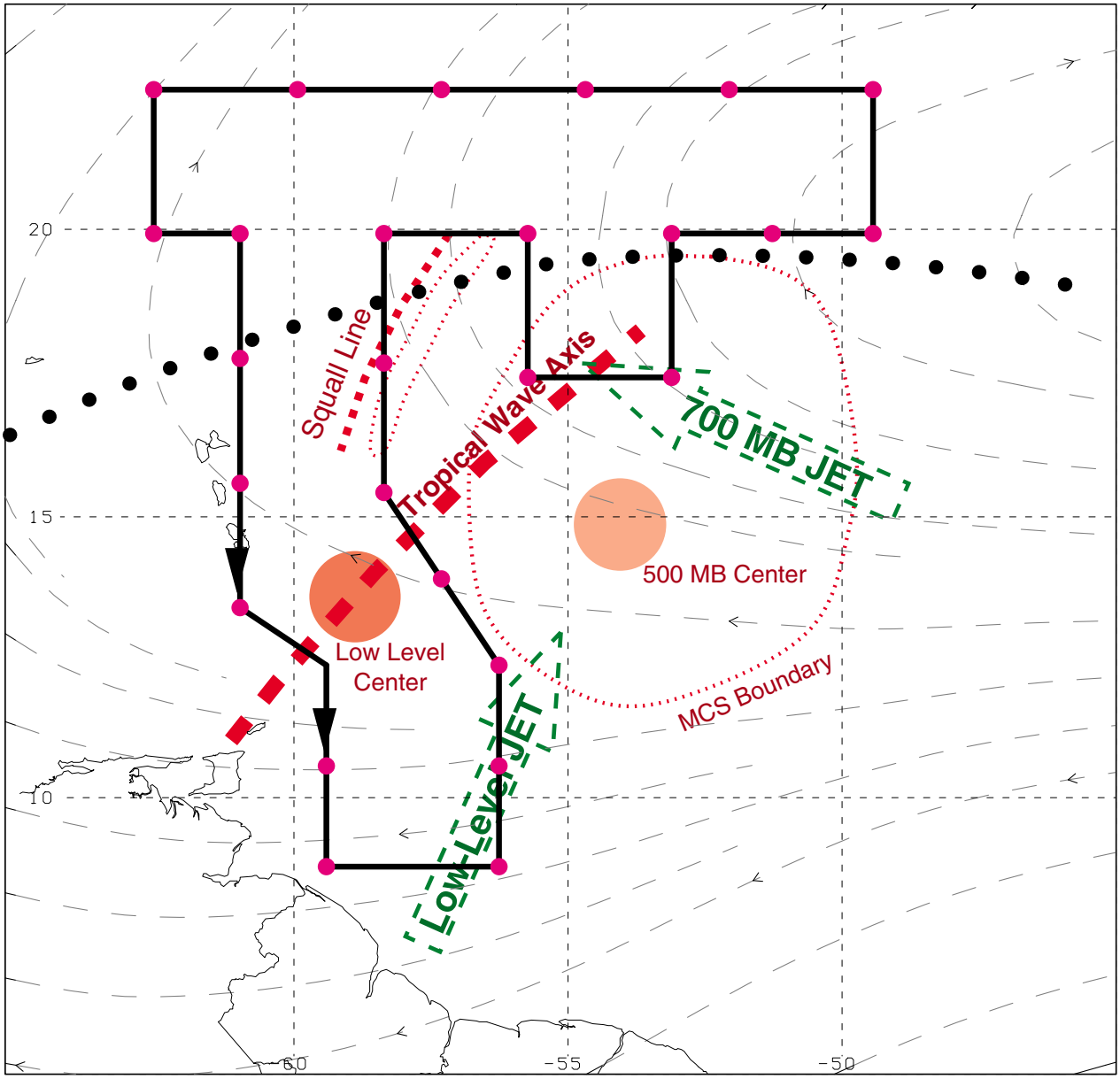

Fig. 10. (a) Cape Verde Region Sample G-IV Pattern

• Note 1.	During the ferry to the **IP**, The G-IV should climb to the 41,000 ft (200 mb) as soon as possible and climb as feasible to maintain the highest altitude for the duration of the pattern.

TROPICAL CYCLOGENESIS EXPERIMENT

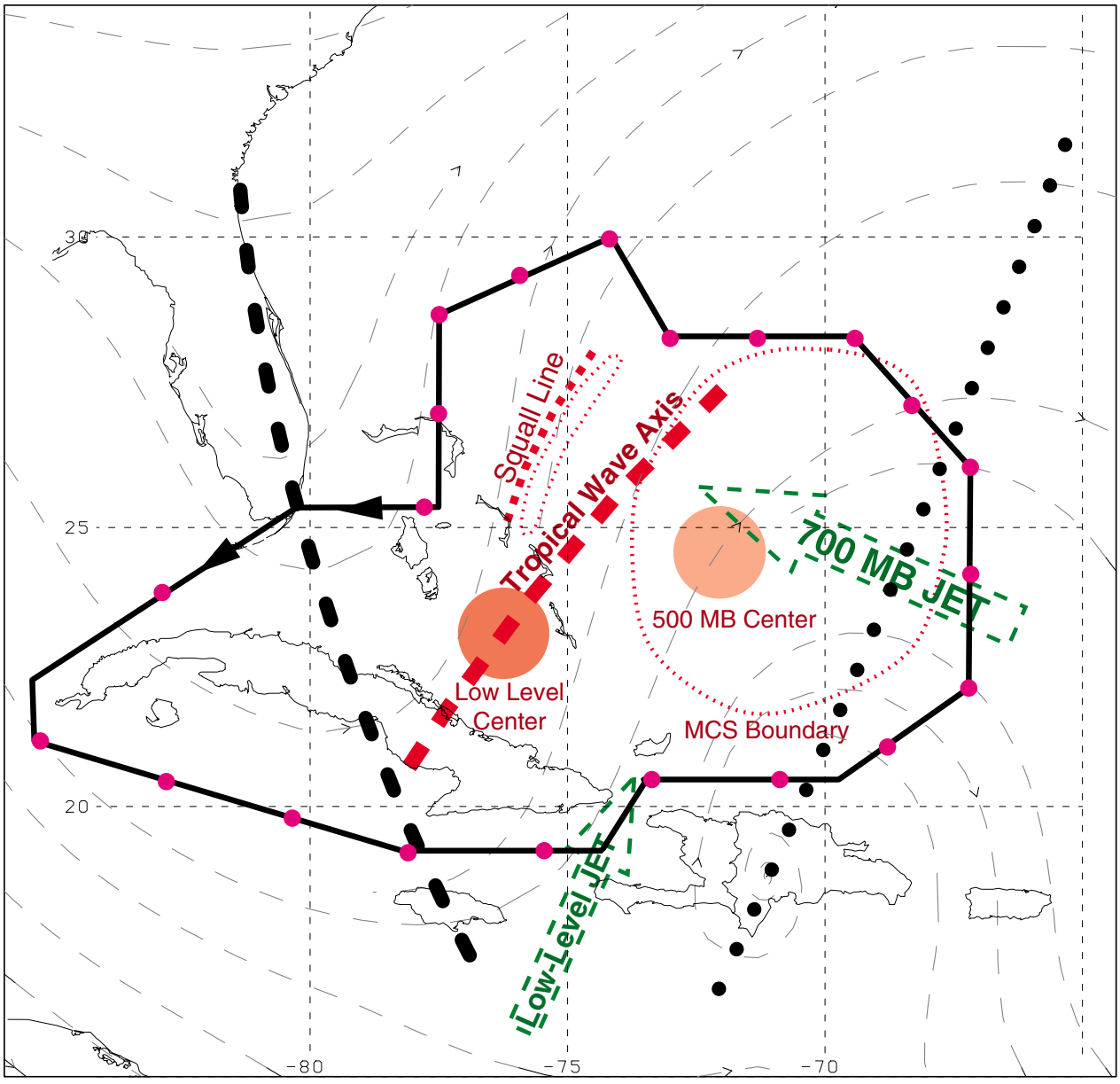

Fig. 10. (b) Bahamas Region Sample G-IV Pattern

• Note 1.	During the ferry to the **IP**, The G-IV should climb to the 41,000 ft (200 mb) as soon as possible and climb as feasible to maintain the highest altitude for the duration of the pattern.

13. Tropical Cyclone Wind Fields at Landfall Experiment

Program Significance: An accurate real-time description of the TC surface wind field near and after landfall is important for warning, preparedness, and recovery efforts. During a hurricane threat, an average of 300 nmi (550 km) of coastline is placed under a hurricane warning , which costs about $50 million in preparation per event. The size of the warned area depends on the extent of hurricane and tropical storm force winds at the surface, evacuation lead-times, and the forecast of the storm's track. Research has helped reduce uncertainties in the track and landfall forecasts, but now there is an opportunity to improve the accuracy of the surface wind fields in TCs, especially near landfall.

HRD is developing a real-time surface wind analysis system to aid the TPC/NHC in the preparation of warnings and advisories in TCs. The real-time system was first tested in Hurricane Emily of 1993, but the system needs further testing before use in operational forecasts and warnings. The surface wind analyses could reduce uncertainties in the size of hurricane warning areas and could be used for post-storm damage assessment by emergency management officials. The surface wind analyses will also be useful for validation and calibration of an operational inland wind forecast model that HRD is developing under Federal Emergency Management Agency (FEMA) sponsorship. The operational storm surge model (SLOSH) could be run in real-time with initial data from the surface wind analysis.

As a TC approaches the coast, surface marine wind observations are normally only available in real-time from National Data Buoy Center (NDBC) moored buoys, C-MAN platforms, and a few ships. Surface wind estimates must therefore be based primarily on aircraft measurements. Low-level (<5,000 ft (1.5 km] altitude) NOAA and Air Force Reserve aircraft flight-level winds are adjusted to estimate surface winds. These adjusted winds, along with C-SCAT and SFMR wind estimates, are combined with actual surface observations to produce surface wind analyses. Such analyses were done after Hurricane Hugo's landfall in South Carolina and Hurricane Andrew's landfall in South Florida, as well as in real-time for Hurricane Emily's (1993) closest approach to the Outer Banks of North Carolina, and for the landfalls of Hurricanes Erin and Opal in 1995, and Fran and Josephine in 1996.

The surface wind analyses may be improved by incorporating airborne Doppler radar-derived winds for the lowest level available (~3,000 ft [1.0 km]). To analyze the Doppler data in real-time, it is necessary to use a Fourier estimation technique. The Velocity-Track Display (VTD) was developed to estimate the mean tangential and radial circulation in a vortex from a single pass through the eye. The technique was applied to Doppler data collected in Hurricane Gloria (1985) and found that the mean winds corresponded well with winds derived by pseudo-dual Doppler (PDD) analysis. The extended VTD (EVTD) was subsequently developed to combine data from several passes through the storm, resolving the vortex circulation up through the wave # 1 component. EVTD was used on data collected during six passes into Hurricane Hugo (1989) to show the development of mean tangential winds >100 kt (50 m s^{-1}) over 7 h. EVTD analyses are computed quickly on the airborne HRD workstation and could be sent to TPC/NHC shortly after their computation. The wind estimates could then be incorporated into the real-time surface wind analyses.

Dual-Doppler analysis provides a more complete description of the wind field in the inner core. While these techniques are still too computationally intensive for real-time wind analysis, the data are quite useful for post-storm analysis. An observational study of Hurricane Norbert (1984), using a PDD analysis of airborne radar data to estimate the kinematic wind field in, found radial inflow at the front of the storm at low levels that switched to outflow at higher levels, indicative of the strong shear in the storm's environment. Another study used PDD data collected in Hurricane Hugo near landfall to compare the vertical variation of winds over water and land. The profiles showed that the strongest winds are often not measured directly by reconnaissance aircraft.

By 1989 both NOAA WP-3D aircraft were equipped with Doppler radars. A study of Eastern Pacific Hurricane Jimena (1991) utilizing several three-dimensional wind fields from true dual-Doppler data collected by two WP-3D's showed that a pulse of radial wind developed in the eyewall with a corresponding decrease in the tangential winds. By the fourth pass, however, the radial pulse was gone and the tangential winds had returned to their previous value. These results suggested that the maintenance of a mature storm may not be a steady-state process. Further study is necessary to understand the role of such oscillations in eyewall maintenance and evolution.

While collection of dual-Doppler radar data by aircraft alone requires two WP-3D aircraft flying in well-coordinated patterns, a time series of dual-Doppler data sets could be collected by flying a single WP-3D toward or away from a ground-based Doppler radar. In that pattern, the aircraft Doppler radar rays are approximately orthogonal to the ground-based Doppler radar rays (Fig. 11), yielding true Dual-Doppler coverage. Starting in 1997 the Atlantic and Gulf coasts were covered by a network of Doppler radars (WSR-88D) deployed by the National Weather Service (NWS), Department of Defense, and Federal Aviation Administration (Fig. 12). Each radar has a digital recorder to store the base data (Archive Level II). In precipitation or severe weather mode the radars will collect volume scans every 5-6 min.

TROPICAL CYCLONE WINDFIELDS NEAR LANDFALL EXPERIMENT

Ground-based/Airborne Doppler Scanning Strategy

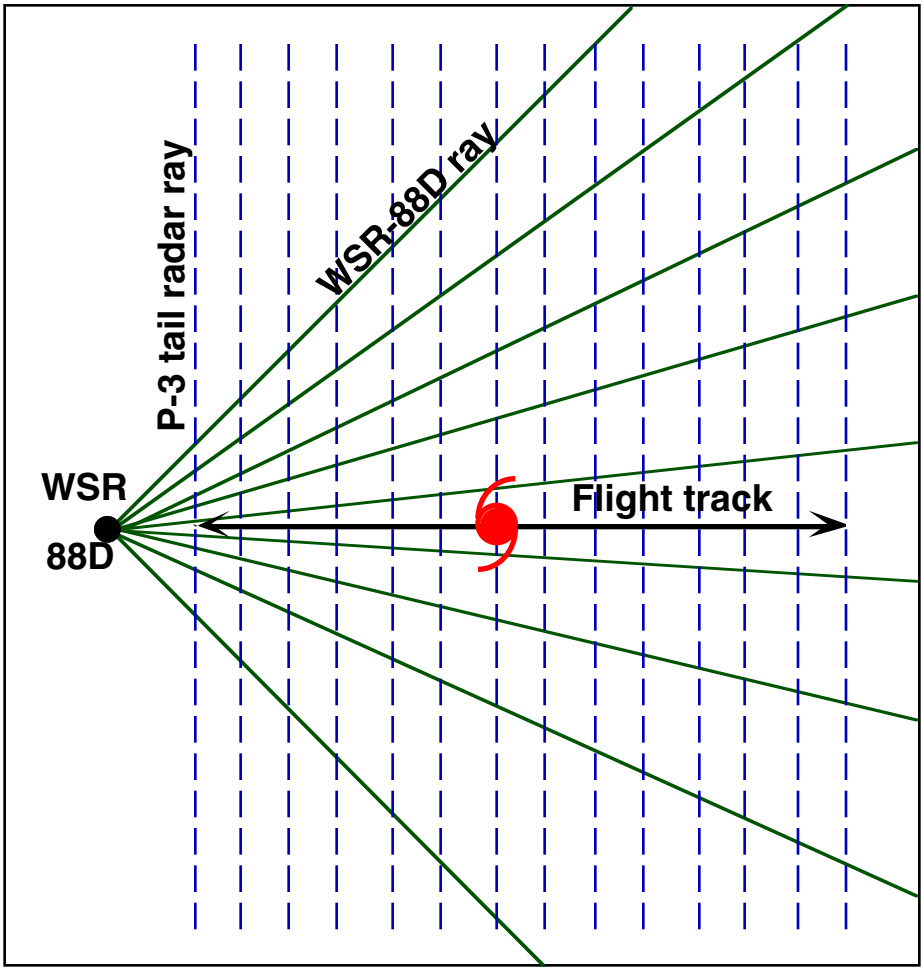

Fig. 11. Airborne Doppler Radar Flight Track

• Note 1.	The legs through the eye may be flown along any compass heading along a radial from the ground-based radar.
• Note 2.	Set airborne Doppler radar to scan continuously perpendicular to the track on all legs.

TROPICAL CYCLONE WINDFIELDS NEAR LANDFALL EXPERIMENT

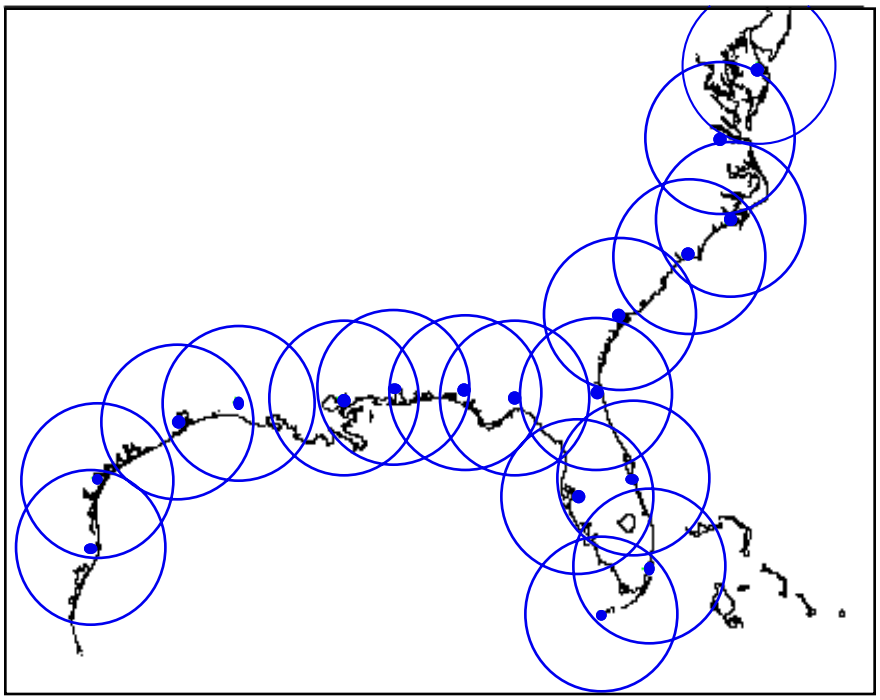

Fig. 12. The locations of the WSR–88D coastal radar sites. Range rings are at 125 nmi (230 km) radius.

If a hurricane or strong tropical storm (i.e., one with sufficient radar scatterers to define the vortex) moves within 125 nmi (230 km) (Doppler range) of a coastal WSR-88D Doppler radar, a WP-3D will obtain Doppler radar data to be combined with data from the WSR-88D radar in dual-Doppler analyses. These analyses could resolve phenomena with time scales <10 min, the time spanned by two WSR-88D volume scans. This time series of dual-Doppler analyses will be used to describe the storm's inner core wind field and its evolution. The flight pattern for this experiment is designed to obtain dual-Doppler analyses at intervals of 10-15 min in the inner core. Unfortunately, these WSR-88D/aircraft dual-Doppler analyses will not be available in real-time, but the Doppler wind fields could be incorporated into post-storm surface wind analyses. The data set will also be useful for development and testing of TC algorithms for the WSR-88D. The Doppler data will be augmented by dropping new GPS-sondes near the coast, where knowledge of the boundary-layer structure is crucial for determining what happens to the wind field as a strong storm moves inland. If conditions permit, GPS-sondes will also be dropped in the eyewall in different quadrants of the TC, to add to the climatology of vertical wind profiles.

To augment the inner core analyses, dual-Doppler data can be collected in the outer portions of the storm (where the aircraft's drift angle is small) from a single aircraft using F/AST. The tail radar is tilted to point 15° forward and aft from the track during successive sweeps. The alternating forward and aft scans intersect at 40°, sufficient for dual-Doppler synthesis of winds.

Several studies indicate that loss of the oceanic moisture source is responsible for the decay of land falling TCs. These studies relied on surface observations that are usually sparse at landfall and require time-to-space compositing techniques that assume stationarity over relatively long time periods. More complete observations could help improve our knowledge of intensity change during and after landfall. Our experience flying over the land in Hurricanes Fran over south eastern North Carolina, and Josephine over northern Florida, showed that, provided that safety requirements are met, the combination of WSR-88D observations with NOAA airborne Doppler radar and flight level measurements allow detailed documentation of the thermodynamic and kinematic structural changes to be made during landfall.

Objectives:

- Collect flight level wind data and make surface wind estimates to improve real-time and post-storm surface wind analyses in TCs.
- Collect single airborne Doppler radar data, analyze with EVTD, and send wind analyses in near real-time to TPC/NHC.
- Collect airborne Doppler radar to combine with WSR-88D radar data in post-storm three-dimensional wind analyses.
- Investigate the incorporation of EVTD wind fields into real-time surface wind analyses.
- Document thermodynamic and kinematic changes in the storm during and after landfall.
- Document changes in microphysics and rainfall characteristics in the storm during and after landfall.
- Obtain a remote sensing data base suitable for evaluation and improvement of satellite and ground validation rainfall estimation algorithms for landfalling TCs.

Mission Description: This experiment will be flown with a single aircraft if a TC moves within 215 nmi (400 km) of the coast of the United States. If the storm moves slowly parallel to the coastline and resources permit, the experiment may be repeated with a second flight. The aircraft must have working lower fuselage and tail radars. The HRD workstation should be on board, so we can transmit radar images and an EVTD analysis back to TPC/NHC. Microphysical data should be collected, to compare rainfall rates with those used in the WSR-88D precipitation products. The SFMR should be operated, to provide estimates of wind speed at the surface. If the C-SCAT is on the aircraft then it should also be operated to provide another estimate of the surface winds. If the storm will be within 125 nmi (230 km) of a WSR-88D, arrangements must be made to ensure that Level II data are recorded.

If the portable Doppler radars (Doppler on Wheels—DOW) and/or portable profilers are able to participate in the experiment then they should be deployed to the region forecast to be outside of the eyewall, in the onshore flow regime. If possible the DOW should be positioned relative to the nearest WSR-88D such that the dual-Doppler lobes cover the largest area of onshore flow possible. In the examples shown below the DOW is positioned north of the Melbourne WSR-88D so that one dual-Doppler lobe is over the coastal waters and the other covers a region ~50-100 km inland. The profiler is positioned in the inland dual-Doppler lobe to provide independent observations of the boundary layer to anchor the dual-Doppler analysis.

The primary module of the experiment, the "real-time module", will support real-time and post-storm surface wind analyses. Two dual-Doppler options can be flown if the storm is near a WSR-88D radar. A coastal-survey option can be flown when the storm is too close to the coast to permit radial penetrations. The flight patterns will depend on the location of the storm relative to surface observing platforms and coastal radars.

Real-time module: The real-time module combines passes over marine surface platforms with one or more figure four patterns in the core of the TC. The aircraft flies at or below 5,000 ft (1.5 km) (possibly at 2,500 ft [750 m]), so that flight level winds can be adjusted to 30 ft (10 m) to combine with measurements from marine surface platforms. Flight-level data and GPS-sondes dropped near the platforms will be used to validate the adjustment method. Doppler data collected in the figure four will be analyzed with EVTD in real-time on the HRD workstation. The lowest level of the EVTD analysis may be sent to TPC/NHC where the Doppler winds can also be adjusted to the surface and made available to HRD's real-time surface wind analysis system. Note that if the storm is outside of WSR-88D Doppler range then the figure four pattern could be repeated before returning home.

For example, if a TC moves within range of a WSR-88D, then the flight pattern should take advantage of buoys or C-MAN sites nearby. The aircraft descends at the initial point and begins a low-level figure-4 pattern, modifying the legs to fly over the buoys (Fig. 13). Whenever the drift angle permits the radar will be in F/AST mode, except in the eye penetrations. If time permits the aircraft would make one more pass through the eye and then fly the dual-Doppler module. In this example the pattern would be completed in about 2.5 h. GPS-sondes would be dropped near the buoys or C-MAN sites.

If the timing is such that the storm is farther off the coast than desired for landfall, then the aircraft can execute the Rainband Thermodynamic Structure Module (Fig. 28) to map the thermodynamic structure of the in-flow. The flight pattern should overfly any buoy or C-MAN sites and if possible, include legs coordinated with a WSR-88D.

Dual-Doppler Option 1: If the TC moves within Doppler range of a coastal WSR-88D 125 nmi (230 km), then we will fly a second module, to collect a time-series of dual-Doppler data from the storm's inner core. Note that the optimal volume scans for this pattern will be obtained when the storm is 32-80 nmi (60-150 km) from the radar, because beyond 80 nmi (150 km) the lowest WSR-88D scan will be above 5,000 ft (1.5 km) which is too high to resolve the low-level wind field. Within 32 nmi (60 km) the volume scan will be incomplete, because the WSR-88D does not scan above 19.5°.

The pattern will depend on the location of the storm relative to the coastal radar. Depending on safety and operational considerations, the aircraft could fly this portion of the experiment at a higher altitude, although 5,000 ft (1.5 km) would still be preferred. After completing the real-time module the aircraft flies to an initial point on the track intersecting the storm center and the coastal radar (Fig. 13). The aircraft then makes several passes through the eyewall (**A-B** in Fig. 13), with the tail radar scanning perpendicularly to the track. Depending on the size of the eyewall each pass should last 10-15 min. It is essential that these passes be flown as straight as possible, because turns to fix the eye will degrade the Doppler radar coverage. After each pass the aircraft turns quickly and heads back along the same track, adjusted to keep the storm center and the coastal radar on the same line. In 2 h, 6-12 volume scans will be collected. The last pass should be followed by a pass through the eye perpendicular to the other legs, to provide data for EVTD and pseudo-dual Doppler analyses. If time permits, the real-time module could be repeated before returning home, or the coastal-survey module could be flown.

Dual-Doppler Option 2: If dual-Doppler data are desired over a larger area, then another module will be flown where the aircraft flies along three WSR-88D radials to survey both the inner core and surrounding rainbands (Fig. 14). In the example shown, this pattern could be flown in about 2 h. Note that the legs outside the inner core should be flown with the tail radar in F/AST mode because the drift angle would be smaller. In the example the module concludes with a coastal-survey pass south along the coast.

Coastal Survey option: When the TC is making landfall, this module will provide information about the boundary layer in the onshore and offshore flow regimes. The WP-3D would fly a coastal survey pattern parallel to the coast, as close as safety permits, at 5,000 ft (1.5 km) or less, and drop GPS-sondes on either side of the storm track, to sample both onshore and offshore flow regimes (Fig. 15). The Doppler radar would be in F/AST mode, to provide wind estimates on either side of the aircraft track. This module could be flown when the TC is making landfall or after the storm moves inland. The pattern could be flown in ~1 h. GPS-sonde drops could be adjusted to be near surface platforms.

Post-landfall option: If the structure of the storm is such that flight patterns with the WP-3D at 10,000 or 15,000 ft (3.0 or 4.5 km) are feasible over land, the pattern shown in Figs. 15 would be flown. The storm can be followed inland as long as time and safety considerations permit. If possible the WP-3D should fly legs along WSR-88D radials with the tail Doppler radar in F/AST scanning mode.

TROPICAL CYCLONE WINDFIELDS NEAR LANDFALL EXPERIMENT

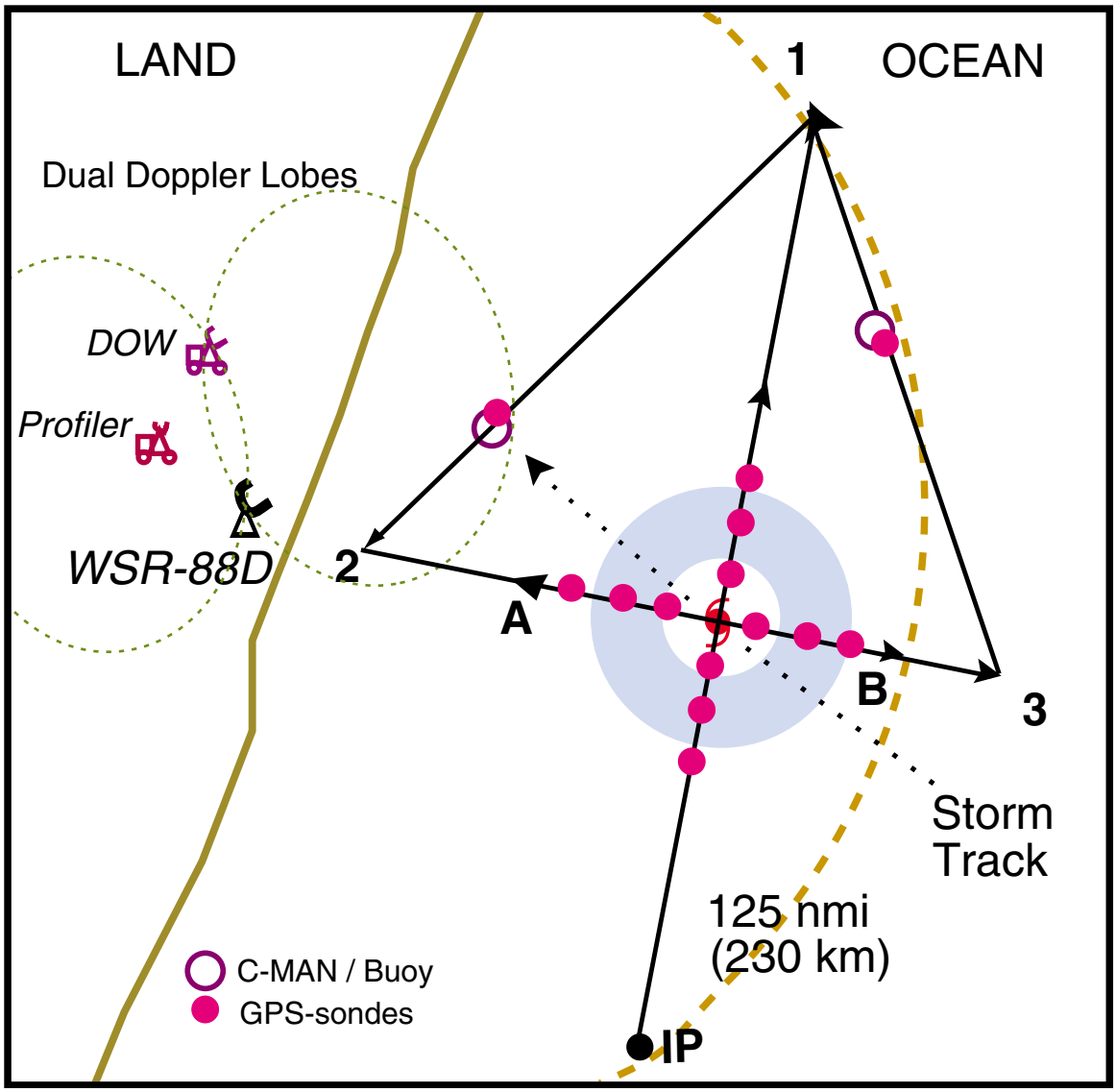

Fig. 13. Flight track for the real-time module with over flights of moored buoys for a storm passing within range of a coastal WSR-88D.

• Note 1.	True airspeed calibration required.
• Note 2.	The legs through the eye may be flown along any compass heading along a radial from the ground-based radar. The **IP** is approximately 100 nmi (185 km) from the storm center. Downwind legs may be adjusted to pass over buoys.
• Note 3.	Dual-Doppler sampling is along a radial from the WSR-88D radar (**A-B**) and may be repeated a number of times.
• Note 4.	Set airborne Doppler radar to scan continuously perpendicular to the track on radial penetrations, and to F/AST on all downwind legs.

TROPICAL CYCLONE WINDFIELDS NEAR LANDFALL EXPERIMENT

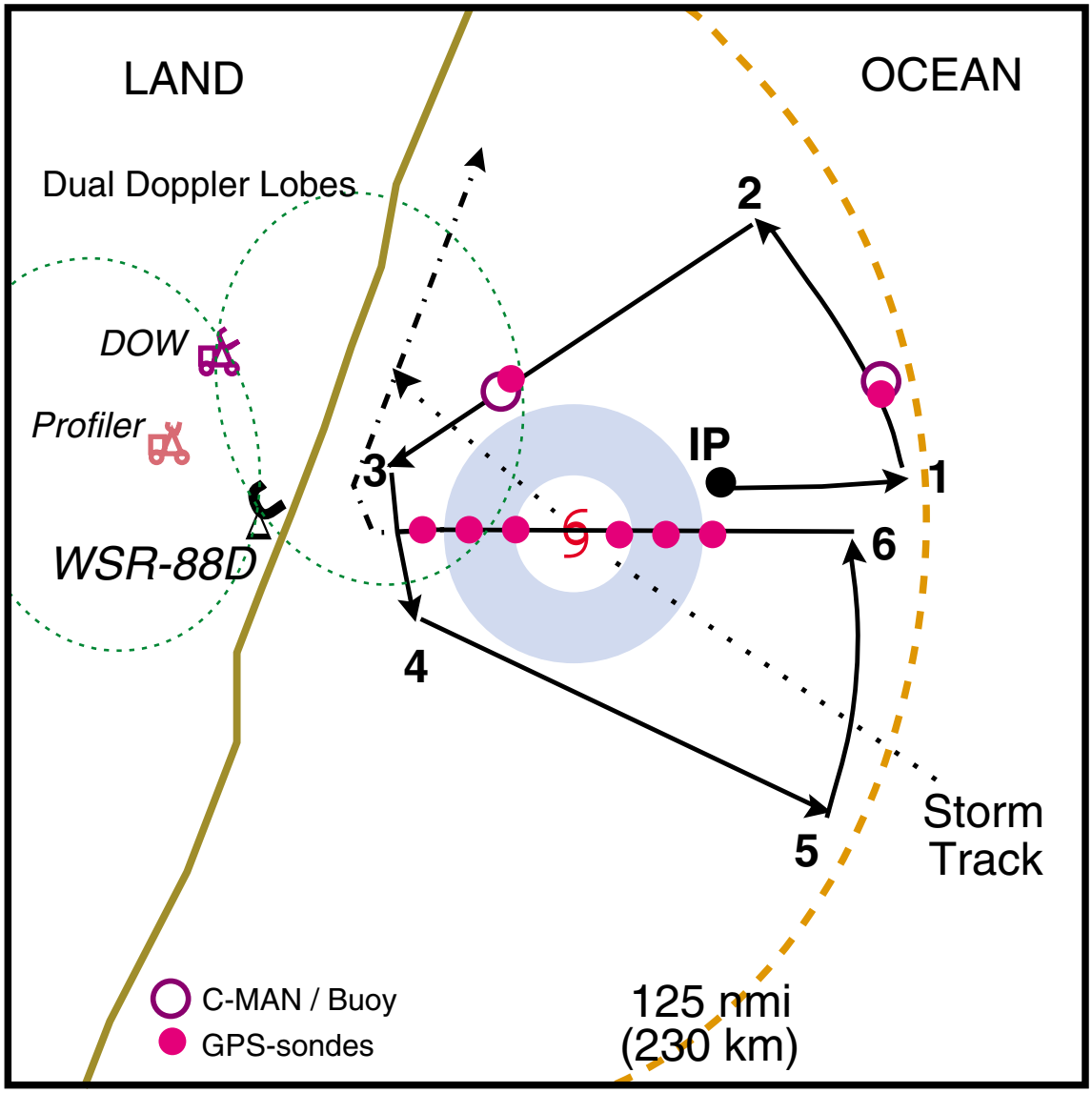

Fig. 14. Flight track for the dual-Doppler option that covers the inner core and surrounding rainbands.

• Note 1.	True airspeed calibration required.
• Note 2.	The legs through the eye may be flown along any compass heading along a radial from the ground-based radar. The **IP** is at the end of the last leg in the real-time module. Downwind legs may be adjusted to pass over buoys.
• Note 3.	Dual-Doppler sampling is along a radial from the WSR-88D radar (**A-B**) and may be repeated a number of times.
• Note 4.	Set airborne Doppler radar to scan F/AST on all legs except from **IP-1**.

TROPICAL CYCLONE WINDFIELDS NEAR LANDFALL EXPERIMENT

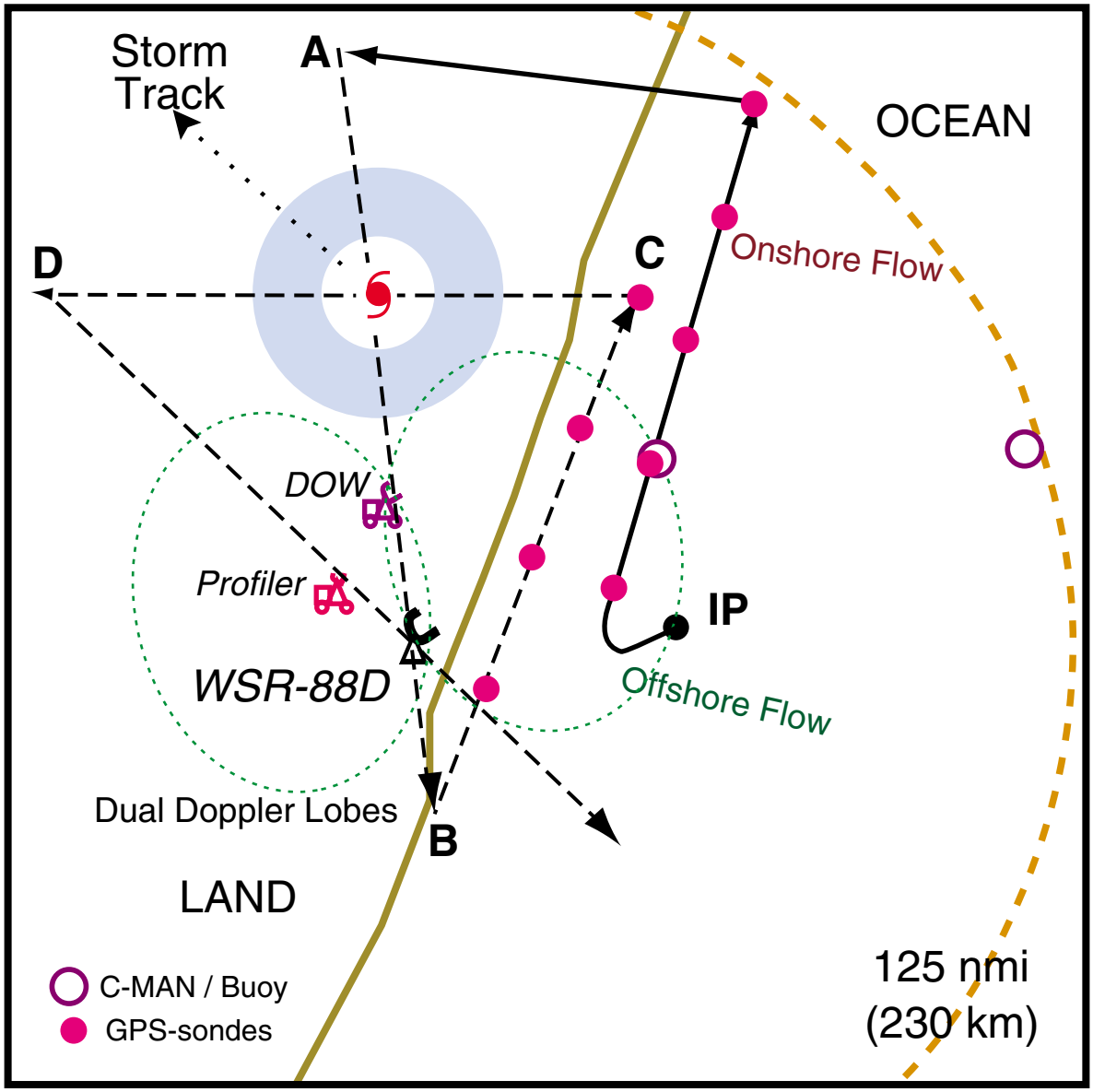

Fig. 15. Flight track for the real-time module with over flights of moored buoys and GPS-sonde drops for a storm after landfall.

• Note 1.	Begin pattern after execution of the coastal survey option. Execute figure-4 or triangle pattern on circulation center with ~60 nmi (110 km) legs at 14,000 ft (4 km) altitude (dashed line).
• Note 2.	GPS-sondes should be dropped at least 10 nmi (18 km) offshore in the onshore flow regime, and as close as possible to the coast in the offshore flow regime.
• Note 3.	Avoid penetration of intense reflectivity or reflectivity gradient areas. Wind center penetrations are optional.
• Note 4.	If possible the legs of the pattern should be lined up on WSR-88D radials. Set airborne Doppler radar to F/AST scanning on all legs.

14. Tropical Cyclone Air-Sea Interaction Experiment

Program Significance: This experiment examines the relationship between TC intensity change and changes in the underlying sea surface temperature (SST) through two types of interactions with the underlying sea surface: (1) Changes in SST due to translation of the storm over pre-existing ocean features; and (2) Changes in SST induced by the TC itself. In the case of (1), three types of features will be examined: (a) permanent, such as the Gulf Stream and Gulf Loop Current, (b) semi-permanent, such as Gulf of Mexico Warm Eddies (GOMWEs) and (c) transitory, such as cold wakes from previous TC's. Underlying SST and Mixed Layer Depth (MLD) changes for the above conditions result in changes of surface maximum wind, surfaced wind field structure, distribution of eyewall and rainband convective activity, rainfall, minimum surface pressure, and thermodynamic structure of the inflow layers. The extent to which these changes can be separated from other external environmental forcing factors, such as mid-latitude troughs and sub-tropical jet streams is the subject of this experiment. While a viable experiment in its own right, this experiment is best run in concert with other single-aircraft experiments such as the XCDX experiment and a G-IV synoptic surveillance mission. The combination of these three experiments are a key ingredient in assessing the importance of internal storm dynamics and environmental interactions on storm intensity change concurrent with air-sea interaction measurements.

It is an important national priority to improve the forecasts of surface wind field intensity, structure and storm surge in landfalling TCs in order to successfully mitigate the problems associated with these storms. The Hurricanes at Landfall (HaL) program was created to improve the analyses and forecasts of the pattern, extent and intensity of damaging winds associated with landfalling TCs in order to bring about a reduction in the current overwarning percentage and an increase in the damage mitigation.

A major source of difficulty in past efforts to predict TC intensity, wind fields and storm surge near landfall has been the inability to measure the surface wind field directly and the inability to predict how it changes in response to external and internal forcing. The surface wind field is parameterized by the magnitude and radius of maximum winds and by the hurricane force, storm force and gale force wind radii (32, 26 and 18m s^{-1} respectively) for each quadrant of the TC. These values must presently be estimated from a synthesis of scattered surface ship and/or buoy observations and aircraft measurements at 5,000-10,000 ft (1.5-3.0 km) altitude. This task is complicated by variations with height of the storms' structure, such as the change with height of storm-relative flow due to environmental wind shear and to the variable outward tilt of the wind maximum with height.

Direct linkages between TC intensity change and observed air-sea changes have been difficult to make since many storms are also exposed to tropospheric environmental influences. In addition, detailed oceanographic and surrounding environmental observations in the atmosphere have been generally lacking from which to make comparisons. Thus, it is a primary goal of this study to establish the link, statistically and physically, between changes in air-sea interaction processes brought about by changes in oceanic features and changes in the TC surface wind field.

To partially overcome these past difficulties, we propose a mobile observing strategy comprised of a mix of in-situ air-deployed surface and subsurface sensors, and airborne remote sensors allowing the surface wind field to be directly measured. We postulate that knowing the surface wind field at landfall is the most important component of HaL for improving, not only wind warnings, but storm surge estimates, including surface wave run-up, and estimates of the rate of inland wind field decay. We further postulate that to improve these estimates we must know, not only the wind field itself, but the tendency in the wind field, that is, whether it is strengthening or weakening, broadening or shrinking. It has been generally agreed that changes in the wind field will be brought about by (1) changes in the large-scale environmental conditions, (2) changes in the underlying boundary and (3) naturally-evolving internal dynamics.

Several dramatic cases suggesting a strong role of air-sea interaction processes on TC intensity changes have occurred in recent years, many of which have been landfalling situations, where intensity change forecasting is especially crucial. Hurricane Andrew (1992) gained strength as it passed over the Gulf Stream just before landfall on South Florida. Hurricane Opal (1995) rapidly intensified as it moved over a warm eddy in the Gulf of Mexico, then rapidly weakened as it moved over the colder shelf water. In over half of the 32 storms that occurred during the 1995 and 1996 hurricane seasons, significant intensity changes were associated with storm translation over SST boundaries, which were either pre-existing or

created by previous storms. Many of these storms also experienced interactions with mid-latitude troughs during the same time period, which has made it difficult to partition the physical processes responsible for the observed intensity changes. The goal of the present study is to establish the link, statistically and physically, between changes in air-sea interaction processes and observed intensity changes.

Objectives: The specific goal of this experiment is to improve the analysis and forecasting of the surface wind field and oceanic response, including storm surge, in landfalling TCs by understanding relevant air-sea interaction processes. In order to achieve this goal, we must:

1) Determine the relationship between changes in the TC surface wind field and changes in the offshore upper ocean structure along its path for time periods before, during and after TC passage over oceanic features near landfall.

2) Determine the relationship between changes in the TC surface wind field and changes in air-sea fluxes.

3) Determine the interaction between the wind field, waves, currents and water-level in generating storm surge at landfall.

4) Incorporate air-sea fluxes, influences of upper oceanic circulations, and interactions between the wind field, waves and storm surge into model initialization, verification and parameterization to improve the TC coastal wind forecasts.

Initial expectations over the next few years are:

- A real-time surface wind remote sensing algorithm and wind field analysis package.

- A statistical relationship between storm intensity change and lower tropospheric/upper ocean variables.

- An improved understanding of the oceanic mixed layer response to TC forcing in the presence of variable background features.

- Determine the extent to which Atmospheric Boundary layer (ABL) maintenance is controlled by SST distribution, mesoscale and convective-scale downdrafts, rainfall evaporation, and between-band subsidence.

- A more accurate representation of air-sea fluxes in the TC ABL.

- Improvements in our understanding of TC generated waves and currents in the deep ocean, over the shelf, and in the near shore region. This information in addition to the better depiction of the wind field can improve the model inputs for storm surge modeling and forecast efforts.

- Improvements of existing ABL parameterizations in numerical TC models that are being developed for forecast applications.

The achievement of these goals is important to NOAA's mission to improve TC forecasts and warnings on both the short and long-term time scales. In the short-term, this investigation seeks to provide real-time measurements of winds at the surface and at typical aircraft flight-levels. In the long term, improved understanding of the behavior of the TC ABL over the ocean and near landfall will lead to improvements in dynamical model predictions and to improved initial data for storm surge models.

Mission Description. While a viable experiment in its own right, this experiment is best run in concert with a G-IV synoptic surveillance mission, and as one of a series of XCDX missions. The combination of these three experiments are a key ingredient in determining what portion of the observed intensity change is a result of internal storm dynamics, large scale environmental forcing, and oceanic forcing. This experiment seeks to measure the surface wind field structure concurrently with the oceanic feature structure using NOAA WP-3D aircraft flights within the TC during four time periods:

1) **Early-Season**: *(1-4 weeks before landfall; one aircraft, two flights)*
One WP-3D aircraft with AXBT/AXCP/AXCTD launching capability is required to map the upper ocean boundary layer structure in a (pre-determined) ocean feature. The flight pattern outlined in Fig. 15a for a symmetric ocean feature such as the GOMWE is designed to accurately measure the ocean feature's undisturbed structure. The pattern is designed to be flown with the initial leg parallel to a TOPEX/POSEIDON satellite altimeter ground track (±32° inclination, from true north, depending on ascending or descending orbits). The expendable probes will be deployed on two single aircraft flights separated by one day with AXBTs being deployed on the first day for the purpose of fine tuning eddy location and regions of maximum subsurface isotherm gradients. AXCPs and AXCTDs will be deployed on the second day. This segment could be conducted as much as one month prior to the arrival of the TC.

2) **Pre-Storm**: *(36-48h before landfall; one aircraft, one flight)*
During the Pre-landfall portion of this experiment one WP-3D aircraft with AXBT/AXCP/AXCTD launching capability is required to map the upper ocean boundary layer structure in a (pre-determined) ocean feature 36-48 h prior to landfall or ~36 h before TC/ocean feature interaction occurs. The Pre-landfall flight patterns outlined in Figs. 15a and 15b (for either symmetric or asymmetric ocean features) are designed to accurately measure the ocean feature's undisturbed structure just prior to the storm. As with the pre-storm case, the pattern is designed to be flown with the initial leg parallel to a TOPEX/POSEIDON satellite altimeter ground track (±32° inclination from true north).Another single aircraft experiment, such as XCDX, is to be conducted at the same time as, or immediately following, the Pre-landfall flight segment to accurately measure internal storm structure prior to TC/ocean feature interaction. This flight should be coordinated with a G-IV synoptic surveillance mission in the environment surrounding the TC.

3) **Near-Storm:** *(12-36 h before landfall; two aircraft, two flights)*
During the near-landfall phase two WP-3D aircraft with AXBT/AXCP/AXCTD launch capabilities is required. The flight plan ,outlined in Fig. 16, commences as the TC begins to interact with either the symmetric or asymmetric ocean feature. This pattern is to be flown by both WP-3Ds, one following the other by 9-12 nmi (15-20 km), and displaced to the upwind side by about 4-9 nmi (7-15 km). The following aircraft will fly at low level, either 2,500 or 5,000 ft (800 m or 1500 m), depending on storm intensity. This aircraft will be equipped with AXCP and AXCTD receiver equipment, the SRA and the NOAA SFMR. The AXCPs and AXCTDs need to be deployed at IAS <200 kt. The lead aircraft will fly at 12,000 ft (3.5 km) and be the primary GPS-sonde- and AXBT-launching aircraft, and will be equipped with the backup AXCP receiver, UMASS C-SCAT/K-SCAT and UMASS SFMR. The downwind displacement and lag time of the following aircraft should be adjusted so that GPS-sondes reach the surface approximately beneath the following aircraft position and flight track.

   As in the Pre-landfall mission, the Near-landfall mission should also be coordinated with a G-IV synoptic surveillance mission in order to determine environmental influences on the TC.

4) **Post-Storm**: *(24 h after landfall; one aircraft)*
The final phase of this experiment requires a single aircraft with AXBT/AXCP/AXCTD launch capabilities. This flight, which is to occur ~ 24 h after TC landfall, is designed to survey the ocean feature's 'post storm' structure. The post-landfall flight plan is identical to the pre-landfall flight patterns illustrated in Figs. 15a and 15b.

The Pre-landfall period defines the initial conditions for model predictions, while the Near- and Post-landfall periods are used for model validation.

Operational reconnaissance flight-level data from AFRES WC-130 aircraft are used throughout the Pre- and Near-landfall periods to assess the role of internal dynamics in modifying TC wind fields. At least three drifting buoy platforms should be deployed by AFRES WC-130 aircraft prior to, or at the beginning of, either the Pre-landfall mission or the Near-landfall mission, depending upon feature location relative to the coast.

To conduct these experiments, the WP-3D should have working lower fuselage and tail Doppler radars, SFMR, C-SCAT/K-SCAT, GPS-sonde system, AXBT/AXCP/AXCTD instrumentation, Scanning Radar Altimeter (SRA), nose, vertical, and side-looking video cameras are required. Sufficient GPS-sondes, AXBTs, AXCPs and AXCTDs must be carried to perform the drops noted in each option. The

availability of an airborne Doppler radar on both WP-3D aircraft and the addition of the SFMR and C-SCAT/K-SCAT is required for high-resolution measurements of surface wind speed and rain rate. The GPS-sondes, AXBTs, AXCPs, AXCTDs and the radome-mounted gust probe (with Lyman-α and Rosemount temperature sensors) insure that valuable supporting data on air-sea stability and turbulent fluxes are obtained. The SRA measures directional wave spectra and mean surface elevation for input to flux parameterizations and storm surge models.

TROPICAL CYCLONE AIR-SEA INTERACTION EXPERIMENT

Early-Season and Pre-Storm Symmetric Ocean Feature Module

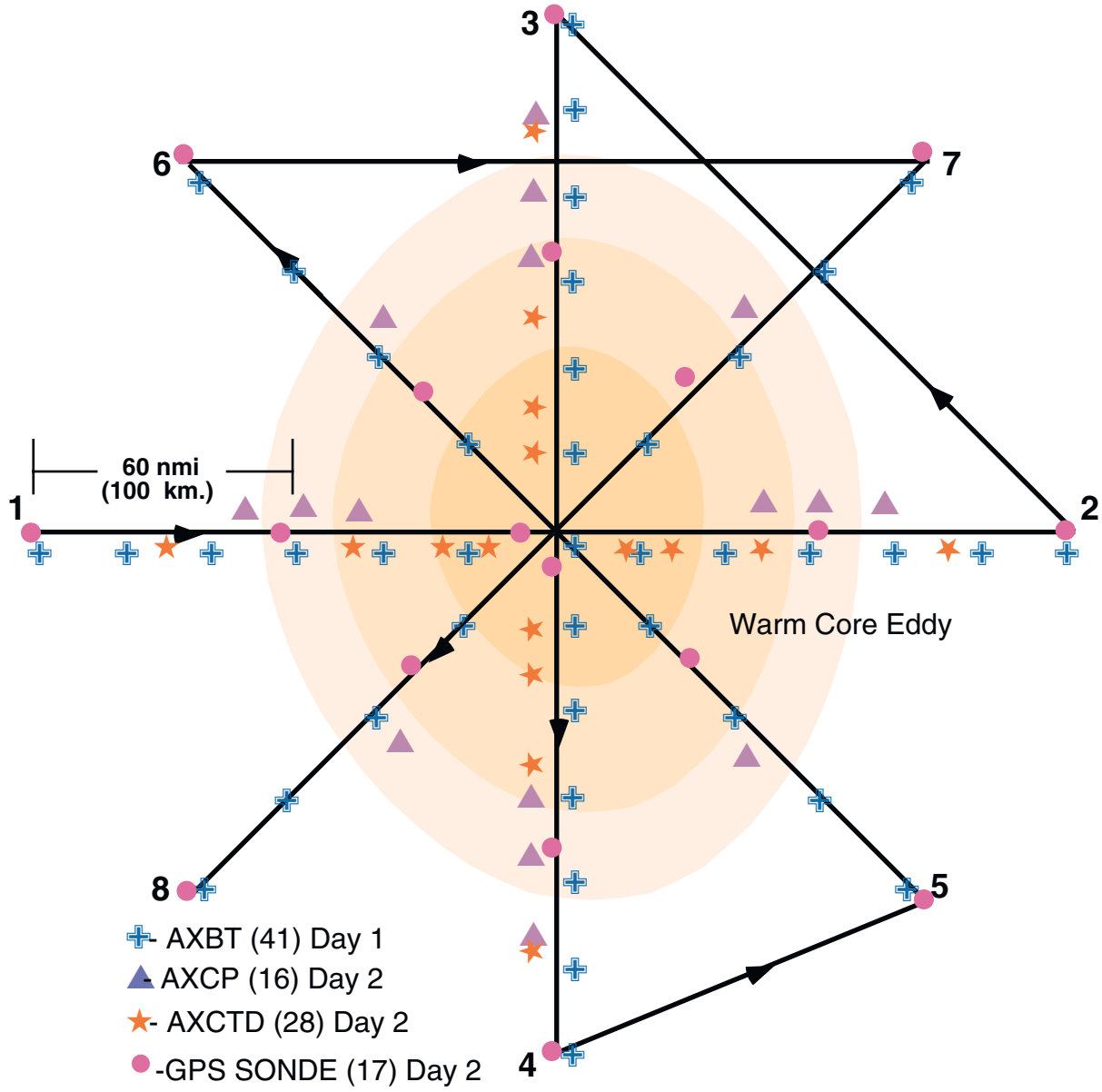

Fig. 15. (a) Sample pattern

• Note 1.	A/C Flies **1-2-3-4-5-6-7-8** at 5,000 ft (1,500 m). Each leg is 120 nm (200 km) radius from the center of the eddy.
• Note 2.	On Day 1 of Early-Season pattern. A/C drops AXBTs to define ocean feature boundaries. On Day 2 of Early-Season or Pre-Storm patterns A/C maps ocean feature circulation and ABL with AXCPs, AXCTDs, and GPS sondes.
• Note 3.	Display specific humidity and θ_e on 1-s display and 10-s listing.
• Note 4.	Set airborne Doppler radar to scan in F/AST on all legs.

TROPICAL CYCLONE AIR-SEA INTERACTION EXPERIMENT

Pre-Storm Asymmetric Ocean Feature Module

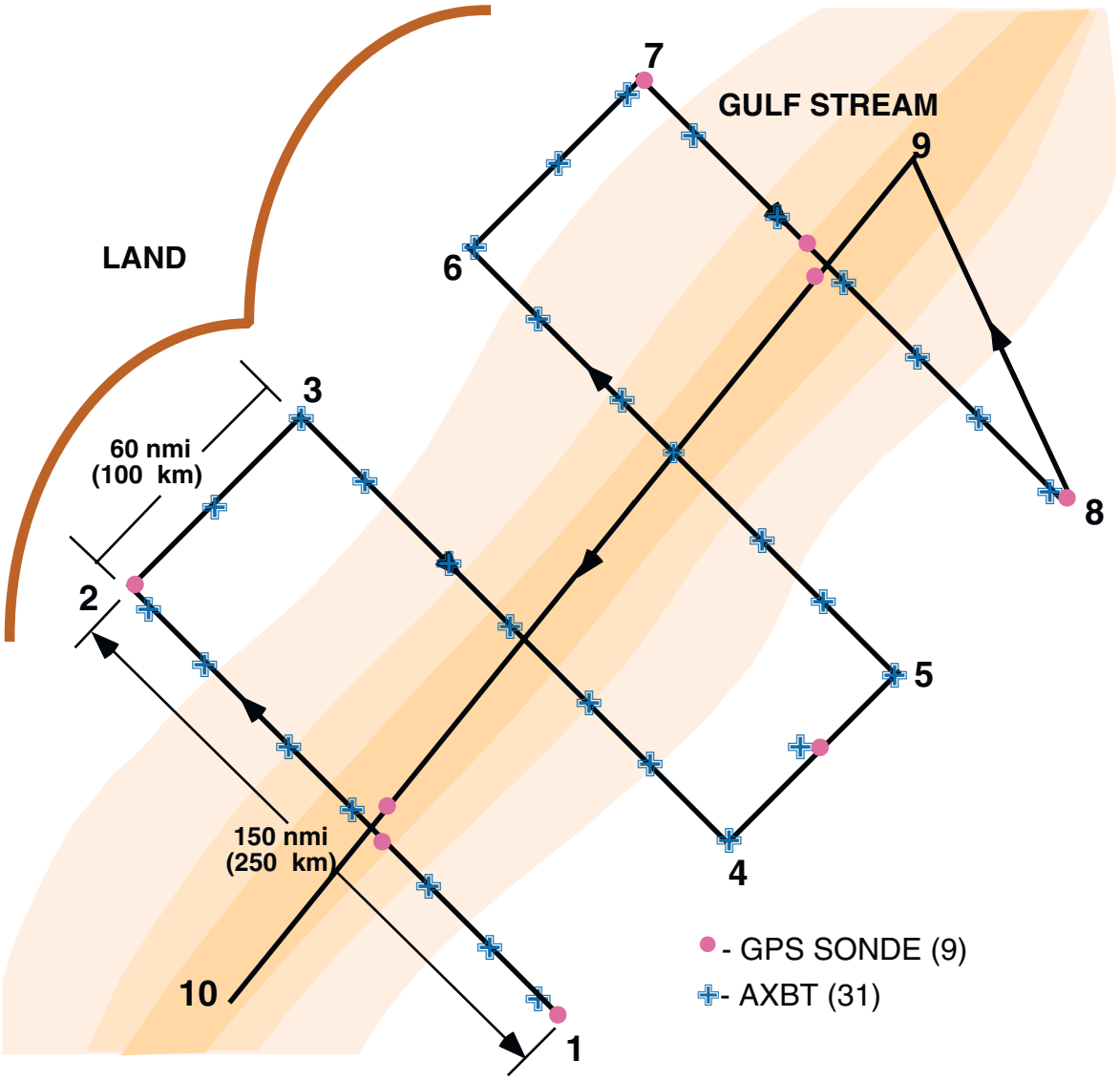

Fig. 15. (b) Sample pattern

• Note 1.	A/C Flies **1-2-3-4-5-6-7-8-9-10** at 5,000 ft (1,500 m).
• Note 2.	Display specific humidity and θ_e on 1-s display and 10-s listing.
• Note 3.	Set airborne Doppler radar to continuously scan perpendicular to the track on all radial penetrations, and F/AST on downwind legs.

TROPICAL CYCLONE AIR-SEA INTERACTION EXPERIMENT

Near-Storm Survey Module

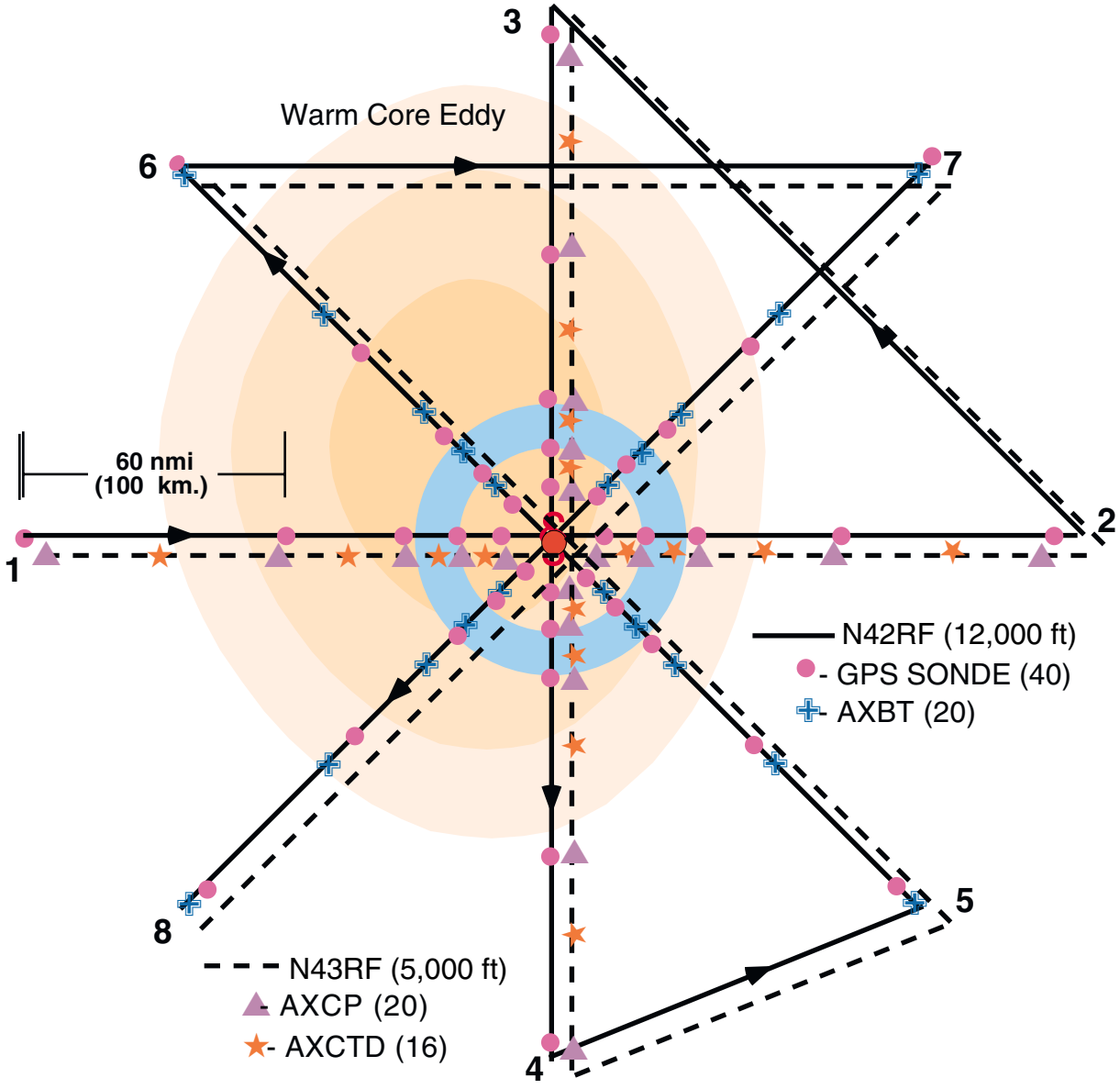

Fig. 16. Sample pattern

• Note 1.	Fly **1-2-3-4-5-6-7-8** at 2,500 ft (800 m) or 5,000 ft (1.5 km) for N43RF and 12,000 ft (3.3 km) for N42RF. Each leg is 120 nmi (200 km) radius from the storm center.
• Note 2.	N42RF drops 10 GPS-sondes and 10 AXBTs each along legs **1-2** and **3-4**, one GPS-sonde and AXBT on each end of the leg, 60 nmi (100 km) from each end of the leg, just outside the eyewall, in the eyewall, and just inside the eye.
• Note 3.	N43RF drops 10 AXCPs and 10 AXCTDs each along legs **1-2** and **3-4.** AXCPs and AXCTDs need to be deployed at IAS <200 kt
• Note 4.	Set airborne Doppler radar to continuously scan perpendicular to the track on all radial penetrations, and F/AST on downwind legs.

15. Rainband Structure Experiment

Program Significance: Over the past few decades, the TC inner core (specifically the eyewall region), has been studied extensively. Numerous aircraft observations have been gathered and many computer models have been developed and run to better understand TCs. An area of research which has been somewhat neglected over the same time period is that of TC rainbands.

Spiral-shaped patterns of precipitation characterize radar and satellite images of TCs. The earliest radar observations of TCs detected these bands, which are typically 3-36 nmi (5-50 km) wide and 55-160 nmi (100-300 km) long. Nevertheless, many aspects of their formation, dynamics, and interaction with the symmetric vortex are still unresolved. The precipitation-free lanes between bands tend to be somewhat wider than the bands. The trailing-spiral shape of bands and lanes arises because the angular velocity of the vortex increases inward and distorts them into equiangular spirals. As the TC becomes more intense, the inward ends of the bands approach the center less steeply approximating arcs of circles. A dynamical distinction exists between convective bands that spiral outward from the center and convective rings that encircle the center.

The detailed case studies which have been accomplished have revealed important aspects of rainbands that were previously unknown. They identified the 'principal band' as a frequent and persistent feature in TCs. Based on the rainband structure determined by these early studies, it was hypothesized that certain rainbands may be able to thermodynamically modify air that attempts to cross a band. Recent studies found a 20 K decrease in low-level θe in a rainband downdraft, and suggested that the draft acted as a barrier to inflow. It was noted that the reduction in boundary-layer energy may inhibit convection near the center. While these case studies have discussed rainbands as important features of the TC circulation and have inferred a relationship between their existence and the TC weakening, very little research has attempted to analyze a large data base of observations from several rainbands. Recent analyses of a large database of radial legs associated with convectively-active rainbands found their kinematic structure were very similar to that of the eyewall. Further, these analyses showed that an outer rainband could provide a barrier to inflowing moist air, and that it is possible that the air may be thermodynamically modified.

At times, rainbands form into full rings that surround the eyewall of the TC. The interaction between the two 'concentric' rings has been shown to be associated with the weakening of TCs. As the outer ring contracts around the inner, the inner eyewall collapses frequently causing a marked weakening of the storm. While this relationship between concentric eyewalls and intensity has been identified, the physics responsible for these changes are poorly understood as we lack both kinematic and thermodynamic measurements in concentric eyewalls necessary to identify how and why they form and how they affect intensity.

The lack of rainband observations leaves us to infer and assume critical elements of rainband structure that may be of fundamental importance to our understanding of the TC. It seems clear that concentric eyewalls can affect TC intensity, and available evidence suggests that convectively-active non-concentric rainbands may play a role in the intensity changes in the TC core. It is extremely important that we understand the structure of rainbands and secondary eyewalls and how they may impact the TC environment. This experiment is designed to address these issues by gathering kinematic data in and around TC rainbands. In addition, with the new GPS-sondes, it is possible to sample some the thermodynamic aspects of the TC ABL.

How do changes in the energy content of the low-level inflow to the eyewall affect TC intensity ? Can we develop techniques that use the new GPS-sondes that will allow one to monitor the changes in the inflow and eventually make forecasts of intensity? Empirical and theoretical studies have developed a relationship ($\delta P = -3\ \delta\theta_e$) that highlights how the increase of the mean equivalent potential temperature ($\delta\theta_e$) of the eyewall updraft column affects the lowering of minimum sea level pressure below a threshold of approximately 1000 mb (δP). If the mean θ_e of the inflow increases 20 K the MSLP of the TC deepens by about 60 mb, all other factors being held constant. Measurement of the evolving energy content will allow estimates of the fluxes at the top and bottom of the inflow layer and provide a clearer view of the air-sea interaction processes that affect TC intensity.

The problem is that the processes that control $\delta\theta_e$ in the inflow have been difficult to quantify. The high sea state and copious amounts of spray push the use of the bulk aerodynamic equations into a realm

for which there are no supporting data. Our understanding of the fluxes at the top of either the mixed layer or the thicker inflow layer is not well known. There are no reliable measurements of the flux at the top of the inflow layer, nor are there reliable estimates of the depth of the inflow. This is despite the conclusions from budget studies and simple numerical models that identify the mixing at the top of these layers as vital part of the TC circulation.

Recently analyses for an intense rainband in Hurricane Gilbert (1988) support the conjecture that the fluxes at the top of the inflow layer are large and downward into the inflow layer. This is counter to the typical situation where the flux of energy is out of the layer and into the middle troposphere. These fluxes can rival the fluxes at the air-sea interface. There appeared to be regions in Gilbert where the inflow layer rapidly increased in θ_e, and other regions where the flux divergence of θ_e resulted in very slowly changing conditions. Rainband circulations have been implicated in this highly asymmetric input of energy into the inflow. Strong rainbands like the one sampled in Gilbert are similar in circulation to an eyewall. We hypothesize that the eyewall circulation itself will have a profound affect on its own inflow, and may lead to a recycling of high θ_e into the top of the inflow layer.

Currently we have little information on the characteristics of the inflow within 45 nmi (75 km) of the eyewall. The new GPS-sondes provide us with an opportunity to sample this region safely and efficiently. This experiment ma, conducted as a piggy-back experiment and would work especially well with reconnaissance missions when a TC is threatening landfall. Eventually we would like to develop the most efficient strategy to deploy the GPS-sondes so we can predict changes in the intensity of the TC. After a few experiments focused on the GPS-sondes are analyzed the experiment can be lengthened to include a more complete sampling of the inflow through the use of in situ turbulent measurements conducted with the WP-3Ds.

Objectives: The general goal of this experiment is to document the structure of non-concentric and concentric rainbands and the environment both inside and outside bands. Data sets from this experiment will be used to determine whether rainbands provide a barrier to the inflow of moist air to the eyewall. Data gathered in this experiment will also allow investigation of the possible thermodynamic effects the rainband may have on the TC environment. Specific goals include:

- Determination of the kinematic and thermodynamic characteristics inside (toward the eye) and outside of TC rainbands, including those that form convective rings.
- Measurement of the characteristics of the middle troposphere and the TC ABL through utilization of GPS-sonde data.
- Determination of the airflow and the rainband structure in all quadrants of the TC.
- Gathering of flight-level and Doppler-derived vertical velocity data in rainbands.
- Documentation of the time evolution and spatial progression of convection within rainbands to determine regions of active and decaying convection.
- Estimate the sensible and latent heat flux divergence for the inflow layer.
- Determine how different inflow trajectories that may pass over land, and warmer or cooler waters alter the energy content of the inflow.
- Determine how the vertical exchange in and near the eyewall affects the energy content of the inflow.
- Develop efficient schemes to monitor energy content of the inflow using the GPS-sondes.
- Assess how changes in the energy content of the inflow affect TC intensity.
- Document changes in microphysics and rainfall characteristics in the storm.
- Obtain a remote sensing data base suitable for evaluation and improvement of satellite and ground validation rainfall estimation algorithms for TCs.

Mission Description: This experiment requires only one day of flying, but a suitable target with a fairly extensive rainband structure or a concentric eyewall structure is necessary. There are two options included in this experiment: a 'principal band' option and a concentric eyewall option. In addition, a separate rainband module is described. For all aircraft missions, GPS-sondes must be available, and lower fuselage and Doppler radars must be operational. In this study, dual-aircraft options require ~40 total GPS-

sondes (20 for each aircraft), single aircraft options require 20 GPS-sondes, and the rainband module requires 4-8 GPS-sondes.

In either option, the two aircraft should stagger their takeoffs. The first aircraft (AC1) will take off ~30-60 min before the second aircraft (AC2) and fly a figure-4 pattern at 10,000 ft (3 km) with ~80 nmi (150 km) legs to document the general reflectivity and wind structure of the storm (**1-2-3-4** in Fig. 17). AC2 will fly ~80 nmi (150 km) legs at ~14,000 ft (4 km) and rendezvous near AC1 at **4** (Fig. 17). GPS-sondes should be dropped inside and outside of the main rainband, and the tail Doppler radar should scan perpendicular to track on radial passes and in F/AST mode on downwind legs. While it is preferred that both aircraft drop sondes and fly legs through the storm, it is essential that the two aircraft arrive at **4** at roughly the same time. To meet this requirement drops can be eliminated and legs can be shortened if necessary.

'Principal band' option: From **4** each aircraft will drop a GPS-sonde and fly downwind. AC1 will remain at 10,000 ft (3 km) and begin its pattern inside the principal rainband (Fig. 18). AC2 will continue to fly at 14,000 ft (4 km) and begin its segment of the pattern outside the rainband. For both aircraft Doppler radar should scan in F/AST mode when flying downwind and perpendicular to the track while crossing the rainband. At **5** the inside aircraft (AC1) will fly across the band to the outside, and AC2 will move to the inside. The aircraft will continue to switch from inside the band to outside the band while dropping sondes as seen in Fig. 18 until the inner aircraft nears the eyewall.

At **7** in Fig. 18, AC2 will continue through the eye (**8**) and rendezvous near AC1 at **9** as both aircraft continue to fly downwind alternating from inside and outside the band as seen in **4-5-6-7**. This pattern is designed to get kinematic and thermodynamic data inside and outside the band. Alternating which aircraft is inside the band assures that neither aircraft proceeds too far ahead of the other while traveling around the storm. It also allows flight level data to be gathered in the band itself. With careful coordination, insuring safety at all times, it may be possible to fly the 'band-crossing' legs to create dual Doppler opportunities in several portions of the rainband.

At. **10**, AC2 (still flying at 14,000 ft - 4 km), will fly a full figure-4 pattern (**10-11-12-13-14** in Fig. 19). AC1 (at 10,000 ft - 3 km) will follow AC2 toward the center and drop sondes on both sides of the rainband and in the storm center. AC2 will not use GPS-sondes on its figure-4 until it is clear of AC1 (as seen in Fig. 19). The estimated flight time for this experiment is 5-6 hours, depending on the radius of the rainband from the storm center.

For a single aircraft mission, a figure-4 pattern with ~80 nmi (150 km) legs will be flown between 10,000 ft (3 km) and 14,000 ft (4 km) to identify the overall structure of the storm and to choose a rainband for investigation. The Doppler radar should scan perpendicular to the flight track when crossing the band and in F/AST mode when flying downwind. A zigzag or sawtooth pattern should be flown across the rainband of interest with GPS-sondes dropped on both sides of the band. At **9**, the aircraft may fly downwind around the storm (flight option 1) or fly upwind to repeat the investigation of the rainband (flight option 2). In either case, GPS-sondes should be dropped along the flight track to gather information on the TC environment. A final figure-4 will complete the flight pattern.

[**NOTE**: As the aircraft get closer to the storm center while following a rainband that is spiraling in toward the center, caution must be exercised.]

Concentric Eyewall Option: This option can be executed with dual aircraft or a single aircraft. For dual aircraft, a flight pattern similar to that seen in Figs. 17-19 will be flown with the aircraft alternating which aircraft is on the inside of the band. Since the rainband of interest would exist in all quadrants of the storm, the aircraft will extend the 'principal band' pattern and fly completely around the storm in a pattern similar to that of Fig. 20 (**4-5-6-7**). GPS-sondes would be dropped as seen in Figs. 17-19.

For a single aircraft mission, a figure-4 pattern with ~80 nmi (150 km) legs will be flown between 10,000 ft (3 km) and 14,000 ft (4 km) to identify the overall structure of the storm. As in the 'principal band' option, the Doppler radar should scan perpendicular to the flight track when crossing the band and in F/AST mode when flying downwind. A zigzag or sawtooth pattern should be flown across the rainband of interest with GPS-sondes dropped on both sides of the band. A final figure-4 will complete the flight pattern.

RAINBAND STRUCTURE EXPERIMENT

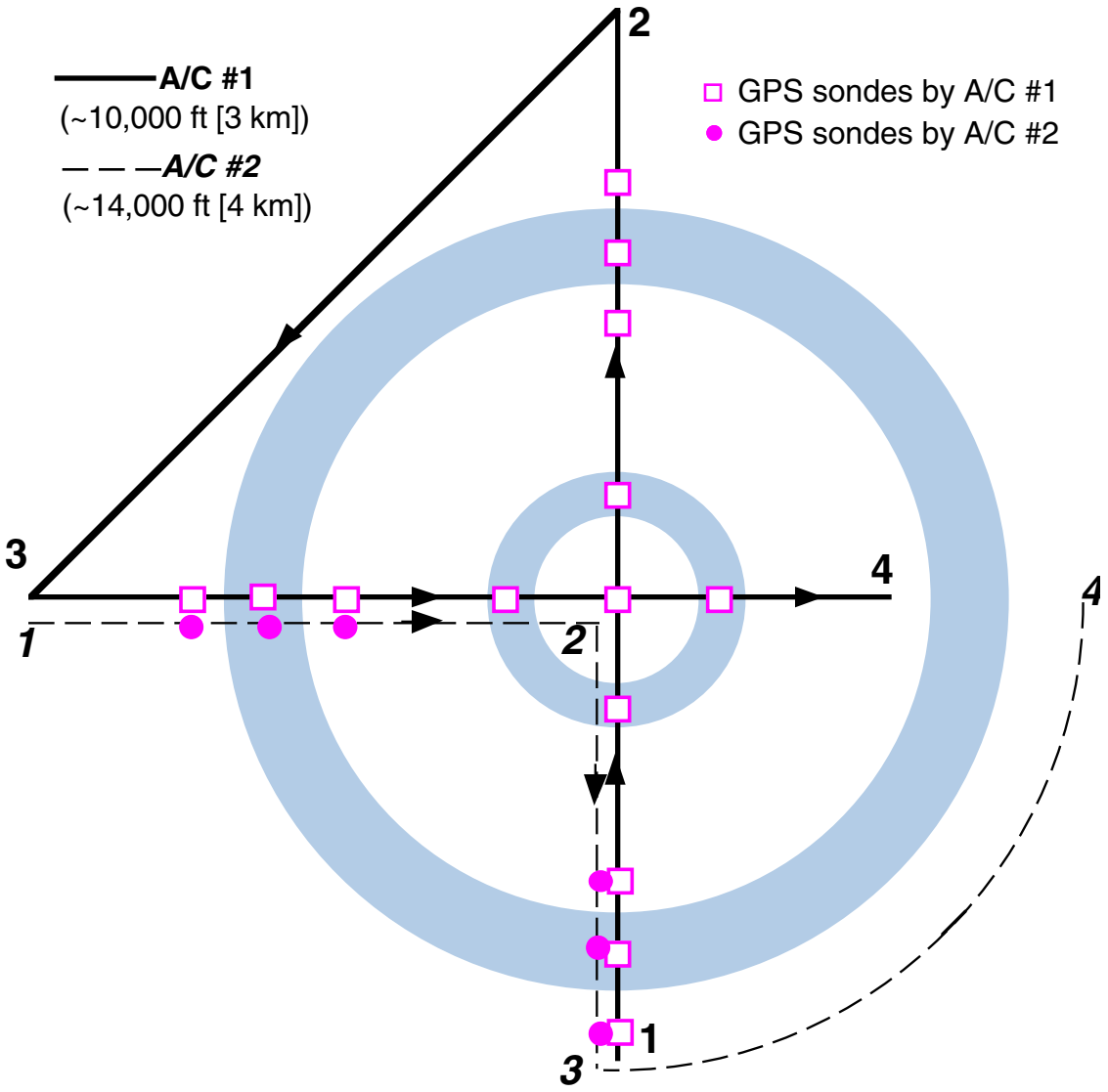

Fig. 17. Beginning Survey Pattern.

• Note 1.	The pattern may be flown along any compass heading.
• Note 2.	**IP** is approximately 80 nmi (150 km) from the storm center.
• Note 3.	Both aircraft should arrive at **4** at the same time. After exiting the eye near **4**, both aircraft begin the downwind rainband portion of experiment.
• Note 4.	Set airborne Doppler radar to continuously scan perpendicular to the track on all radial penetrations, and F/AST on downwind legs.

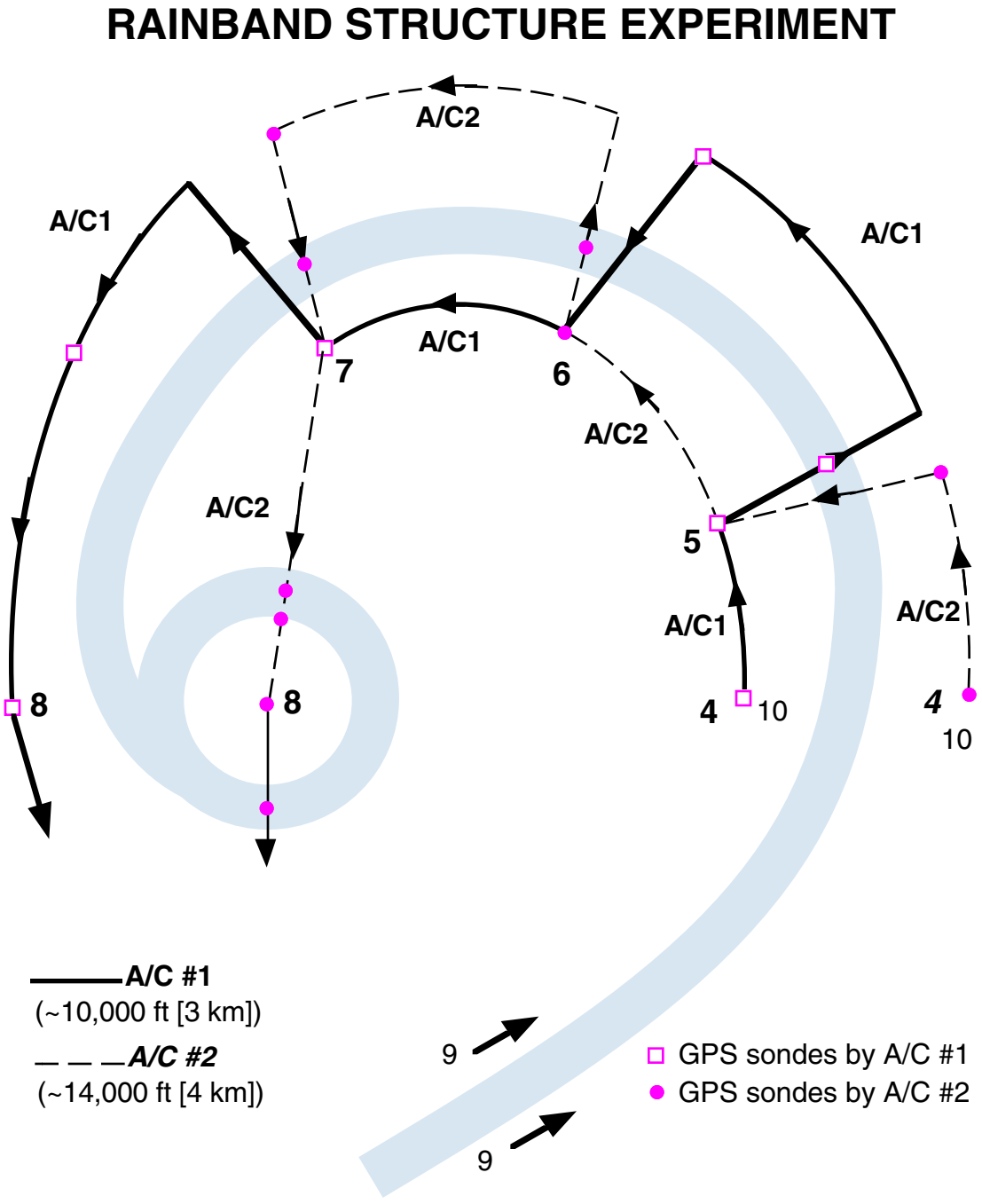

Fig. 18. Principal Band /Concentric Eyewall Option.

• Note 1.	A/C#1 should not fly closer than 33 nmi (60 km) from the storm center. Aircraft separation should not exceed 25 nmi (45 km) on the downwind legs.
• Note 2.	Turn points and drops should be coordinated between aircraft to ensure flight safety.
• Note 3.	Set airborne Doppler radar to F/AST on downwind legs.

RAINBAND STRUCTURE EXPERIMENT

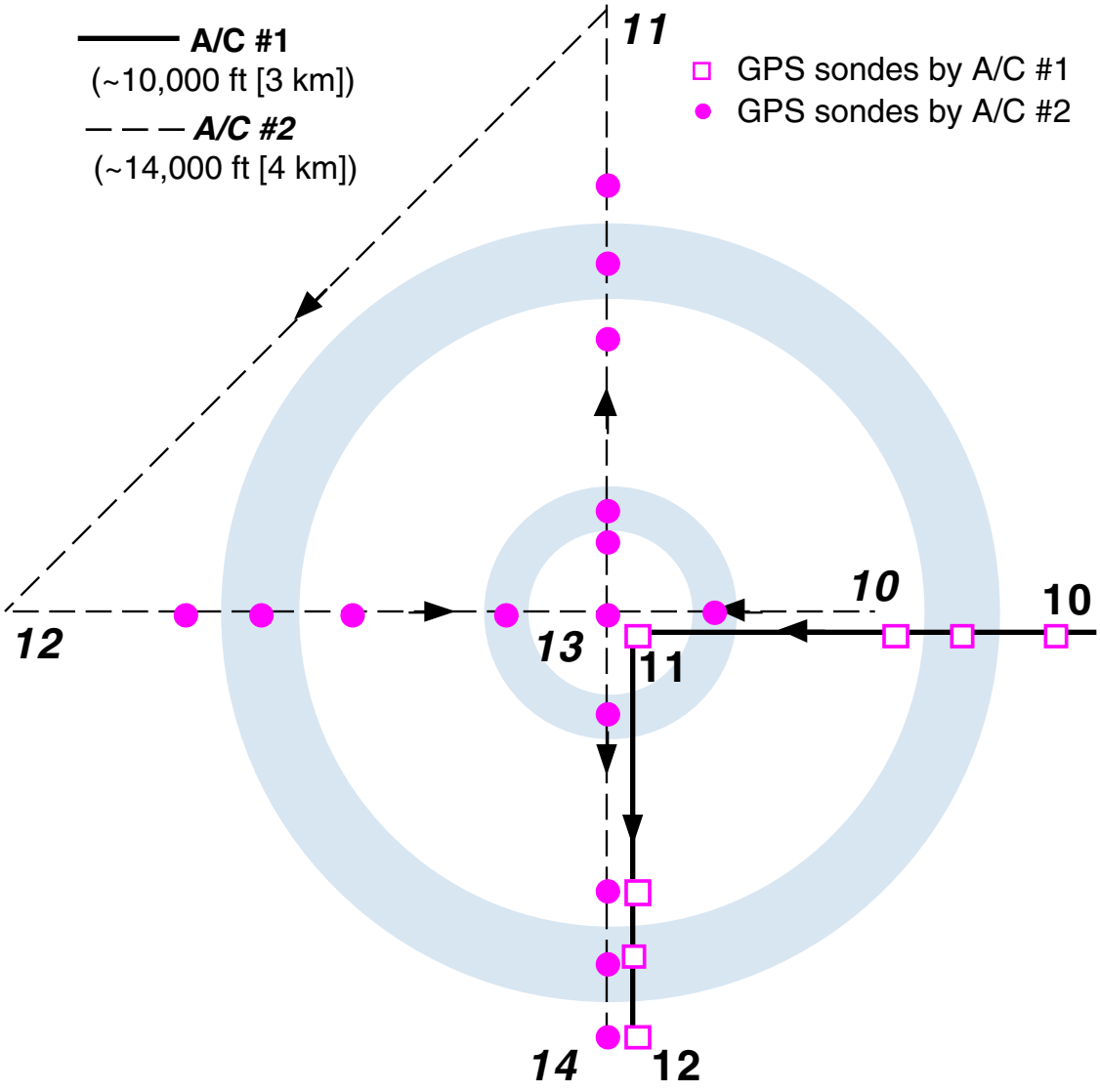

Fig. 19. Final Survey.

• Note 1.	The pattern may be flown along any compass heading.
• Note 2.	**10** is approximately 80 nmi (150 km) from the storm center.
• Note 3.	AC2 will not drop sondes until clear of AC1 on the track to **11**.
• Note 4.	Set airborne Doppler radar to continuously scan perpendicular to the track on all radial penetrations, and F/AST on downwind legs.

- **Rainband module**: The single aircraft rainband module has been designed to be flown with other experiments in "rainbands of opportunity" and last 30-60 min (Fig. 20). The goal of the module is to gather data inside, outside, and across several rainbands of several storms over several seasons. It was successfully flown in Hurricane Bonnie (1998). While individual data sets will increase our understanding of the structure of rainbands, the primary objective here is to develop a database of rainband observations for future comprehensive study.

- **Rainband Thermodynamic Structure Module**: This module requires one WP-3D flying above the inflow layer (8,000 to 10,000 ft). The WP-3D deploys 6-8 GPS-sondes and an occasional AXBT along a curved track approximately 60 nmi (100 km) long that roughly mimics the inflow trajectory for air in the subcloud and lower cloud layers. Deployment of the GPS-sondes occurs between the eyewall outer edge and the inner edge of any convective rainband found at greater radial distance. If there are no rainbands then sonde deployment may cease at approximately 60 nmi (100 km) radial distance from the circulation center. Fig. 21a is a plan view of the experiment, Fig. 21b is a radius-height cross-section of the scheme. Note that shorter times between each GPS launch are preferred when the aircraft is near the eyewall. A sonde should also be deployed in the eye. The mission easily can be accomplished when the aircraft is conducting a reconnaissance mission for NHC. Instead of cardinal headings to and from the eye the aircraft follows a spiral path in and out of the circulation center. A typical spiral path should be 20-40° from a tangent to a given radius. Flight time for 60 nmi (100 km) is about 15-20 min.

GPS-sondes are deployed every 6-9 nmi (10-15 km) starting from about 6 nmi (10 km) from the outer edge of the eyewall to insure that the sonde falls outside of the main updraft and rain. After four sondes are in the air and the first sonde splashes down a new one may be deployed. The design assumes that 4 sondes may be in the air simultaneously and that the sonde descends at about 12 m s^{-1}.

A single spiral in or out will provide a view of how energy content changes along a trajectory for one portion of the storm. If several trajectories are sampled then energy content and cyclone intensity can be studied. Judicious choice of the inflow trajectories to be flown is made by the airborne mission scientist and would likely include sampling inflow from the southeast and from the northwest as shown in Fig. 21a.

Turbulent flux option: If a WP-3D is equipped with the high frequency temperature and moisture sensors then a series of legs may be flown in the region where sondes were previously dropped between the eyewall and a convective rainband. These legs are again approximately parallel to the low level inflow and are designed to allow one to estimate the sensible and latent heat flux divergence in the inflow layer. The levels chosen are a function of the structure revealed by one or more of the GPS-sondes. Legs should be 37-50 nmi (60-80 km) long. Typical altitudes would be 8,000, 6,500, 5,000, 3,000, 2,000, 1,000, and 500 ft; these levels may be adjusted depending on the altitude of the top of the inflow and mixed layers. It is desirable to have 2 legs above the inflow, the rest within the inflow. The lower levels are flown only if the turbulence and visibility are assessed as safe. At no time does the aircraft need to fly into rainbands, the eyewall, or any strong cells in between these two features. On the first, highest leg the aircraft should deploy sondes at every 12 nmi (20 km) to assess any evolution of the inflow from the prior GPS deployment stage. Fig. 21c shows the flight pattern. The total time for this option is about 2 h.

The turbulent flux option is recommended *only* if the flux instrumentation is operational and after a few experiments with the GPS alone have been accomplished.

RAINBAND STRUCTURE EXPERIMENT

Single Aircraft Option

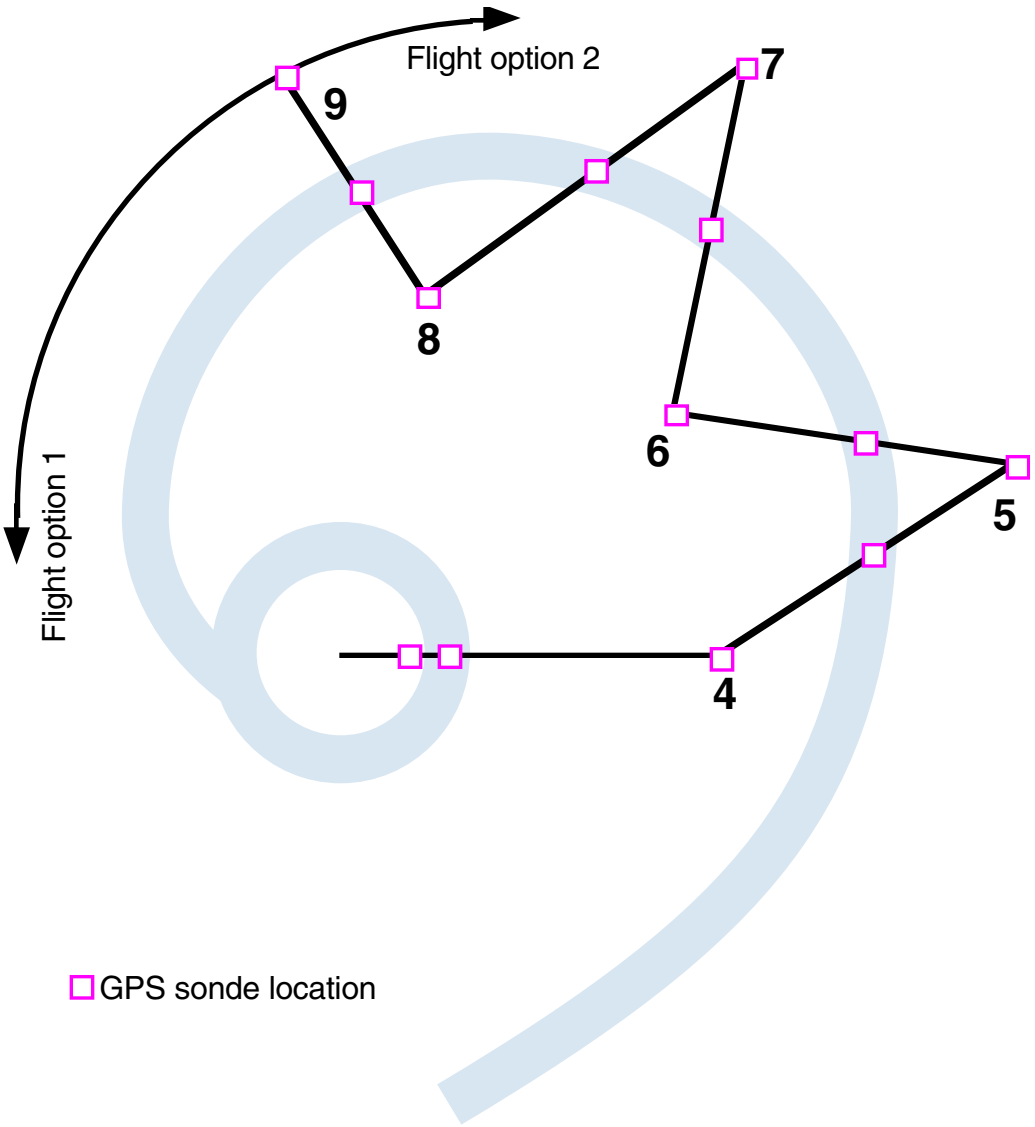

Fig. 20. Rainband Module—Single Aircraft Option.

• Note 1.	Fly zig-zag legs **4-9** at 10,000-14,000 ft (3-4 km) altitude, below the melting level. Each leg is approximately 25 nmi (45km) long. Outside turns of 270°-300° are at the end of each zig-zag leg. GPS-sondes will be dropped on both sides of the band.
• Note 2.	At **9** fly downwind around the eyewall (option 1), or upwind along rainband (option 2) to a point near the beginning of the zig-zag legs.
• Note 3.	Repeat pattern in different parts of the storm as time permits.
• Note 4.	Set airborne Doppler radar to continuously scan perpendicular to the track on all radial penetrations or zig-zag legs, and F/AST on upwind or downwind legs.

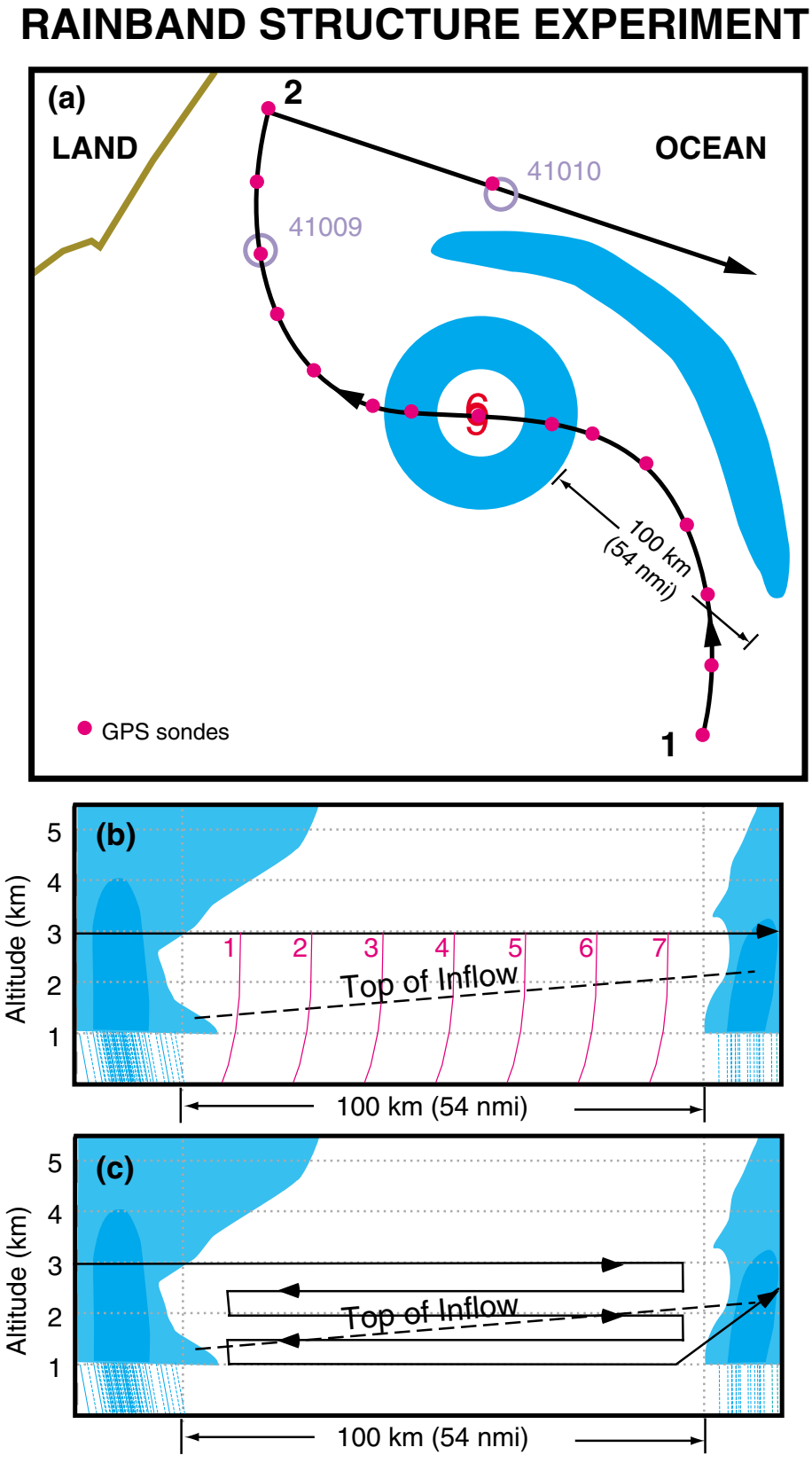

Fig. 21. **Rainband Thermodynamic Structure Module (a) Plan view; and Aircraft track-height depiction of (b) the GPS-sonde deployment experiment and (c) turbulent flux experiment.**

16. Electrification of Tropical Cyclone Convection Experiment

Program Significance: Cloud electrification has been a topic of great scientific interest for many years, but the lack of suitable instruments for measuring electric fields and particle charges in clouds has hindered research. From anecdotal evidence, meteorologists have considered that TCs usually have little electrical activity. However, the introduction of wide-area lightning detection systems along the U.S. coast has resulted in several case studies of lightning from tropical storms and hurricanes. These data show that a larger proportion of TCs produce cloud-to-ground (CG) lightning than was previously known.

Neither the microphysical nor electrical structure of TC clouds that exhibit lightning is known. Laboratory experiments have shown that more charge is separated when ice crystals collide with a rimed target in the presence of supercooled water than is separated without supercooled water. They also showed that the sign of the charge transferred reversed at about -20°C. Other laboratory experiments showed that the growing conditions encountered by the ice particles determined the sign of the charge that was transferred between them during collisions. Observations in continental thunderstorms support this hypothesis and suggest that charge separation occurs most rapidly on the boundary between the main updraft and the downdraft near -15°C. More recent observations showed that sublimating graupel acquire negative charge and graupel undergoing deposition acquire positive charge. As these processes depend critically upon the graupel temperature and cloud liquid water content, it is highly desirable to obtain suitable measurements in natural clouds.

In mature TCs, updraft velocities are usually low. In addition, graupel and ice particles are plentiful, but supercooled cloud water is rare in TCs at temperatures as warm as -5°C. Studies of two mature Atlantic TCs have shown that the little supercooled water present in the strongest eyewall updrafts was immediately adjacent to areas that contained high concentrations of small ice particles. When one considers the lack of supercooled water in mature TCs, it is not surprising that mature TCs are not always electrified. However, the National Lightning Detection Network (NLDN) detected lightning in several hurricanes and tropical storms as they approached land.

A recent investigation noted that there appeared to be a relationship between the occurrence of CG lightning in the eyewall and a subsequent intensification of the TC. A similar relationship was proposed by studies of lightning observations in two developing TCs. In each case, lightning was qualitatively associated with exceptionally strong convection, which occurred when the storms were rapidly intensifying. In addition, recent observational studies of CG lightning in TCs using data from the NLDN showed that CG lightning is most prevalent in the outer convective rainbands of TCs with little CG lightning near the eyewall. An apparent paradox is thus created as research shows that vertical velocities in rainbands are weaker than those in the eyewall. It is important to note, however, that rainbands >54 nmi (100 km) outside of the eyewall remain virtually unsampled.

Although these observational studies analyzed lightning in TCs, none of them included cloud microphysics or vertical velocity measurements. The inclusion of these data are critical to better understanding the relationship between cloud physics, vertical velocity, and CG lightning. Combining these data sets allow further investigation of the implications CG lightning has to intensity changes in TCs.

In view of these observations, we believe that supercooled water and charge separation occasionally occur in the strong convection in TCs. Recent additions to the WP-3D instrumentation that make electrification studies possible are four rotating vane field mills that measure the vector electric field and an induction ring that measures the charge on individual particles.

Objectives: The objectives of this experiment are to study the temporal evolution of the electric field and microphysical and kinematic properties in TCs. The specific goals are:

- Measure the sign and magnitude of the vector electric field near the eyewall and in an outer convective rainband.
- Document the three dimensional wind field in electrified clouds, including the vertical winds estimated from the Doppler radar.
- Determine the polarity and magnitude of the charge on ice precipitation at several temperature levels above the melting level.
- Estimate the transport of electrical charge in the storm.

- Record the types and concentrations of all particle types observed in the electrically active portions of the storm.
- Document changes in microphysics and rainfall characteristics in the storm.
- Obtain a remote sensing data base suitable for evaluation and improvement of satellite and ground validation rainfall estimation algorithms for TCs.

Mission Description: This experiment documents the microphysical characteristics of electrically active convection using a single aircraft. The new Particle Measuring System (PMS) 2-D greyscale probes, the new PMS FSSP-100, and the University of Nevada, Desert Research Institute (DRI) field mills are essential. The DRI induction ring, the tail Doppler radar, and the cloud liquid water probes (Johnson-Williams [JW] and King) are highly desirable. Horizontal and vertical wind field measurements will be obtained from the Doppler radar. The aircraft should execute a standard true airspeed (TAS) calibration in clear air prior to entering the storm if conditions permit.

This study requires that one aircraft be equipped with the DRI electric field instruments in addition to the standard instrumentation. The PMS probes must be the best available, and the radars must be fully operational. The experiment is composed of three options. In all options, it is desirable to have 4 to 6 GPS-sondes to obtain soundings outside the convection in the inflow near the areas of interest. The aircraft should loiter in the eye or any other suitable area when it is necessary to service equipment.

Eyewall option: To execute this option, the aircraft will fly radial legs out and back at constant radar altitude upon a reciprocal track through the eyewall at successively higher altitudes starting at the stratiform area melting level (~16,000 ft [4.8 km]) until the maximum operational altitude is reached. An dropwindsonde should be dropped outside the eyewall on the highest altitude leg to obtain a vertical sounding. Each successive radial pass (out and back) shall be 1,500 ft (500 m) higher than the previous one. Climbs and descents should occur in clear areas outside the eyewall (**2** in Fig. 22), and leg lengths shall be altered as necessary to achieve this. This out and back pattern (**1-2-1** in Fig. 22) should be repeated until the aircraft reaches its maximum attainable altitude. The Doppler radar should be operated in a 360° scan mode during the radial passes. Upon completion of the radial legs, an equilateral triangle Doppler pattern will be executed, starting from inside the eye. The starting azimuth (Fig. 22) will be 60° upstream from the upstream edge of the strongest radar reflectivity feature in the eyewall or innermost convection. The legs should be ~43 nmi (80 km) long, with the inbound leg connected to the outbound leg by a downwind leg. The inbound leg should penetrate the convection at the downstream edge of the strong reflectivity area previously identified. Each triangle will require 10-20 min to complete, depending upon the leg length.

Rainband option: If a convective outer rainband is available >80 nmi (150 km) from the eye, it should first be surveyed for evidence of electric fields. The survey consists of flying along the band until the field mills register a space charge or the Doppler radar reveals the presence of vigorous convection. When an interesting area is located, the aircraft should either seek a clear area and climb to maximum altitude or descend to the 0°C (~16,000 ft [4.8 km]) altitude, whichever is closer, and start making passes downwind (Fig. 23) through the middle of the band the feature. Each downwind pass (Fig. 23, **1-2**) should maintain a track along the axis of the band and be about 50 nmi (93 km) long and 1,500 ft (500 m) higher (lower) than the previous one. During this portion of the pattern, the Doppler radar should make 360° scans normal to the aircraft track. After the downwind pass is completed, the aircraft should exit the band on the outer side, climb (descend), and return (Fig. 23, **3-4**) upwind to the start of the band. The Doppler data will be obtained on the upwind pass using the F/AST method. This pattern will require about 20 min to execute. Pass length may be altered as circumstances dictate. Repeat this pattern until the maximum altitude is reached, or seek a new area as desired. As an alternate, a zig-zag path downwind through the convective band may be flown if necessary for flight safety.

(**Note**: If the feature of interest is not translating, radial legs should be flown on a constant track instead of a constant heading. The length of the radial legs depends upon the diameter of the eye and the width of the rainband, respectively. Turns should be initiated into the wind.)

Landfalling storm option: The purpose of this option is to investigate the relationship between cloud physics, vertical velocity, and the occurrence and location of CG lightning. Outer convective rainbands are of primary interest since they are the most likely features to be electrified. Vertically pointing Doppler rays are used to estimate vertical air motions during passes through active convection in both tropical storms and hurricanes. Along with the vertical velocities, coincident microphysics and electric field

ELECTRIFICATION OF TROPICAL CYCLONE CONVECTION EXPERIMENT

Eyewall Module

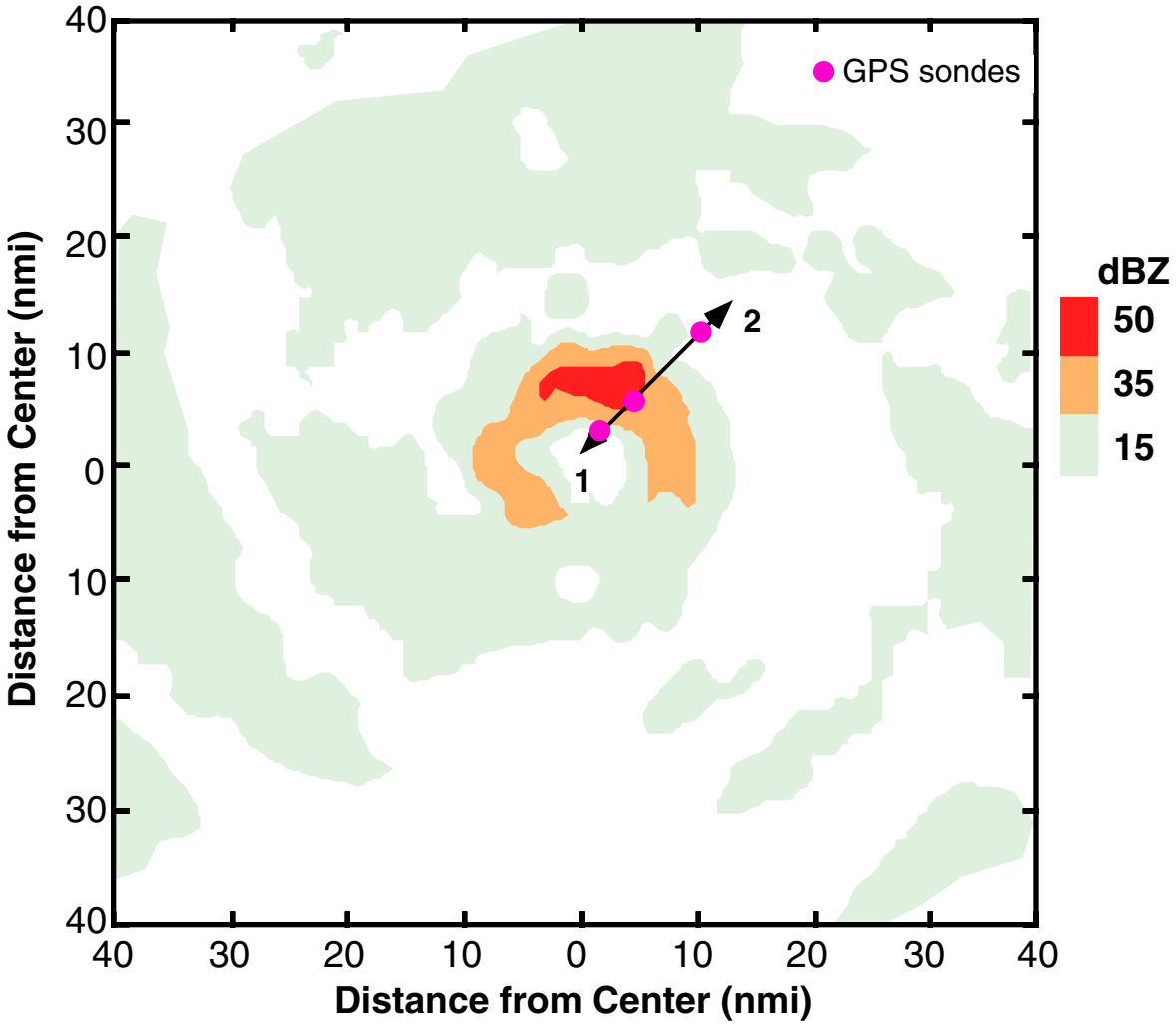

Fig. 22. Convection/Eyewall module flight pattern.

• Note 1.	True airspeed calibration is required.
• Note 2.	The pattern may be entered along any compass heading.
• Note 3.	Radial penetrations are separated by 1,500 ft (500 m) altitude and occur along track **1-2-1**.
• Note 4.	Set airborne Doppler radar to continuously scan perpendicular to the track on radial penetrations.

ELECTRIFICATION OF TROPICAL CYCLONE CONVECTION EXPERIMENT

Rainband Module

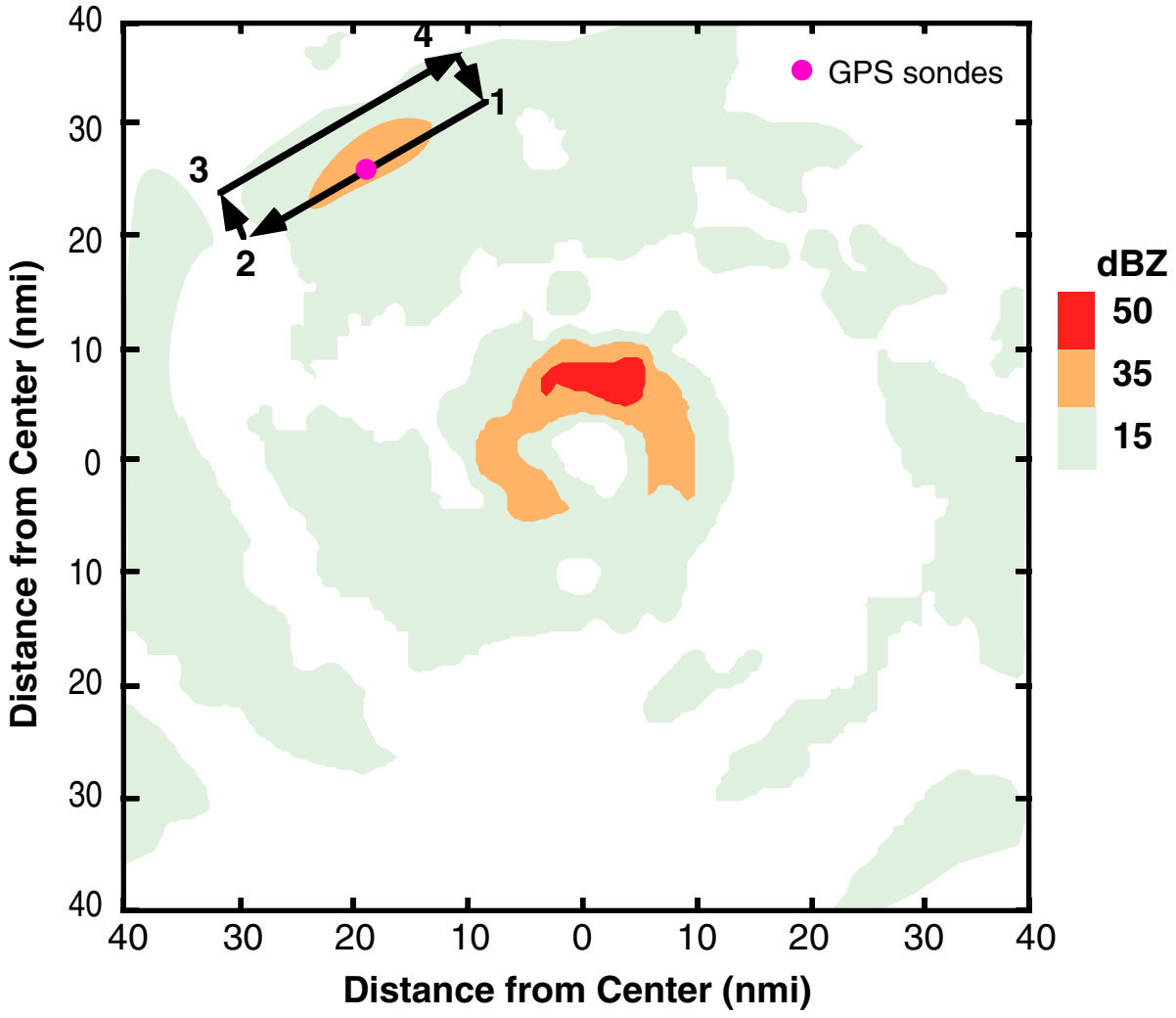

Fig. 23. Convection/Rainband module flight pattern.

• Note 1.	True airspeed calibration is required.
• Note 2.	The pattern may be flown along any compass heading.
• Note 3.	Rainband passes **1-2** are separated by 1500 ft (500 m) altitude. Climbs occur along **3-4** away from the convection.
• Note 4.	Set airborne Doppler radar to continuously scan perpendicular to the track from **1-2**, and F/AST on all other legs.

measurements are made at heights above the melting level. Three-dimensional wind fields of the convective areas can be constructed from a Pseudo-dual Doppler technique and from the F/AST Doppler data. CG lightning data are available within 325 nmi (600 km) range of the NLDN (Fig. 24). Together, these data sources and techniques should lead to a better understanding of the characteristics of the convective processes that lead to lightning in TCs and, possibly, to intensity changes of the storms.

For this option, the aircraft will initially fly a survey figure-4 pattern (Fig 25a) at ~18,000 ft (5.5 km) altitude. The figure-4 pattern would be completed in 1.5-2.0 h with radial legs 80 nmi (150 km) in length. The second part of this option (Fig. 25b) concentrates on rainbands that are located within the useful range of the NLDN. Upon exiting the eye at **4**, the aircraft should climb as high as possible on the way to the rainband of interest (**5**). A sawtooth pattern is flown downwind (Doppler operating in standard mode) with repeated crossings of the rainband to **6**. We prefer to fly directly down the band as noted in Fig. 23, but for reasons of safety, a sawtooth pattern may be flown. An upwind leg, flown outside of the band, is performed with the tail radar operating in the F/AST mode. The sawtooth pattern across the band is repeated with an exit toward the eye at **7**. After entering the eye, the aircraft turns toward the second rainband at **8**. The sawtooth crossings and the F/AST downwind leg are repeated as in the first rainband. A final center fix is made (time permitting) before returning to base from **10**. About one hour should be spent in each of the rainbands. If only one rainband is present within the useful range of the NLDN, a second study of the same band can be performed after a circuit through the storm center.

ELECTRIFICATION OF TROPICAL CYCLONE CONVECTION EXPERIMENT

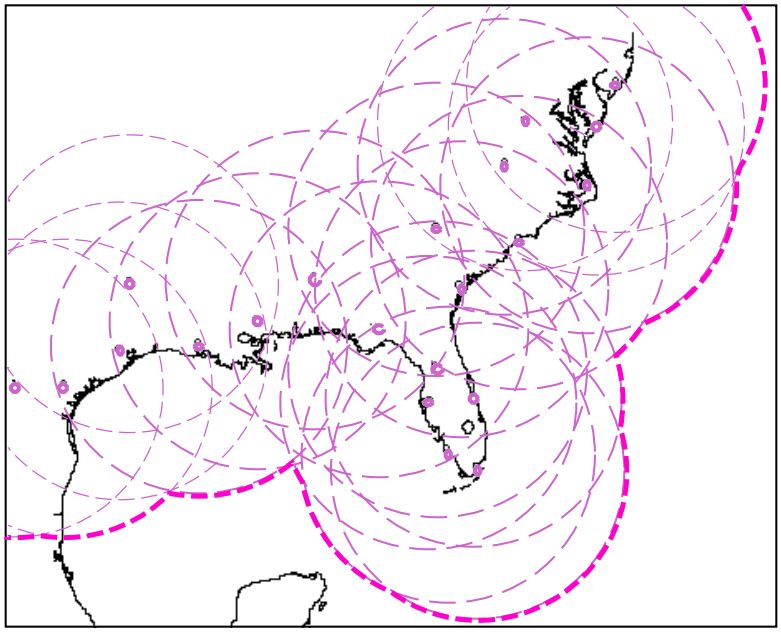

Fig. 24. Lightning direction finders (DFs) of the NLDN. Rings are at 325 nmi (600 km) radius from each site. The o denotes DF location.

ELECTRIFICATION OF TROPICAL CYCLONE CONVECTION EXPERIMENT

Survey Module

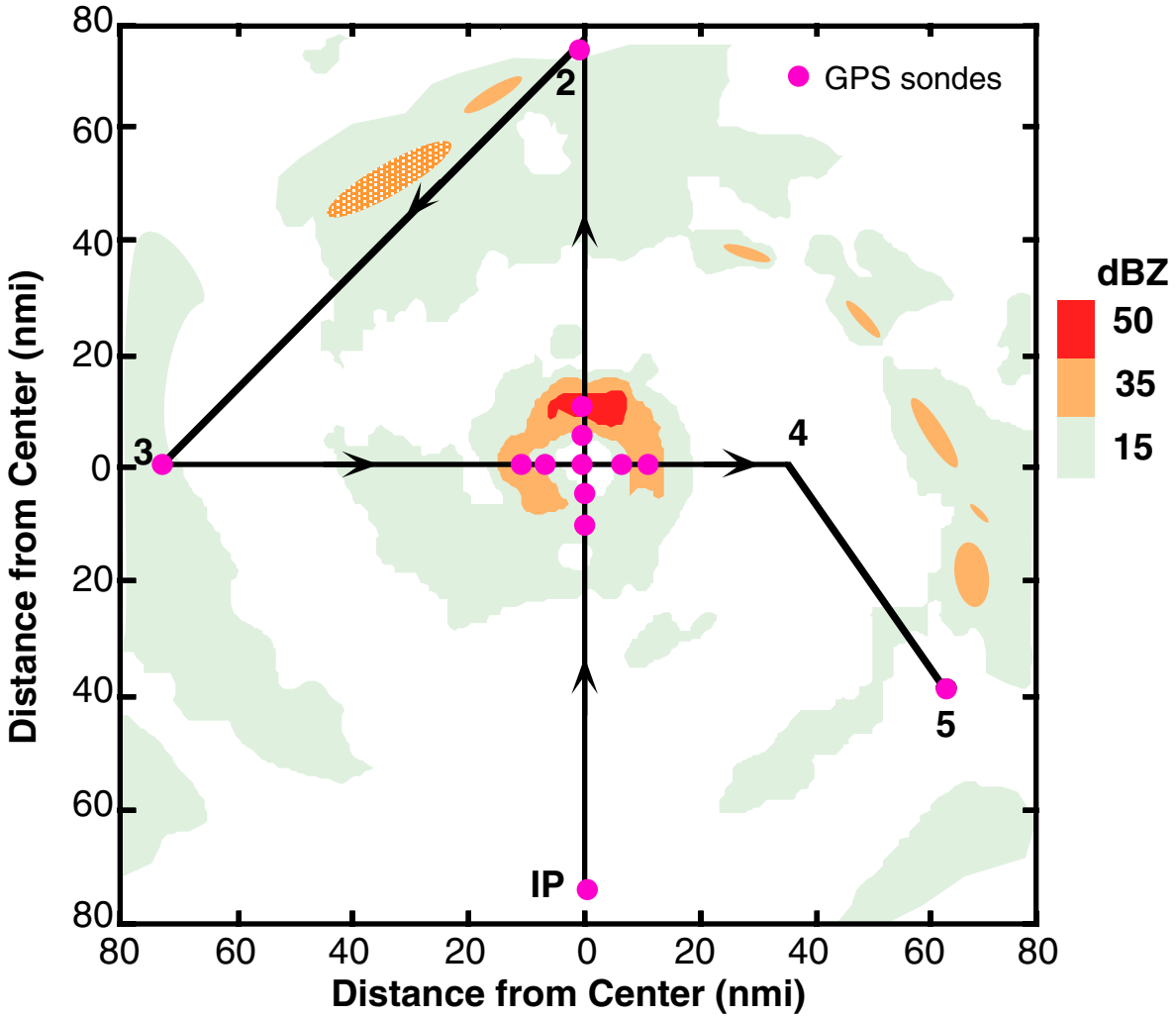

Fig. 25. (a) Convection/Survey module flight pattern.

• Note 1.	The pattern may be flown along any compass heading.
• Note 2.	Fly **IP-2-3-4** at 18,000 ft (5.5 km). **IP** is approximately 80 nmi (150 km) from the storm center.
• Note 3.	After exiting the eye near **4**, select upwind portion of a rainband for rainband portion of experiment.
• Note 4.	Set airborne Doppler radar to continuously scan perpendicular to the track on all radial penetrations, and F/AST on downwind legs.

ELECTRIFICATION OF TROPICAL CYCLONE CONVECTION EXPERIMENT

Rainband Module

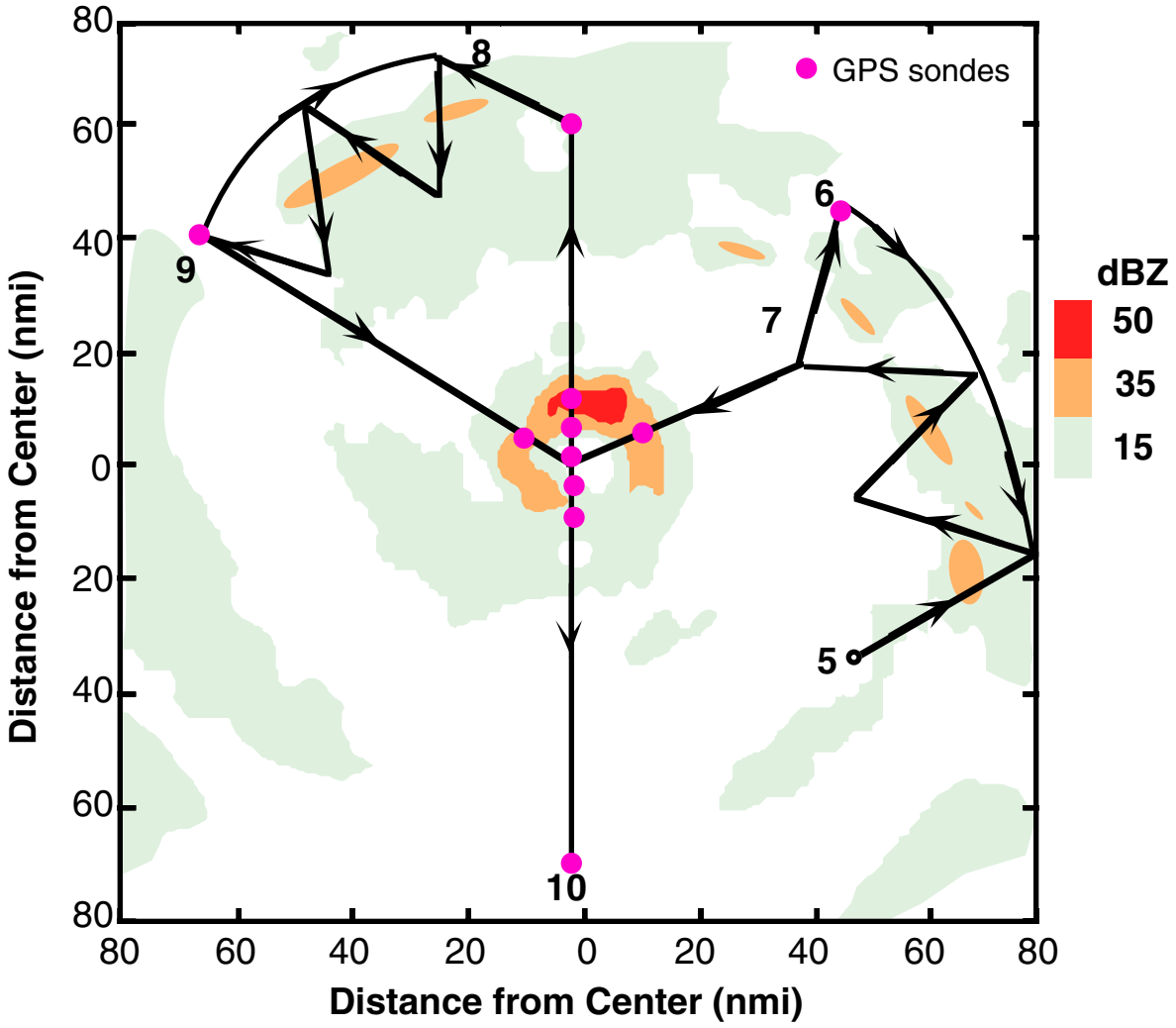

Fig. 25. (b) Convection/Survey rainband module flight pattern.

• Note 1.	Fly zig-zag legs **5-6** and **8-9** at highest possible altitude. Each leg is approximately 25 nmi (45km) long. Outside turns of 270°-300° are at the end of each zig-zag leg.
• Note 2.	At **6** and **9** fly upwind leg along rainband at highest possible altitude to a point near the beginning of the zig-zag legs.
• Note 3.	Repeat pattern in different parts of the storm as time permits.
• Note 4.	Set airborne Doppler radar to continuously scan perpendicular to the track on all radial penetrations or zig-zag legs, and F/AST on upwind legs along the rainband.

17. Structure of Eyewall Convection Experiment (SECE)

Program significance: Knowledge of the three-dimensional structure of air motions in the eyewall are crucial for understanding the internal processes that govern intensification of the TC. The TC eyewall is the primary region for organized, deep convection. Outward-sloping updrafts can extend several kilometers in both the horizontal and vertical and transport moisture-laden air from the sea-surface to the upper troposphere. The largest and strongest 10% of the eyewall updrafts are responsible for ~90% of the upward mass transport necessary to maintain the intensity of the TC. Downdrafts typically are smaller and slightly weaker than the updrafts, do not exhibit any radial slope, yet may be important in vertical momentum transports that can affect the boundary-layer winds. The remote-sensing capability of the Doppler radar on the WP-3D aircraft, combined with the GPS-sondes, allows for the study of the eyewall convective structure in greater detail than was formerly available.

Recent wind and thermodynamic observations from GPS-sondes have provided unprecedented detail of the structure of the TC eyewall. Large vertical variations in the wind structure have been documented. Included in these variations are pronounced low-level wind maxima that are apparently related to convective features in the eyewall. Theses wind maxima are usually correlated with strong updrafts or downdrafts, occur at heights from just above the sea surface to heights of ~3,000 ft (1 km), and can extend several hundred meters in the vertical. Observations from multiple dropwindsondes released in rapid succession along a radial leg through the eyewall have suggested that these convective wind features extend 6-12 nmi (10-20 km) radially, albeit at different altitudes. Little information is available on the azimuthal continuity of the convective wind features. This knowledge would be beneficial for numerical modeling efforts of the TC and for real-time assessment of the structure of the surface wind field.

Observations from GPS-sondes, dual-Doppler analysis and vertical-incidence Doppler data from coordinated, parallel flight tracks of both WP-3D aircraft can be used to study the three-dimensional wind and thermodynamic structure of eyewall convection. The GPS navigation provides accurate positioning of the aircraft, relative to the storm center, resulting in smaller errors in the total wind field, including vertical velocity estimates. Data collected simultaneously from both aircraft in two adjacent radius-height profiles through the eyewall can be used to infer the azimuthal continuity of the largest up- and downdrafts. Observations from multiple dropwindsonde releases along a downwind leg just inside of the visual eyewall (at altitude) can provide additional information on the continuity of low-level wind maxima associated with convective features. The dual-Doppler analysis provides the basic flow in the eyewall in which these convective features are embedded. Comparisons of vertical velocity estimates from the vertical-incidence data and the dropwindsondes can be compared and used in a vertical air motion analyses. The data collected from this experiment will be used to expand knowledge of the relation between the convective structure and intensity change, to provide a basis for use in numerical modeling efforts of TC eyewall processes, and towards a better understanding of variations in the surface wind field.

Objectives:

- To map the three-dimensional spatial structure of the TC eyewall convection from dual-vertical incidence data, dual-Doppler analysis, and GPS-sonde observations.
- To investigate the relation between the convective structure in the TC eyewall to vertical variations in the horizontal wind.
- Compare and validate the horizontal and vertical wind estimates from GPS-sondes and Doppler data.
- To refine the conceptual model of the three-dimensional structure of the eyewall for use as ground truth in numerical models of the TC.
- Document changes in wind and rainfall characteristics in the storm.
- Obtain a remote sensing data base suitable for evaluation and improvement of satellite and ground validation of the surface wind field in TCs

Mission Description: This experiment uses both WP-3D aircraft flying highly coordinated flight patterns to map the three-dimensional structure of eyewall convection. The primary requirement is for the target storm to have a well-developed eyewall with substantial areas of deep convection. Both aircraft must have fully operational tail radar systems and at least one aircraft must have a working lower fuselage

radar. Recording of cloud physics data is desired but not necessary. The aircraft will fly at two altitudes, one at 14,000 ft (4.2 km) and the other at 16,000 ft (4.8 km). Each aircraft should have up to 36 GPS-sondes available for deployment in the eye, eyewall, and outside of the eyewall.

The first and last portions of the mission includes coordinated "figure-4" patterns (Fig. 26a) with leg lengths nominally set at 60 nmi (110 km). The length may vary depending on the size of the eye. After completing the initial "figure 4", the aircraft will rendezvous in a relatively clear area outside of the eyewall to coordinate an inbound leg into the eye (Fig. 26b). The aircraft should fly at the same ground speed so as to be parallel to each other along the radial leg. The horizontal spacing between aircraft can vary from 1,500 ft (0.5 km) to 6,500 ft (2.0 km) and the vertical separation can be 2,000 ft (600 m) or greater, depending on safety considerations.

The dual vertical-incidence module (Fig. 26b) consists of coordinated radial legs into and out of the eye with downwind legs flown outside of the eyewall between the outbound and inbound legs. The radial legs will typically be 40-60 nmi (70-110 km) long, depending on the eye size. The upper aircraft should be slightly downwind of the lower plane so that dropwindsondes can be released from each aircraft simultaneously. Coordination between aircraft should be done in clear air in the eye and outside of the eyewall at the end of the downwind legs. If the eye diameter is too small to maneuver the aircraft, straight legs through the eye and eyewall may be used. Otherwise, if conditions permit, the aircraft can separate in the eye to perform short downwind legs along the inner edge of opposite sides of the eyewall. These legs (Fig. 26c) are to be flown in "clear air" radially-inward of the visible edge of the eyewall with four GPS-sondes released in rapid succession (~10 s apart). After completing this module, the aircraft can coordinate in the eye to continue the dual vertical-incidence module. These series of radial legs should be repeated so as to maximize the coverage of the eyewall, but to allow time for a coordinated "figure-4" pattern at the end of the flight.

STRUCTURE OF EYEWALL CONVECTION EXPERIMENT

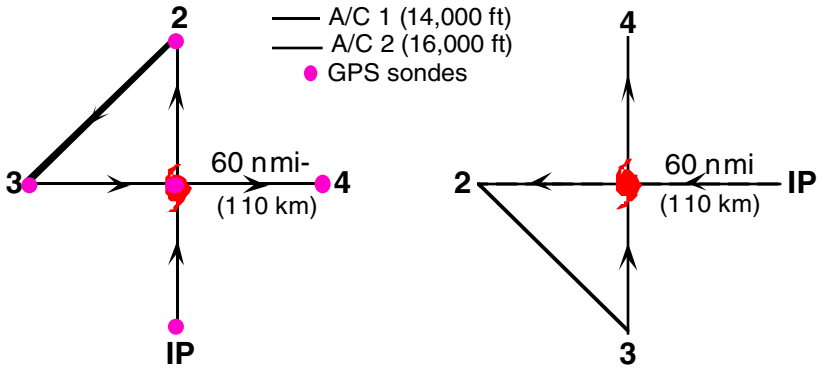

Fig. 26. (a) Coordinated dual-Doppler pattern

• Note 1.	Dual-Doppler pattern flown at beginning and end of mission.
• Note 2.	Set airborne Doppler radar to continuously scan perpendicular to the track on all radial penetrations, and F/AST on upwind legs .

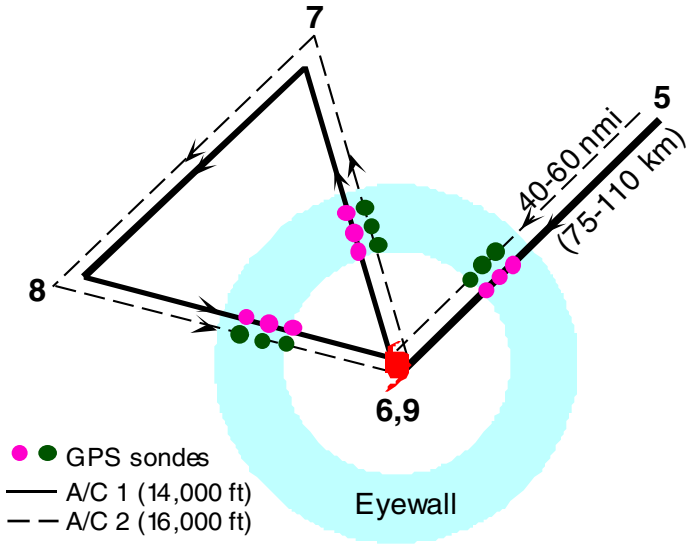

Fig. 26. (b) Eyewall dual-vertical incidence module

• Note 1.	A/C coordinate at **5** and fly parallel at the same ground speed with horizontal spacing of ~1 nmi (2 km).
• Note 2.	Coordination points in relatively clear air at points **5,6,8,** and **9**.
• Note 3.	Straight legs through the eye and eyewall may be used if the eye size is too small to maneuver the aircraft.
• Note 4.	At **6 or 9**, aircraft can break off for short downwind leg along inner edge of eyewall.
• Note 5.	Repeat pattern (**6-7-8-9**), rotating 60° downwind allowing time for final figure-4.
• Note 6.	Set airborne Doppler radar to continuously scan perpendicular to the track on all radial penetrations, and F/AST on upwind legs

STRUCTURE OF EYEWALL CONVECTION EXPERIMENT

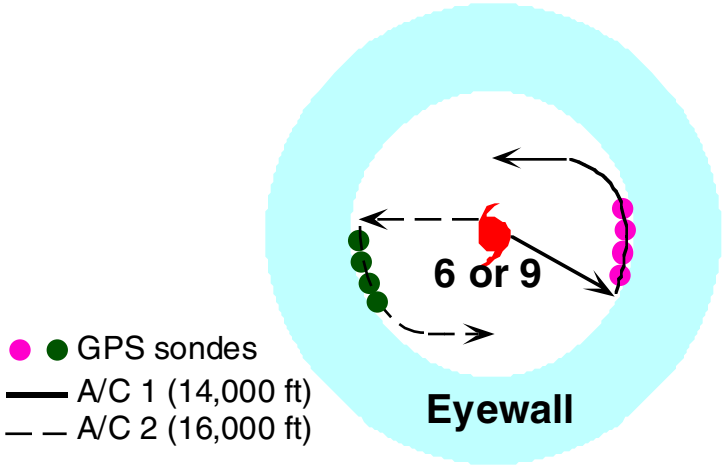

Fig. 26. (c) Inner edge downwind module

• Note 1.	After completion return to dual vertical-incidence module.
• Note 2.	Set airborne Doppler radar to scan F/AST on legs along the eyewall.

18. Clouds and Climate

Program Significance: It has become widely recognized that the physics of clouds and precipitation must be considered in any realistic study of climate change. Clouds and water vapor play a pivotal role in the Earth's heat and radiation budgets. They control the amount of solar energy absorbed by the climate system as well as the infrared radiation emitted to space, and they strongly influence the redistribution of heat throughout the climate system, particularly in the tropics. Tropical clouds and cloud systems, because they lie in the zone of maximum solar input into the atmospheric system, have an important, and probably direct climatic effect. Together with the release of latent heat, the radiative heating of layered clouds in the upper tropical troposphere is a significant source of energy for driving the global circulation. A wide spectrum of tropical cloud types and sizes are important from a climate viewpoint. In some instances, the very small scale microphysical characteristics of the clouds, and interactions with the cloud dynamics, are important on the climate scale.

Small precipitating tropical cumuli, even though their fraction of active convective updrafts may be rather small at any given instant, have an aggregate fraction of total cloud cover, including decaying clouds that is in the range of 20-30%. Hence, they have a direct effect on the radiative transfer in the tropics. In addition, they have an effect on the turbulent mixing in the upper ocean through changes in radiative heating of the sea surface, and through precipitation into the sea surface. The behavior of these small clouds is linked to the ocean, and the ocean to the behavior of these clouds. As sea surface temperature influences the atmosphere on various time and space scales, clouds and upper ocean dynamics are inextricably linked.

This study is complimentary to our continuing work on studies of the dynamics and microphysics of TC convection. The oceanic cumulus provides a simple, easily observed convective entity that has more similarities to TC convective clouds than differences. One advantage is that the precise stage of an oceanic cumulus in its life cycle is usually definable. Thus answering questions about this simpler entity will complement the TC observation program, and greatly aid in the interpretation of more complex data sets from large international field programs. We can exploit our extensive observational capability in the natural convective laboratory at our doorstep (Florida Bay, Bahamas, and the Caribbean Sea) for a relatively meager investment of resources. The result will be an increased understanding of principles that are applicable to convection in general.

The detailed microphysical measurements will also be useful to studies of the characteristics of precipitation in the tropics. The precipitation characteristics derived from this proposed experiment will provide a data base for statistical rainfall studies underway in support of the Florida Bay Restoration Act, the Climate and Global Change Initiative, TOGA COARE, and TRMM. This data set will provide data on isolated topical convective clouds.

Objectives: The experiment will document the kinematics and microphysics of a representative sample of convection, with the initial emphasis being on small precipitating convective cells. We are particularly interested in these clouds` life cycle evolving from first condensation to a precipitating stage (glaciated or not). The specific scientific objectives of this experiment include:

- Building a data base, or census, of small precipitating cumulus; e.g., dimensions (top height, diameter, and depth) and precipitation characteristics that has potential uses in several facets of climatic analysis.

- Documenting the thermodynamic and wind environment of the clouds. Mapping the three dimensional flow field within an active convective feature, and computing the hydrometeor trajectories into the region surrounding the storm using the airborne Doppler radar.

- Collecting rainfall statistics of oceanic convection for use in statistical rainfall studies.

- Perform underflights of the TRMM satellite to obtain a data base suitable for evaluation and improvement of satellite and ground validation rainfall estimation algorithms.

- Testing the capability of determining the hydrometeor distributions from the reflectivity and Doppler mean velocity data at, or near, vertical incidence.

- Documenting the initial electrification and the evolution of the electric field within a sample of clouds.

- Documenting the characteristics of significant convective updrafts - water mass flux, the evolution of ice particles in the updrafts and the conversion rates to ice.

- Studying the relationship between initial and subsequent precipitation formation and the interaction between precipitation loading and the dynamics of the convective cell.

- Studying the interactions between warm cloud and ice microphysics at different stages of cloud development. Emphasis will be placed on the warm rain development versus rain from glaciation.

Mission Description: The experiment calls for a basic one-aircraft cloud structure and evolution sampling module (Fig. 27). This simple module could be executed during dedicated flights over Florida Bay or the Keys, or on targets of opportunity during deployments. Sampling during dedicated flights will emphasize combinations of remote sensing and cloud penetrations, while remote sensing will be used during deployments.

The basic cloud sampling module utilizes one aircraft, equipped with the airborne Doppler radar and microphysics instrumentation, to investigate maritime convective clouds. Desired candidates for study should be convective clouds that can be followed through nearly their entire life cycle. The flight patterns of the basic cloud sampling module are shown in Fig. 27, and are relatively straightforward. The aircraft will make rapid repeated penetrations of the cloud, to sample the microphysical and electric field development at a constant distance below the cloud top. The attempt will be to document the microphysics and electric field development near cloud top from first condensation through a mature cloud stage. At each pass through the cloud, vertical incidence Doppler data will be collected to document the evolution of the vertical velocity field as the cloud matures. These patterns, or penetrations, will be oriented based upon the environmental wind shear vector. The aircraft will release a GPS-sonde or perform an aircraft sounding in the environment of each cloud sampled (in the clear, upwind of the cloud). The aircraft will also attempt to sample the boundary layer air flow, rainfall characteristics, the warm cloud microphysics, and photo-document the cloud behavior.

CLOUDS AND CLIMATE EXPERIMENT

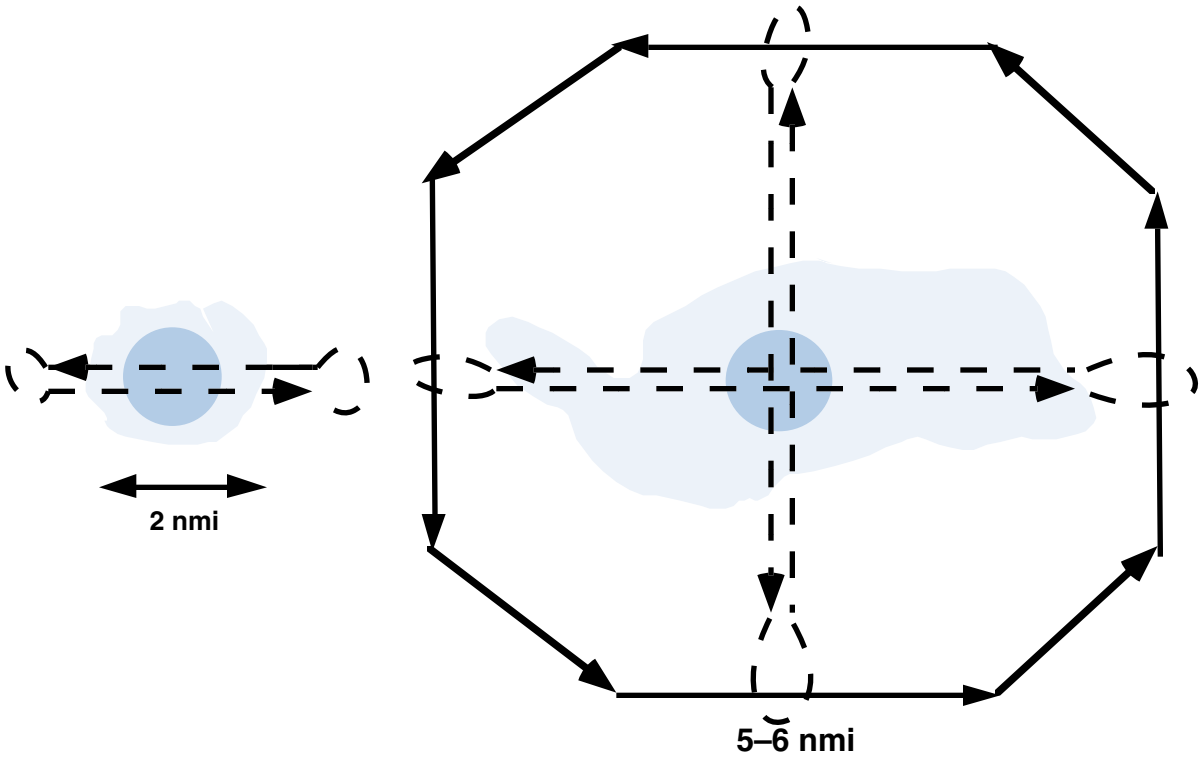

Fig. 27. (a) Initial Cloud Stage **Fig. 27. (b) Growing Stage**

• Note 1.	True airspeed calibration is required.
• Note 2.	The pattern may be flown along any compass heading.
• Note 3.	During initial cloud stage the aircraft conducts rapid penetrations climbing with cloud top from 12,000 ft (3.5 km), climbing with the cloud top on each successive pass. Passes are separated by 1,500 ft (500 m) altitude. Climbs occur away from the convection.
• Note 4.	During the growing stage the aircraft conducts circumnavigation at 5,000 ft (1.5 km) with 5-6 nmi (10-12 km) legs centered on cell to provide F/AST Doppler mapping. The circumnavigation is followed by penetration of the cell at 3,000 (1 km) or 5,000 ft (1.5 km).
• Note 5.	Set the airborne Doppler radar to F/AST scan on all circumnavigation legs, and to scan perpendicular to the track on all penetration legs.

APPENDIX A:

DECISION AND NOTIFICATION PROCESS

DECISION AND NOTIFICATION PROCESS

The decision and notification process is illustrated in Fig. A-1. This process occurs in four steps:

1) A research mission is determined to be probable within 72 h [field program director]. Consultation with the director of HRD and the AOC Project Manager determines: flight platform availability, crew and equipment status, and the type of mission(s) likely to be requested.

2) The Field Program Advisory Panel [Director, HRD, Marks, M. Black, P. Black, R. Black, Cione, Dodge, Gamache, Houston, Kaplan, Powell, Landsea, Willis, McFadden (or AOC designee) meets to discuss possible missions and operational modes. Probable mission determination and approval to proceed is given by the HRD director (or designee).

3) Primary personnel are notified by the field program director [Marks].

4) Secondary personnel are notified by their primary affiliate (Table A-2).

General information, including updates of program status, are provided continuously by tape. Call (305) 221-3679 to listen to the recorded message. During normal business hours, callers should use (305) 361-4400 for other official inquiries and contacts. During operational periods, an MGOC team member is available by phone at (305) 229-4407 or (305) 221-4381. MGOC team leader, and the HRD field program director. (Appropriate telepager phone numbers will be provided to program participants before the start of the field program.)

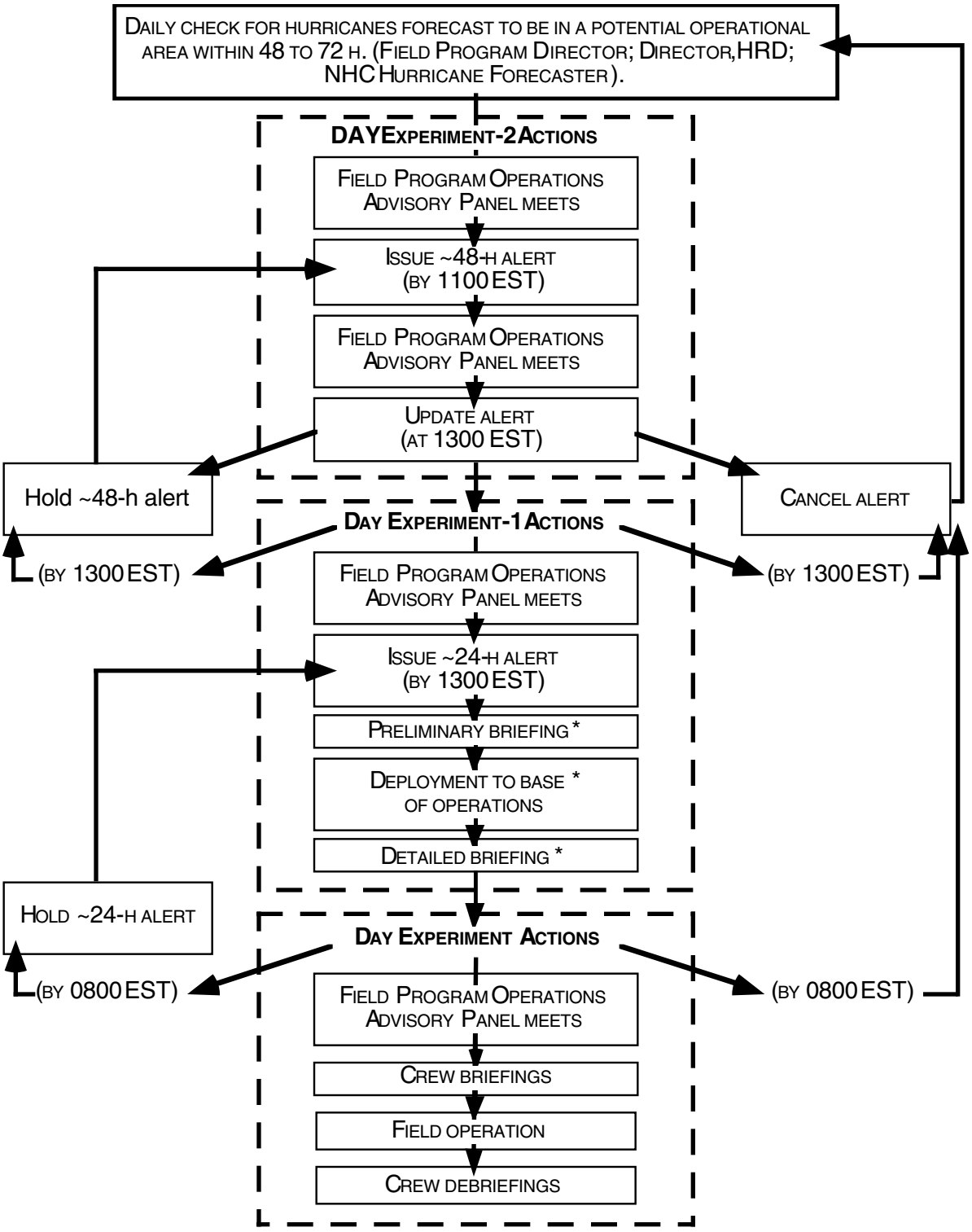

* Time of briefings and deployments are dictated by the crew, scientist, aircraft and storm locations and conditions.

Fig. A-1. Decision and notification process.

Table A-1. Primary Contacts

Name	Agency/title	Home phone	Work phone
H. Willoughby	HRD/Director	305-665-4080	305-361-4502
F. Marks	HRD/Field Program Director	305-271-7443	305-361-4321
P. Black	HRD/Assistant Field Program Director	305-596-4473	305-361-4320
H. Friedman	HRD/MGOC Senior Team Leader	954-962-8021	305-361-4319
J. McFadden	AOC/Project Manager for Hurricane Research	305-666-3622 813-839-7550	813-828-3310 x3076
J Parrish	AOC/Alternate Project Manager for Hurricane Research	813-933-2302	813-828-3310 X3077
S. White	AOC/Project Manager for Hurricane Surveillance	813-837-6276	813-828-3310 x3072
J. Pavone	CARCAH/Liaison	305-248-3422 434-3420[1]	305-229-4474
Synoptic Analysis Branch	NESDIS/Liaison		301-763-8444 301-763-8445
K. Katsaros	AOML/Director	305-361-5543	305-361-4302 305-361-4300
J. Goldman	OAR/PA		301-713-2483
F. Lepore	TPC/NHC/PA	305-235-6670	305-229-4404
MacDill Global[2]			813-828-3109 813-828-3356 813-828-3881

1 DSN: Defense Switched Network (replaced Autovon).

2 MacDill Global phone patch; used to contact the NOAA aircraft during missions.

Table A-2. Secondary Contacts

Name/group	Home phone	Work phone	Contacted by
HRD participants			F. Marks/MGOC
AOC participants			J. McFadden
R. McCann/AOC	813-522-3515	813-828-3310 x3125	J. McFadden
FAA			AOC
LT.COL Gale Carter	601-928-7681	601-377-3207	CARCAH
53rd Wea. Recon. Sqdn.		597-3207[1]	
J. Jarrell/TPC/NHC	305-234-5389	305-229-4488	F. Marks/MGOC
C. Burr/TSAF/TPC/NHC	305-667-9932	305-229-4430	F. Marks/MGOC
Sr. Duty Meteorologist/NCEP	----	301-763-8298 301-763-8364 301-763-8076	F. Marks/MGOC
E. Walsh	303-447-1694	303-497-6357	F. Marks
W.-C. Lee/NCAR	303-939-8291	303-497-8814	F. Marks
P. Hildebrand/NCAR	303-443-6648	303-497-2050	F. Marks
S. Lord/NCEP	301-249-7713	301-763-8005	S. Aberson
C. Velden/U. Wisconsin	608-274-5500	608-262-9168	S. Aberson
Craig Bishop/PSU		814-865-9500	S. Aberson
Julian Heming/UKMO		44-0-1344-854494	S. Aberson
Rolf Langland/NRL		831-656-4786	S. Aberson
Zoltan Toth/NCEP		301-763-8545	S. Aberson
J. Hallett/DRI	702-747-0776	702-677-3117 702-784-6780	R. Black
J. Carswell/ U. Massachusetts	413-549-7467	413-545-4867	P. Black
P. Chang/NESDIS	703-670-8285	301-763-8231x167	P. Black
T. Gobel/OFCM	301-589-5771 717-637-1284	301-427-2002	P. Black
I. Popstefanija/Quadrant	413-549-0567	413-545-2136	P. Black
H. Selsor/NRL	504-641-5674	601-688-4760	P. Black
P. Vachon/AES	613-825-8425	613-995-1575	P. Black
E. Meindl/NDBC	228-466-9529	228-688-1717	M. Powell/S. Houston
M. Burdett/NDBC	601-798-1151	228-688-2868	M. Powell/S. Houston
T. Rienhold/Clemson University	----	864-656-5941	M. Powell/S. Houston
J. Schroeder/TTU	----	806-742-3476x288	M. Powell/S. Houston
J. Straka/U. Oklahoma	----	405-325-6561	M. Powell/S. Houston
R. Jensen/USACE	----	601-634-2101	S. Houston
S. Gill/NOS	----	301-713-2840	S. Houston
K. Knupp/U. Alabama/Huntsville	----	205-922-5762	P. Dodge / S. Houston
B. McCaul/U. Alabama/Huntsville	----	205-922-5837	P. Dodge/ S. Houston
J. Wurman/U. Oklahoma	----	405-325-7689	P. Dodge/ S. Houston

[1] DSN: Defense Switched Network (replaced Autovon).

APPENDIX B:

Aircraft Scientific Instrumentation

Aircraft Scientific Instrumentation

Table B lists the basic instrumentation systems normally available on NOAA/AOC WP-3D aircraft missions (N42RF and N43RF). Because of operational constraints, all of the instrumentation listed in the table may not be available on a single sortie.

Table B. NOAA/AOC WP-3D instrumentation

	N42RF	N43RF
NAVIGATIONAL		
Position, position update	INE and GPS	INE and GPS
Radar and pressure altitude	Radar and pressure altimeters	Radar and pressure altimeters
METEOROLOGICAL		
Free air temperature (derived)	Rosemount total temperature	Rosemount total temperature
Static and dynamic pressure	Rosemount	Rosemount
Dew point temperature	General Eastern	General Eastern
Horizontal wind (computed)	INE/TAS (computed); GPS	INE/TAS (computed); GPS
Vertical wind (computed)	High-resolution angle of attack, pitch angle, vertical acceleration	High-resolution angle of attack, pitch angle, vertical acceleration
Temperature and momentum flux	Radome-mounted gust probe and fast-response total temperature	Radome-mounted gust probe and fast-response total temperature
RADIATION		
Sea surface temperature	AOC modified PRT-5	AOC modified PRT-5
CO_2 air temperature	AOC modified PRT-5	AOC modified PR-5
CLOUD PHYSICS		
Small cloud droplet spectrum	FSSP forward scattering probe	FSSP forward scattering probe
Cloud droplet spectrum	PMS Knollenberg 2-D Gray probe	PMS Knollenberg 2-D Gray probe
Hydrometeor size spectrum	PMS Knollenberg 2-D Gray probe	PMS Knollenberg 2-D Gray probe
Cloud liquid water	Johnson-Williams hot wire	Johnson-Williams hot wire
Total liquid water	PMS King probe	
Cloud particle charge	DRI Particle charge probe	
RADAR		
Radar reflectivity	C-band PPI lower-fuselage (LF), 360° scan (horizontal)[1]	C-band PPI lower-fuselage (LF), 360° scan (horizontal)[1]
Radar reflectivity and radial velocity	Doppler X-band RHI tail (TA), 360° scan (vertical)[1] (French antenna)	Doppler X-band RHI tail (TA), 360° scan (vertical)[1] (AOC antenna) WARDS C-band nose (NO), 180° scan (horizontal)
MISCELLANEOUS		
Cloud structure; surface wind	Video photography (3 axis)	Video photography (3 axis)
Vertical atmospheric sounding	GPS Dropwindsonde system	GPS Dropwindsonde system
Oceanic temperature, current and salinity profile	AXBT, AXCP, AXCTD receivers and laptop	AXBT, AXCP, AXCTD receivers and laptop
Stable water isotope ratio	University of Houston water collection device	University of Houston water collection device
Data transmission	Aircraft-satellite-data-link (ASDL)[2]	ASDL[2]
Two components of electric field	DRI system	
Clear-air winds	Chaff sondes	
Surface wind speed & direction	KuSCAT/CSCAT SFMR[3]	SFMR[3]
Surface wave spectra & altimetry		SRA[4]
Ozone concentration		AOML O_3 instrument

[1] LF radar data recorded every other scan. TA radar recorded every scan.

[2] An HRD airborne workstation will be installed on each NOAA/AOC WP-3D.

[3] Ku-band and C-band scatterometer and Stepped frequency microwave radiometer

[4] Scanning radar altimeter

APPENDIX C:

Calibration; Scientific Crew Lists; Data Buoys; DOD/NWS RAWIN/RAOB and NWS Coastal Land-based Radar Locations/Contacts

Calibration; Scientific Crew Lists; Data Buoys; DOD/NWS RAWIN/RAOB and NWS Coastal Land-based Radar Locations/Contacts

C.1 En-Route Calibration of Aircraft Systems

Instrument calibrations are checked by flying aircraft intercomparison patterns whenever possible during the hurricane field program or when the need for calibration checks is suggested by a review of the data. In addition, an over flight of a surface pressure reference is advisable en route or while on station when practicable. Finally, all flights en route to and from the storm are required to execute a true airspeed (TAS) calibration pattern. This pattern is illustrated in Fig. C-1.

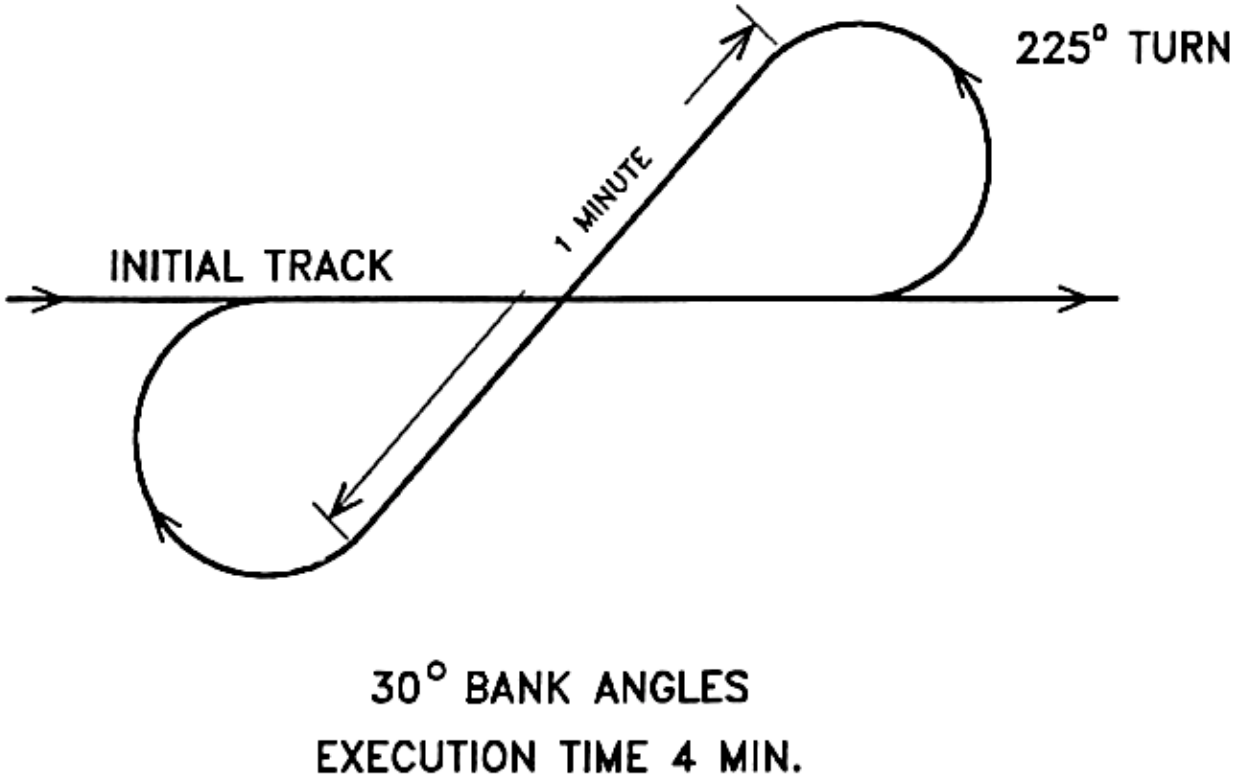

Fig. C-1 En-Route TAS calibration pattern.

C.2 Aircraft Scientific Crew Lists

Table C-2.1 Hurricane Synoptic-Flow Experiment (single-option, dual-aircraft mission)

Position	N42RF	N43RF
Lead Project Scientist	F. Marks	J. Gamache
Cloud Physics Scientist	(radar scientist)	(radar scientist)
Radar/Doppler Scientist	M. Black	S. Goldenberg
Dropwindsonde Scientists	J. Kaplan	S. Aberson or C. Landsea
Workstation Scientist	P. Leighton	P. Dodge
C-SCAT/SFMR Scientist	P. Chang or J. Carswell	

Table C-2.2 Extended Cyclone Dynamics Experiment (single-option, single-aircraft mission)

Position	N43RF	N42RF	N43RF
Lead Project Scientist	H. Willoughby	P. Black	F. Marks
Cloud Physics Scientist	R. Black	(radar scientist)	J. Cione
Radar/Doppler Scientist	S. Goldenberg	J. Gamache	N. Dorst
Dropwindsonde Scientist	M. Black	J. Kaplan	C. Landsea
Workstation Scientist	P. Leighton	J. Griffin	P. Dodge
C-SCAT/SFMR Scientist		P. Chang or J. Carswell	

Table C-2.3 Vortex Motion and Evolution Experiment (single-option, dual-aircraft mission)

Position	N43RF	N42RF
Lead Project Scientist	M. Black	J. Gamache
Cloud Physics Scientist	R. Black	(radar scientist)
Radar/Doppler Scientist	J. Cione	N. Dorst or S. Goldenberg
Dropwindsonde Scientist	F. Marks	S. Aberson or C. Landsea
Workstation Scientist	P. Leighton	P. Dodge
C-SCAT/SFMR Scientist	P. Chang or J. Carswell	P. Black

Table C-2.4 Tropical Cyclogenesis Experiment (single-option, dual-aircraft mission)

Position	N43RF	N42RF
Lead Project Scientist	P. Black	H. Willoughby
Cloud Physics Scientist	R. Black	S. Goldenberg
Radar/Doppler Scientist	J. Gamache	N. Dorst or J. Cione
Dropwindsonde Scientist	M. Black	F. Marks
Workstation Scientist	P. Leighton	P. Dodge
SRA and C-SCAT/SFMR Scientists	E. Walsh	P. Chang or J. Carswell

Table C-2.5 Tropical Cyclone Wind fields Near Landfall Experiment (dual-option, single-aircraft mission)

Position	N43RF
Lead Project Scientist	P. Dodge
Cloud Physics Scientist	(radar scientist)
Radar/Doppler Scientist	J. Gamache
Dropwindsonde Scientist	C. Landsea
Workstation Scientist	P. Leighton
SRA Scientist	E. Walsh

Table C-2.6 Tropical Cyclone Air-sea interaction Experiment (multi-option, mulit-aircraft mission)

Position	N42RF	N43RF
Lead Project Scientist	P. Black	L. Shay
Cloud Physics Scientist	(radar scientist)	(radar scientist)
Radar/Doppler Scientist	J. Gamache	M. Black
Boundary Layer Scientist	J. Cione	E. Uhlhorn
Dropwindsonde Scientist	(boundary layer scientist)	(boundary layer scientist)
Workstation Scientist	P. Leighton	P. Dodge
C-SCAT/SFMR/SRA Scientist	P. Chang or J. Carswell	E. Walsh

Table C-2.7 Rainband Structure Experiment (dual-option, dual-aircraft mission)

Position	N42RF	N43RF
Lead Project Scientist	P. Black	F. Marks
Cloud Physics Scientist	R. Black	J. Cione
Radar/Doppler Scientist	J. Gamache	N. Dorst
Dropwindsonde Scientist	M. Black	S. Goldenberg
Workstation Scientist	P. Leighton	P. Dodge
C-SCAT/SFMR and SRA Scientists	P. Chang or J. Carswell	E. Walsh

Table C-2.8 Electrification of Tropical Cyclone Convection (dual-option, single-aircraft mission)

Position	N42RF
Lead Project Scientist	R. Black
Cloud Physics Scientist	N. Dorst
Radar/Doppler Scientist	M. Black
Dropwindsonde Scientist	S. Goldenberg
Workstation Scientist	P. Leighton
C-SCAT/SFMR Scientist	P. Chang or J. Carswell

Table C-2.9 Structure of Eyewall Convection Experiment (SECE) (single-option, dual-aircraft mission)

Position	N43RF	N42RF
Lead Project Scientist	F. Marks	M. Black
Cloud Physics Scientist	R. Black	N. Dorst
Radar/Doppler Scientist	J. Gamache	P. Dodge
Dropwindsonde Scientist	S. Aberson	S. Goldenberg
Workstation Scientist	P. Leighton	J. Griffin
SRA and C-SCAT/SFMR Scientists	E. Walsh	P. Chang or J. Carswell

Table C-2.10 Clouds and Climate Study (single-option, single-aircraft mission)

Position	N42RF
Lead Project Scientist	P. Willis
Cloud Physics Scientist	R. Black
Radar/Doppler Scientist	P. Dodge or J. Cione
Dropwindsonde Scientist	C. Landsea
Workstation Scientist	P. Leighton

C.3 Buoy/Platform Over flight Locations[1]

Table C-3.1 Moored Buoys

Station Identifier	Type of Station[2]	Location Lat. (N)	Location Lon (W)	Area	Special Obs/ Comments[4]
44007*	3D /D	43.53	70.14	PORTLAND	A
44005*	6N /D	42.90	68.89	GULF OF MAINE	A
44013	3D /D	42.35	70.69	BOSTON	---
44011*	6N /D	41.08	66.58	GEORGES BANK	A
44008*	3D /V	40.50	69.43	NANTUCKET	A
44025	3D /D	40.25	73.17	LONG ISLAND	DW
44004*	6N /D	38.46	70.69	HOTEL	---
44009*	3D /V	38.46	74.70	DELAWARE BAY	---
44014	3D /D	36.58	74.83	VIRGINIA BEACH	DW
41001*	6N /D	34.68	72.64	E. HATTERAS	A
41002*	6N /D	32.28	75.20	S. HATTERAS	---
41004*[3]	3D /D	32.51	79.10	EDISTO	DW
41009	6N /D	28.50	80.18	CANAVERAL	---
41010	6N /D	28.89	78.55	CANAVERAL EAST	---
42036*	3D /D	28.51	84.51	W. TAMPA	DW
42003*	10D /V	25.94	85.91	E. GULF	A
42040	3D /D	29.18	88.29	MOBILE SOUTH	A
42007*	3D /V	30.10	88.77	OTP	A
42001*[3]	10D /V	25.93	89.65	MID GULF	A
42002*	10D /V	25.89	93.57	W. GULF	A
42035*	3D /V	29.25	94.41	GALVESTON	---
42019*	3D /D	27.92	95.35	FREEPORT	---
42020*[3]	3D /D	26.92	96.70	CORPUS CHRISTI	
41008*[3]	3D /V	31.40	80.87	GRAYS REEF	
42039	3D /V	28.78	86.04	PENSACOLA S.	A

[1] Tables C-3.1 and C-3.4 were updated with information from the **Data Platform Status Report (May 14, 1999)**, NOAA/National Data Buoy Center (NDBC), Stennis Space Center, MS 39529-6000, for the period **May 6 – May 13, 1999**. (Also, the NDBC report lists the location of drifting buoys o/a **May 6 – May 13, 1999**). See subsequent editions of this weekly NDBC report for later information. Tables C-3.2, C-3.3, and portions of C-3.4 were updated with information from **National Weather Service Offices and Stations** (May 1999), NOAA/NWS, W/MB31, Silver Spring, MD.

[2]

Hull Type		Anemometer Height	
10D	-	10-m discus buoy	10.0 m
6N	-	6-m NOMAD buoy	5.0 m
3D	-	3-m discus buoy	5.0 m

Payload types: /G = GSBP; /D = DACT; /V = VEEP.

[3] Note remarks section of NDBC report (**May 7, 1999**); see latest edition of NDBC **Data Platform Status Report** for current status.

[4] A = 10-min data (continuous); R = rainfall; DW = directional wave spectra.

* Base funded station of the National Weather Service (NWS); however, all stations report data to NWS.

Table C-3.2 Automated over-water surface buoy and instrumented platform locations

Station Identifier/Name	Type of Station[1]	Location Lat. (N)	Location Lon (W)	Area
MIBF/Miami Beach	DARDC	25.8	80.1	FL COAST
FLGF/Flamingo	DARDC	25.2	80.9	FL COAST
NAPF/Naples	DARDC	26.1	81.8	FL COAST
—/Sunshine Skyway Bridge	PORTS	27.7	82.6	FL COAST
TUPF1/Turkey Point	DARDC	29.9	84.5	FL COAST
—/Springmaid Pier	DARDC	36.7	78.9	SC COAST
—/Holden Beach	DARDC	33.9	78.7	NC COAST
—/Kure Beach	DARDC	34.0	77.9	NC COAST
—/Topsail Beach	DARDC	34.5	77.4	NC COAST
Mobile Platforms:				
P92/Salt Point	RAMOS	29.5	91.6	GULF MEX

[1] AMOS = Automatic Marine (Meteorological) Observing Station (full parameter)
DARDC = Device for Automatic Remote Data Collection (partial parameter)
PORTS = Physical Oceanographic Real-Time System (NOS)
RAMOS = Remote Automatic Meteorological Observing Station (full parameter)

Table C-3.3 C-MAN sites[1]

Station Identifier	Station Name/ Payload Type	Location		Area	Comments[3]	Height (m)
		Lat. (N)	Lon (W)			
MDRM1*	Mt. Desert Rock, ME/D	43.97	68.13	ME COAST	---	22.6
MISM1*	Matinicus Rock, ME/D	43.78	68.86	ME COAST	---	16.5
IOSN3*	Isle of Shoals, NH/D	42.97	70.62	NH COAST	---	19.2
BUZM3*	Buzzards Bay, MA/V	41.40	71.03	MA COAST	A	24.8
ALSN6*[2]	Ambrose Light, NY/V	40.46	73.83	NY COAST	---	49.1
TPLM2*	Thomas Point, MD/V	38.90	76.44	MD COAST	---	18.0
CHLV2*	Chesapeake Light, VA/D	36.90	75.71	VA COAST	A	43.3
DUCN7*[2]	Duck Pier, NC/V	36.18	75.75	NC COAST	A	20.4
DSLN7*[2]	Diamond Shoals Light, NC/D	35.15	75.30	NC COAST	A, DP	46.6
CLKN7*	Cape Lookout, NC/V	34.62	76.52	NC COAST	A	9.8
FPSN7*[2]	Frying Pan Shoals, NC/D	33.49	77.59	NC COAST	A	44.2
FBIS1*	Folly Island, SC/D	32.68	79.89	SC COAST	A	9.8
SPGF1*	Settlement Point, GBI/M	26.70	78.99	GR BAHAMA	A	9.8
SAUF1*	St. Augustine, FL/V	29.86	81.26	FL COAST	A	16.5
LKWF1*	Lake Worth, FL/M	26.61	80.03	FL COAST	A	13.7
FWYF1*	Fowey Rocks, FL/V	25.59	80.10	FL COAST	A	43.9
MLRF1*	Molasses Reef, FL/V	25.01	80.38	FL COAST	---	15.8
SMKF1*	Sombrero Key, FL/M	24.63	81.11	FL COAST	---	48.5
SANF1*	Sand Key, FL/V	24.46	81.88	FL COAST	A	13.1
LONF1*	Long Key, FL/M	24.84	80.86	FL COAST	---	7.0
DRYF1*	Dry Tortugas, FL/M	24.64	82.86	FL COAST	---	5.7
VENF1*[2]	Venice, FL/V	27.07	82.45	FL COAST	A	11.6
CDRF1*[2]	Cedar Key, FL/V	29.14	83.03	FL COAST	A	10.0
CSBF1*	Cape San Blas, FL/M	29.67	85.36	FL COAST	A	9.8
KTNF1*	Keaton Beach, FL/M	29.82	83.59	FL COAST	A	10.0
DPIA1*[2]	Dauphin Island, AL/V	30.25	88.07	AL COAST	---	17.4
BURL1*	Southwest Pass, LA/M	28.90	89.43	LA COAST	A	30.5
GDIL1*	Grand Isle, LA/M	29.27	89.96	LA COAST	A	15.8
SRST2*	Sabine, TX/M	29.67	94.05	TX COAST	A	12.5
PTAT2*	Port Aransas, TX/M	27.83	97.05	TX COAST	A	14.9

1 Coastal-Marine Automated Network (C-MAN) stations are located on coastal headlands, piers, or offshore platforms. Payload types, shown next to the station's name (after the "/") are: D = DACT; V = VEEP; M=MARS; and I = Industry-supplied. C-MAN anemometer heights are listed in the **C-MAN User's Guide**.

2 Note remarks section of NDBC report (**May 14, 1999**); see latest edition of NDBC **Data Platform Status Report** for current status.

3 A = 10-min data (continuous); DP = dew point; R = rainfall; DW = directional wave spectra.

* Primarily for National Weather Service (NWS) support; however, all stations report data to NWS.

Table C-3.4 NOS next generation meteorological-tide stations*

Station Name	Location Lat. (N)	Lon (W)
Bermuda Pier, St. Georges Island	32.37	64.70
Eastport Bay, ME	44.90	66.98
Bergen Point West, NY	40.63	74.14
Solomons Island, MD	38.32	76.45
Kiptopeke, VA	37.17	75.98
Lewisetta, Potomac River, VA	37.99	76.45
Sewells Point, VA	36.95	76.32
Chesapeake Bay Bridge, VA	36.97	76.10
Duck, FRF Pier, NC	36.18	75.74
Cape Hatteras Fishing Pier, NC	35.22	75.63
Mayport, FL	30.39	81.42
St. Augustine Beach, FL	29.85	81.25
Virginia Key, FL	25.72	80.15
Naples, FL	26.12	81.80
St. Petersburg, FL	27.75	82.62
McKay Bay, FL[1]	27.90	82.42
Clearwater Beach, FL	27.97	82.43
Apalachicola Bay, FL	29.72	85.00
Panama City Beach, FL	30.20	85.87
Morgans Point, TX	29.47	94.92
Eagle Point, TX	29.35	94.77
Port Bolivar, TX	29.30	94.79
Galveston Pier, TX	29.28	94.78
Galveston (offshore), TX	29.12	94.50
Freeport, TX	28.94	95.30
Corpus Christi, TX	27.57	97.22
Port Mansfield, TX	26.55	97.42
Cochino Pequeno	15.85	86.50

* Quality controlled data from these platforms can be obtained from NDBC's **Seaboard Bulletin Board Service** soon after the fact. For information contact NDBC or Sam Houston at (305) 361-4509.

1 Special project stations that have no satellite radio and non-real time data.

Table C-3.5 Automated Surface Observing System (ASOS) sites

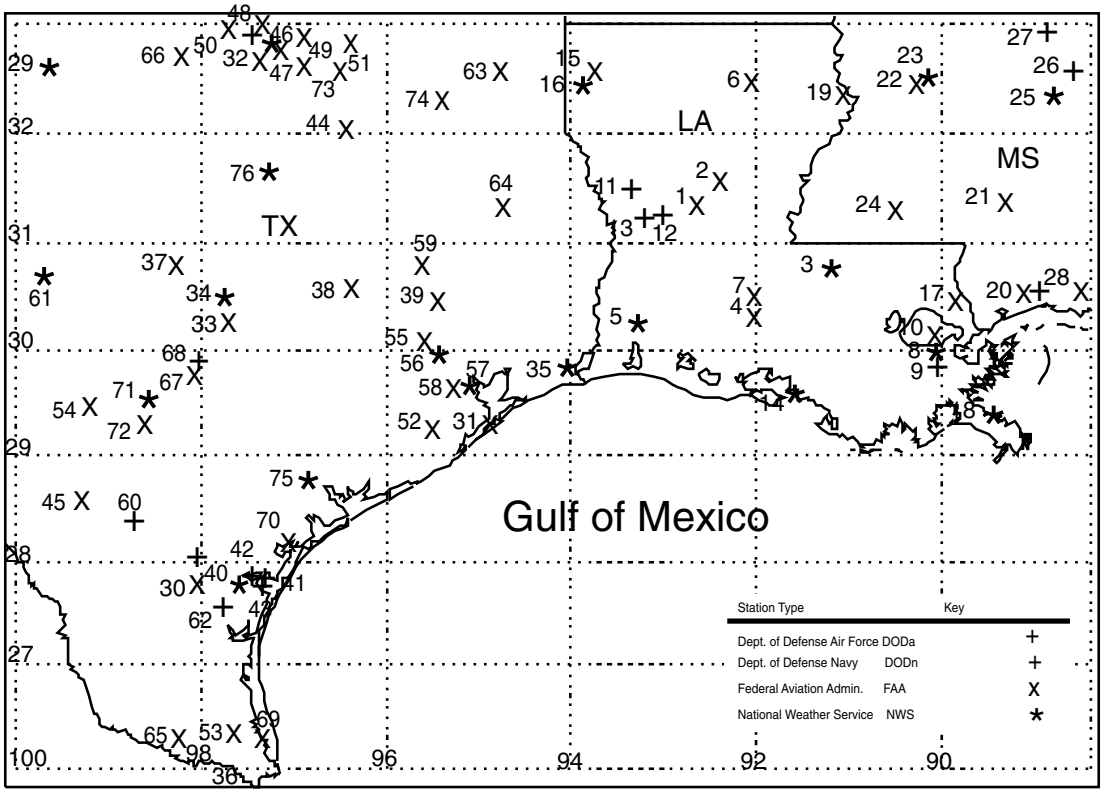

#	ID	Agency	Site Name	Lat. (N)	Lon (W)	#	ID	Agency	Site Name	Lat. (N)	Lon (W)
1	KAEX	FAA	Alexandria, LA	31.33	92.56	39	KCXO	FAA	Conroe, TX	30.36	95.41
2	KESF	FAA	Alexandria, LA	31.40	92.29	40	KCRP	NWS	Corpus Christi, TX	27.77	97.51
3	KBTR	NWS	Baton Rouge, LA	30.54	91.95	41	KNGP	DODn	Corpus Christi, TX	27.68	97.29
4	KLFT	FAA	Lafayette, LA	30.20	91.99	42	KNGW	DODn	Corpus Christi, TX	27.72	97.44
5	KLCH	NWS	Lake Charles, LA	30.12	93.23	43	KNVT	DODn	Corpus Christi, TX	27.63	97.31
6	KMLU	FAA	Monroe, LA	32.51	92.03	44	KCRS	FAA	Corsicana, TX	32.03	96.40
7	KARA	FAA	New Iberia, LA	30.29	91.99	45	KCOT	FAA	Cotulla, TX	28.45	99.22
8	KMSY	NWS	New Orleans, LA	29.99	90.02	46	KDAL	FAA	Dallas, TX	32.85	96.86
9	KNBG	DODn	New Orleans, LA	29.84	90.02	47	KRBD	FAA	Dallas, TX	32.68	96.86
10	KNEW	FAA	New Orleans, LA	30.05	90.03	48	KDFW	NWS	Dallas/Fort Worth, TX	32.90	97.02
11	FTPK1	DODa	Fort Polk, LA	31.41	93.30	49	KFTW	FAA	Fort Worth, TX	32.83	97.36
12	FTPK2	DODa	Fort Polk, LA	31.11	92.97	50	KNFW	DOD	Fort Worth, TX	32.77	97.43
13	FTPK3	DODa	Fort Polk, LA	31.12	93.16	51	KAFW	FAA	Fort Worth, TX	32.97	97.32
14	KP92	NWS	Salt Point, LA	29.56	91.53	52	KGLS	FAA	Galveston, TX	29.27	94.86
15	KDTN	FAA	Shreveport, LA	32.54	93.74	53	KHRL	FAA	Harlingen, TX	26.23	97.66
16	KSHV	NWS	Shreveport, LA	32.45	93.82	54	KHDO	FAA	Hondo, TX	29.36	99.17
17	KASD	FAA	Slidell, LA	30.34	89.82	55	KDWH	FAA	Houston, TX	30.07	95.56
18	K7R1	NWS	Venice, LA	29.26	89.36	56	KIAH	NWS	Houston, TX	29.99	95.36
19	KTVR	FAA	Vicks./Tallulah, LA	32.35	91.03	57	KHOU	NWS	Houston, TX	29.64	95.28
20	KGPT	FAA	Gulfport, MS	30.41	89.08	58	KT02	FAA	Houston, TX	29.52	95.24
21	KHBG	FAA	Hattiesburg, MS	31.27	89.26	59	KUTS	FAA	Huntsville, TX	30.74	95.59
22	KHKS	FAA	Jackson, MS	32.34	90.22	60	KNMT	DODn	Ingleside, TX	28.24	98.72
23	KJAN	NWS	Jackson, MS	32.32	90.08	61	KJCT	NWS	Junction, TX	30.51	99.77
24	KMCB	FAA	McComb, MS	31.18	90.47	62	KNQI	DODn	Kingsville, TX	27.50	97.81
25	KMEI	NWS	Meridian, MS	32.34	88.75	63	KGGG	FAA	Longview, TX	32.39	94.71
26	KNMM	DODn	Meridian, MS	32.55	88.54	64	KLFK	FAA	Lufkin, TX	31.23	94.75
27	KNJW	DODn	Meridian Range, MS	32.80	88.83	65	KMFE	FAA	McAllen, TX	26.18	98.24
28	KPQL	FAA	Pascagoula, MS	30.46	88.53	66	KMWL	FAA	Mineral Wells, TX	32.78	98.06
29	KABI	NWS	Abilene, TX	32.41	99.68	67	K3R5	FAA	New Braunfels, TX	29.71	98.05
30	KALI	FAA	Alice, TX	27.74	98.02	68	KNOG	DODn	Orange Grove, TX	27.89	98.04
31	KLBX	FAA	Angelton/L. Jack., TX	29.12	95.46	69	KT31	FAA	Port Isabel, TX	26.16	97.34
32	KF54	FAA	Arlington, TX	32.66	97.10	70	KRKP	FAA	Rockport, TX	28.08	97.04
33	KBSM	FAA	Austin, TX	30.18	97.68	71	KSAT	NWS	San Antonio, TX	29.53	98.46
34	KAUS	NWS	Austin, TX	30.29	97.70	72	KSSF	FAA	San Antonio, TX	29.34	98.47
35	KBPT	NWS	Beau./Port Art., TX	29.95	94.02	73	KTRL	FAA	Terrel, TX	32.71	96.27
36	KBRO	NWS	Brownsville, TX	25.91	97.42	74	KTYR	FAA	Tyler, TX	32.36	95.40
37	KBMQ	FAA	Burnet, TX	30.74	98.23	75	KVCT	NWS	Victoria, TX	28.86	96.93
38	KCLL	FAA	College Station, TX	30.58	96.36	76	KACT	NWS	Waco, TX	31.62	97.23

Table C-3.5 Automated Surface Observing System (ASOS) sites (continued)

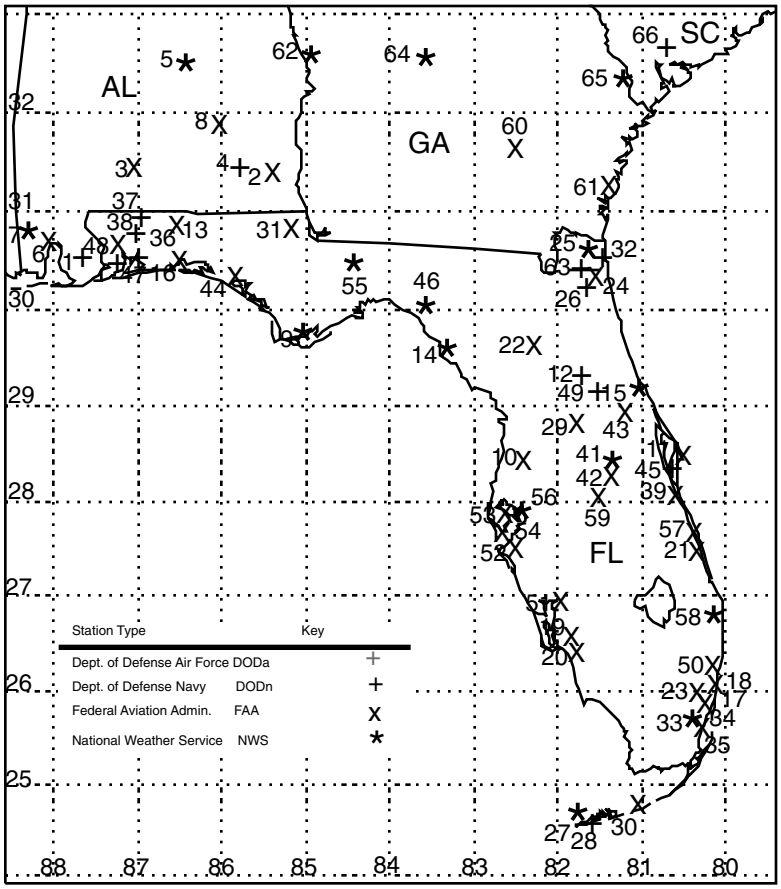

#	ID	Agency	Site Name	Lat. (N)	Lon (W)	#	ID	Agency	Site Name	Lat. (N)	Lon (W)
1	KNBJ	DODn	Barin, AL	30.39	87.63	34	KOPF	FAA	Miami, FL	25.91	80.23
2	KDHN	FAA	Dothan, AL	31.31	85.44	35	KTMB	FAA	Miami, FL	25.64	80.43
3	KGZH	FAA	Evergreen, AL	31.42	87.05	36	KNDZ	DODn	Milton, FL	30.70	87.02
4	KLOR	DODn	Fort Rucker, AL	31.36	85.75	37	KNFJ	DODn	Milton, FL	30.51	86.95
5	KMGM	NWS	Montgomery, AL	32.30	86.41	38	KNSE	DODn	Milton, FL	30.73	87.02
6	KBFM	FAA	Mobile, AL	30.61	88.06	39	KMLB	FAA	Melbourne, FL	28.10	80.64
7	KMOB	NWS	Mobile, AL	30.69	88.25	41	KMCO	NWS	Orlando, FL	28.42	81.33
8	KTOI	FAA	Troy, AL	31.86	86.01	42	KORL	FAA	Orlando, FL	28.55	81.34
9	KAQQ	NWS	Apalachicola, FL	29.73	85.02	43	KSFB	FAA	Orlando, FL	28.78	81.25
10	KBKV	FAA	Brooksville, FL	28.47	82.45	44	KPFN	FAA	Panama City, FL	30.21	85.89
11	CCAS1	FAA	Cape Canaveral, FL	28.48	80.58	45	PAFB1	DODa	Patrick AFB, FL	28.23	80.60
12	KNZC	DODn	Cecil, FL	30.21	81.87	46	K40J	NWS	Perry Foley, FL	30.07	83.57
13	KCEW	FAA	Crestview, FL	30.77	86.52	47	KNPA	DODn	Pensacola, FL	30.36	87.32
14	KCTY	NWS	Cross City, FL	29.55	83.11	48	KPNS	FAA	Pensacola, FL	30.48	87.19
15	KDAB	NWS	Daytona Beach, FL	29.17	81.06	49	KNAE	DODn	Pinecastle, FL	29.14	81.63
16	KDTS	FAA	Destin, FL	30.39	86.47	50	KPMP	FAA	Pompano Beach, FL	26.25	80.11
17	KFLL	FAA	Fort Lauderdale, FL	26.07	80.15	51	KPGD	FAA	Punta Gorda, FL	26.92	81.99
18	KFXE	FAA	Fort Lauderdale, FL	26.20	80.13	52	KSRQ	FAA	Sar./Braden., FL	27.41	82.56
19	KFMY	FAA	Fort Myers, FL	26.58	81.86	53	KPIE	FAA	St. Peter./Clear., F	27.91	82.69
20	KRSW	FAA	Fort Myers, FL	26.53	81.77	54	KSPG	FAA	St Petersburg FL	27.77	82.63
21	KFPR	FAA	Fort Pierce, FL	27.50	80.38	55	KTLH	NWS	Tallahassee, FL	30.39	84.35
22	KGNV	FAA	Gainesville, FL	29.69	82.28	56	KTPA	NWS	Tampa, FL	27.96	82.54
23	KHWO	FAA	Hollywood, FL	26.00	80.24	57	KVRB	FAA	Vero Beach, FL	27.66	80.41
24	KCRG	FAA	Jacksonville, FL	30.34	81.51	58	KPBI	NWS	West Palm Beach, FL	26.68	80.10
25	KJAX	NWS	Jacksonville, FL	30.49	81.69	59	KGIF	FAA	Winter Haven, FL	28.06	81.76
26	KNIP	DODn	Jacksonville, FL	30.23	81.67	60	KAMG	FAA	Alma, GA	31.54	82.51
27	KEYW	NWS	Key West, FL	24.55	81.75	61	KSSI	FAA	Brunswick, GA	31.15	81.39
28	KNQX	DODn	Key West, FL	24.57	81.68	62	KCSG	NWS	Columbus, GA	32.52	84.94
29	KLEE	FAA	Leesburg, FL	28.82	81.81	63	KNBQ	DODn	Kings Bay, GA	30.79	81.56
30	KMTH	FAA	Marathon, FL	24.73	81.05	64	KMCN	NWS	Macon, GA	32.69	83.65
31	KMAI	FAA	Marianna, FL	30.84	85.18	65	KSAV	NWS	Savannah, GA	32.12	81.20
32	KNRB	DODn	Mayport, FL	30.40	81.42	66	KNBC	DODn	Beaufort, SC	32.49	80.70
33	KMIA	NWS	Miami, FL	25.79	80.32						

Table C-3.5 Automated Surface Observing System (ASOS) sites(continued)

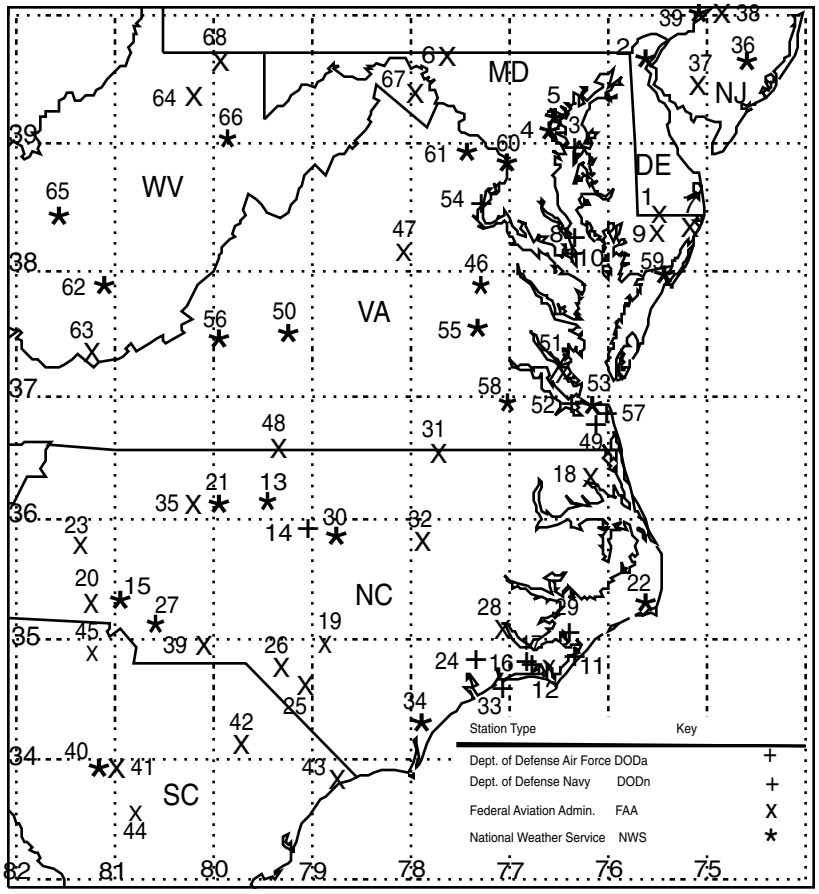

#	ID	Agency	Site Name	Lat. (N)	Lon (W)	#	ID	Agency	Site Name	Lat. (N)	Lon (W)
1	KGED	FAA	Georgetown, DE	38.69	75.36	35	KINT	FAA	Winston Salem, NC	36.13	80.22
3	KNAK	DODn	Annapolis, MD	38.99	76.43	36	KACY	NWS	Atlantic City, NJ	39.46	74.59
4	KBWI	NWS	Baltimore, MD	39.17	76.68	37	KMIV	FAA	Millville, NJ	39.37	75.08
5	KDMH	NWS	Baltimore, MD	39.28	76.61	38	KVAY	FAA	Mount Holly, NJ	39.94	74.84
6	KHGR	FAA	Hagerstown, MD	39.71	77.73	39	KPNE	NWS	Philadelphia, PA	40.08	75.01
7	KN80	FAA	Ocean City, MD	38.31	75.12	40	KCAE	NWS	Columbia, SC	33.94	81.11
8	KNHK	DODn	Patuxent River, MD	38.28	76.41	41	KCUB	FAA	Columbia, SC	33.97	80.99
9	KSBY	FAA	Salisbury, MD	38.34	75.50	42	KFLO	FAA	Florence, SC	34.18	79.73
10	KNUI	DODn	St Inigoes, MD	38.15	76.42	43	KCRE	FAA	Myrtle Beach, SC	33.82	78.72
11	KNLT	DODn	Atlantic City, NC	34.89	76.34	44	KOGB	FAA	Orangeburg, SC	33.46	80.85
12	KMRH	FAA	Beaufort, NC	34.73	76.66	45	K29J	FAA	Rock Hill, SC	34.98	81.06
13	KBUY	NWS	Burlington, NC	36.05	79.47	46	KOFP	NWS	Ashland, VA	37.71	77.43
14	KIGX	DODn	Chapel Hill, NC	35.93	79.06	47	KCHO	FAA	Charlottesville, VA	38.14	78.46
15	KCLT	NWS	Charlotte, NC	35.21	80.95	48	KDAN	FAA	Danville, VA	36.57	79.35
16	KNKT	DODn	Cherry Point, NC	34.90	76.88	49	KNFE	DODn	Fentress, VA	36.70	76.13
17	KNIS	DODn	Cherry Point, NC	34.89	76.86	50	KLYH	NWS	Lynchburg, VA	37.32	79.21
18	KECG	FAA	Elizabeth City, NC	36.26	76.18	51	KPHF	FAA	Newport News, VA	37.13	76.49
19	KFAY	FAA	Fayetteville, NC	34.99	78.88	52	KNGU	DODn	Norfolk, VA	36.93	76.30
20	KAKH	NWS	Gastonia, NC	35.20	81.16	53	KORF	NWS	Norfolk, VA	36.90	76.19
21	KGSO	NWS	Greensboro, NC	36.10	79.94	54	KNYG	DODn	Quantico, VA	38.51	77.29
22	KILG	NWS	Wilmington, DE	39.67	75.60	55	KRIC	NWS	Richmond, VA	37.51	77.32
22	KHSE	NWS	Hatteras, NC	35.23	75.62	56	KROA	NWS	Roanoke, VA	37.32	79.97
23	KHKY	FAA	Hickory, NC	35.74	81.38	57	KNTU	DODn	Virginia Beach, VA	36.82	76.03
24	KNCA	DODn	Jacksonville, NC	34.71	77.44	58	KAKQ	NWS	Wakefield, VA	36.98	77.00
25	KLBT	FAA	Lumberton, NC	34.61	79.06	59	KWAL	NWS	Wallops Island, VA	37.94	75.46
26	KMEB	FAA	Maxton, NC	34.79	79.37	60	KDCA	NWS	Washington, DC	38.84	77.03
27	KEQY	NWS	Monroe, GA	35.02	80.60	61	KIAD	NWS	Washington, DC	38.93	77.45
28	KEWN	FAA	New Bern, NC	35.07	77.05	62	KBKW	NWS	Beckley, WV	37.80	81.12
29	KNBT	DODn	Piney Island, NC	35.02	76.46	63	KBLF	FAA	Bluefield,	0.00	37.30
30	KRDU	NWS	Raleigh/Durham, NC	35.87	78.79	64	KCKB	FAA	Clarksburg, WV	39.30	80.22
31	KRZZ	FAA	Roanoke Rapids, NC	36.44	77.71	65	KCRW	NWS	Charleston, WV	38.38	81.59
32	KRWI	FAA	Rocky Mount Wil., NC	35.85	77.90	66	KEKN	NWS	Elkins, WV	38.89	79.85
33	KNJM	DODn	Swansboro, NC	34.69	77.03	67	KMRB	FAA	Martinsburg, WV	39.40	77.98
34	KILM	NWS	Wilmington, NC	34.27	77.91	68	KMGW	FAA	Morgantown, WV	39.65	79.92

Table C-3.5 Automated Surface Observing System (ASOS) sites(continued)

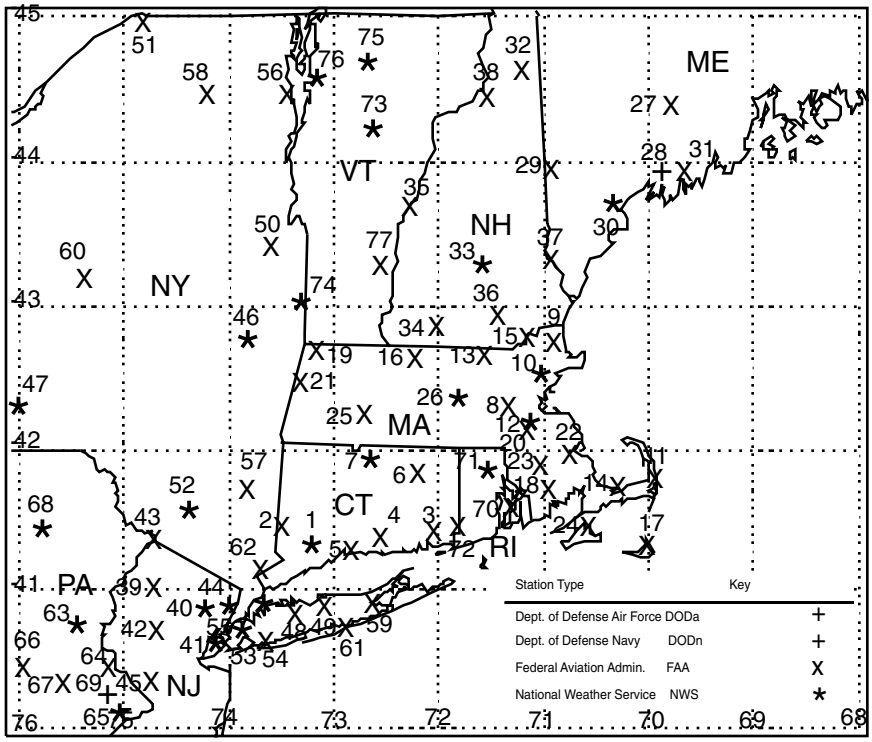

#	ID	Agency	Site Name	Lat. (N)	Lon (W)	#	ID	Agency	Site Name	Lat. (N)	Lon (W)
1	KBDR	NWS	Bridgeport, CT	41.16	73.13	39	K12N	NWS	Andover, NJ	41.01	74.74
2	KDXR	FAA	Danbury, CT	41.37	73.48	40	KCDW	FAA	Caldwell, NJ	40.88	74.28
3	KGON	FAA	Groton/N. Lon, CT	41.33	72.05	41	KEWR	NWS	Newark, NJ	40.68	74.17
4	KHFD	FAA	Hartford, CT	41.33	72.65	42	KN52	FAA	Somerville, NJ	40.62	74.67
5	KHVN	FAA	New Haven, CT	41.26	72.89	43	KFWN	FAA	Sussex, NJ	41.20	74.63
6	KIJD	FAA	Willimantic, CT	41.74	72.18	44	KTEB	NWS	Teterboro, NJ	40.85	74.06
7	KBDL	NWS	Windsor Locks, CT	41.94	72.68	45	KTTN	FAA	Trenton, NJ	40.28	74.82
8	KBED	FAA	Bedford, MA	42.47	71.29	46	KALB	NWS	Albany, NY	42.75	73.80
9	KBVY	FAA	Beverly, MA	42.58	70.92	47	KBGM	NWS	Binghamton, NY	42.21	75.98
10	KBOS	NWS	Boston, MA	42.36	71.01	48	KFRG	FAA	Farmingdale, NY	40.73	73.42
11	KCQX	FAA	Chatham, MA	41.69	69.99	49	KISP	FAA	Islip, NY	40.79	73.10
12	KMQE	NWS	East Milton, MA	42.21	71.11	50	KGFL	FAA	Glens Falls, NY	43.34	73.61
13	KFIT	FAA	Fitchburg, MA	42.55	71.56	51	KMSS	FAA	Massena, NY	44.93	74.85
14	KHYA	FAA	Hyannis, MA	41.67	70.27	52	KMGJ	NWS	Montgomery, NY	41.51	74.27
15	KLWM	FAA	Lawrence, MA	42.71	71.13	53	KNYC	NWS	New York City, NY	40.78	73.97
16	KORE	FAA	Orange, MA	42.57	72.28	54	KJFK	NWS	New York City, NY	40.64	73.76
17	KACK	FAA	Nantucket, MA	41.25	70.06	55	KLGA	NWS	New York City, NY	40.78	73.88
18	KEWB	FAA	New Bedford, MA	41.68	70.97	56	KPLB	FAA	Plattsburgh, NY	44.68	73.53
19	KAQW	FAA	North Adams, MA	42.70	73.17	57	KPOU	FAA	Poughkeepsie, NY	41.63	73.88
20	KOWD	FAA	Norwood, MA	42.19	71.17	58	KSLK	FAA	Saranac Lake, NY	44.39	74.20
21	KPSF	FAA	Pittsfield, MA	42.43	73.29	59	KHWV	FAA	Shirley, NY	40.82	72.87
22	KPYM	FAA	Plymouth, MA	41.91	70.73	60	KUCA	FAA	Utica, NY	43.14	75.38
23	KTAN	FAA	Taunton, MA	41.88	71.02	61	KFOK	FAA	West Hampton Bch, NY	40.85	72.62
24	KMVY	FAA	Vineyard Haven, MA	41.39	70.62	62	KHPN	FAA	White Plains, NY	41.06	73.70
25	KBAF	FAA	Westfield, MA	42.16	72.71	63	KABE	NWS	Allentown, PA	40.65	75.45
26	KORH	NWS	Worcestor, MA	42.27	71.87	64	KN88	FAA	Doylestown, PA	40.33	75.12
27	KAUG	FAA	Augusta, ME	44.32	69.80	65	KPNE	NWS	Philadelphia, PA	40.08	75.01
28	KNHZ	DODn	Brunswick, ME	43.90	69.94	66	KRDG	FAA	Reading, PA	40.37	75.96
29	KIZG	FAA	Fryeburg, ME	43.99	70.95	67	KPTW	FAA	Pottstown, PA	40.24	75.56
30	KPWM	NWS	Portland, ME	43.64	70.30	68	KAVP	NWS	Wilkes B./Scran., PA	41.34	75.73
31	KIWI	FAA	Wiscasset, ME	43.96	69.71	69	KNXX	DODn	Willow Grove, PA	40.19	75.14
32	KBML	FAA	Berlin, NH	44.58	71.18	70	KUUU	FAA	Newport, RI	41.53	71.23
33	KCON	NWS	Concord, NH	43.20	71.50	71	KPVD	NWS	Providence, RI	41.72	71.43
34	KAFN	FAA	Jaffrey, NH	42.81	72.00	72	KWST	FAA	Westerly, RI	41.35	71.80
35	KLEB	FAA	Lebanon, NH	43.63	72.31	73	KMPV	NWS	Barre/Montpelier, VT	44.20	72.57
36	KMHT	FAA	Manchester, NH	42.93	71.44	74	KDDH	NWS	Bennington, VT	42.89	73.25
37	K6B1	FAA	Rochester, NH	43.28	70.92	75	KMPV	NWS	Burlington, VT	44.47	73.15
38	KHIE	FAA	Whitefield, NH	44.37	71.55	76	KMVL	NWS	Morrisville, VT	44.20	72.57
						77	KVSF	NWS	Springfield, VT	43.34	72.52

Table C-3.5 Automated Surface Observing System (ASOS) sites (continued)

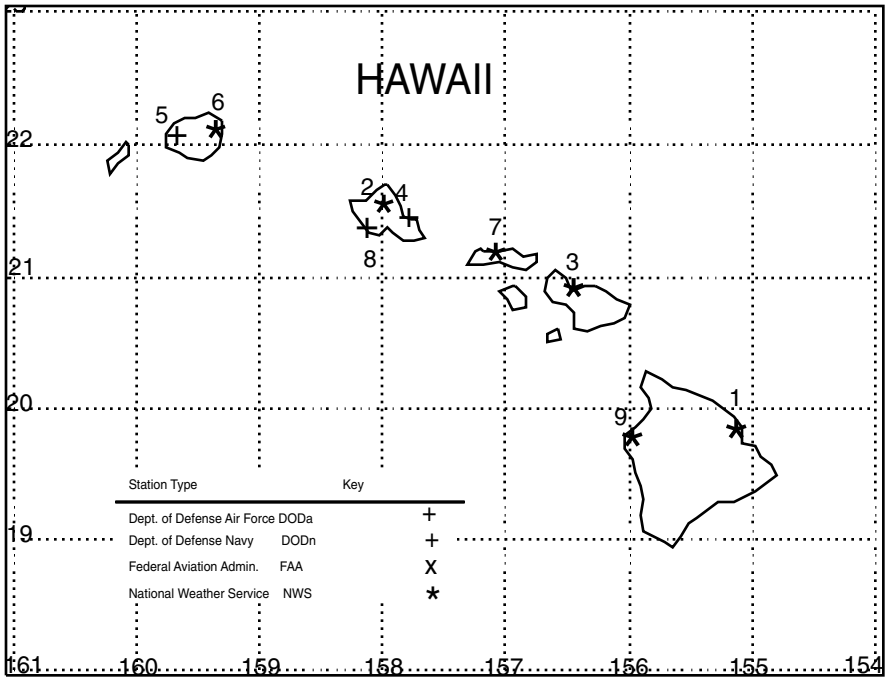

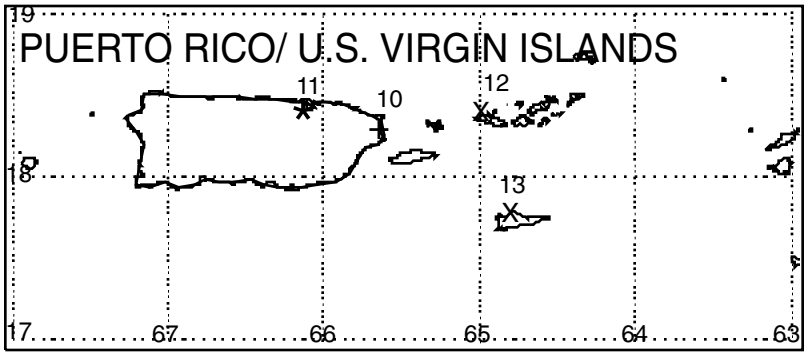

#	ID	Agency	Site Name	Lat. (N)	Lon (W)
1	PHTO	NWS	Hilo, HI	19.72	155.05
2	PHNL	NWS	Honolulu, HI	21.32	157.94
3	PHOG	NWS	Kahului, HI	20.89	156.43
4	PHNG	DODn	Kaneohoe, HI	21.45	157.77
5	PHBK	DODn	Kekaha, HI	22.04	159.79
6	PHLI	NWS	Lihue, HI	21.98	159.34
7	PHMK	NWS	Molokai, HI	21.16	157.10
8	PHNA	DODn	Oahu, HI	21.31	158.07
9	PHKO	NWS	Kailua/Kona, HI	19.74	156.05
10	TJNR	DODn	Roosevelt Roads, PR	18.26	65.64
11	TJSJ	NWS	San Juan, PR	18.43	66.01
12	KSTT	FAA	Charlotte Amali, VI	18.34	64.98
13	KSTX	FAA	Christiansted, VI	17.70	64.81

C.4 NWS and DOD Locations/Contacts - 1999

Table C-4.1 DOD RAWIN/RAOB locations/contacts

Station Identifier	Address/Location	Sqdrn. Co/Fac. Cmdr.	Telephone Numbers
COF (74795)	45th Wea. Squadron/CC 1201 Edward H. White St. Patrick AFB, FL 32925-3238	Col. David Urbanski Squadron Commander Lt. Col. Dewey Harms Chief of Systems	407-494-7012 407-494-7426 407-854-7426 FAX: 407-853-4315 DNS[1]: 853-8211 FAX: 407-853-8295
VPS (72221)	46th W5 601 W. Choctawhatchee Suite 60 Eglin AFB, FL 32542-5719	Lt. Col. Robert Lafbare Squadron Commander Joe Kerwin Chief, Range Support	850-882-5449 850-882-4800 850-882-5224 850-882-5960 850-872-5323 DSN[1]: 872-5323 FAX: 850-882-3341
TXKF[2] (78016)	P.O. Box 123 St. Georges Bermuda GEBX	Mr. Roger Williams	441-293-5339 441-293-5078 FAX: 441-293-6658

[1] DSN: Defense Switched Network.

[2] The facility at Bermuda is not military. Mr. Roger Williams is the manager of the meteorology office.

Note 1: AT&T can be used to call Bermuda from HRD/AOML; however, you must have an AT&T FTS 2000 credit card (see Gladys Medina if you need an AT&T FTS 2000 credit card for official business).

To place a call using an AT&T FTS 2000 card:
(a) Follow instructions on the back of your AT&T FTS 2000 credit card.
(b) Division secretaries or Gladys Medina can assist placing calls.

Note 2: In recent years, CSR operated the meteorological station at Antigua under a contract with the USAF. Meteorological operations at Antigua were terminated May 1, 1993. During the 1999 field program, if additional rawinsonde/radiosonde data from the eastern Caribbean area are required, the MGOC representative should contact the Meteorological Office, Saint Martin (Saint Maarten), Netherlands Antilles [TNCM (78866)]. Petier Trappenberg is the Director of the facility. He can be contacted as follows:

AT&T: 011-599-9-683933 (FAX: 011-599-9-683999)

For further information or assistance, contact Albert Mongeon (NWS) at 301-713-0882, ext. 140.

Note 3: Additional rawinsondes/radiosondes from DOD rawinsonde sites, including Patrick AFB, Eglin AFB, and NAS Guantanamo (Cuba), can be requested through the CARCAH at TPC/NHC (see Appendix F, section F.3, 3g)].

Note 4: When requesting additional RAWINs/RAOBs from any DOD or other facility, the MGOC representative should:

(a) State the beginning and ending date(s) and time(s) [UTC].
(b) Specify the desired frequency of rawinsondes/radiosondes (3-, 6-, or 12-hourly intervals).
(c) State that rawinsondes/radiosondes should be "flown" (at least) to the 100-mb level.
(d) Request that all data (*i.e.,* raw data **and** worked-up soundings) be sent to Howard A. Friedman, AOML/HRD, 4301 Rickenbacker Causeway, Miami, Florida, 33149.

Table C-4.2 NWS/Eastern Region RAWIN/RAOB locations/contacts[1]

Station Identifier	Address/Location	MIC/OIC	Telephone Numbers
CHS (72208)	NWS/WSO, NOAA 5777 S. Aviation Avenue Charleston, SC 29406	Steve Rich MIC Stephen.Rich@noaa.gov	843-744-0303 843-744-0211 843-727-4395 FAX: 843-747-5405
GSO (72317)	NWS/WSO, NOAA Centennial Campus NCSU 1005 Capability Dr. Research Building III, Suite 300 Raleigh, NC 27606	Steve Harned MIC Steve.Harned@noaa.gov	919 515-8209
MHX (72305)	NWS/WSO, NOAA 533 Roberts Road Newport, NC 28570	Thomas Kriehn MIC Thmoas.Kriehn@noaa.gov	252-223-5122 252-223-5631 252-223-2328 FAX: 252-223-3673 1-800-697-7374
OKX (72501)	NWS/WSFO, NOAA 175 Brookhaven Avenue Bld. # NWS 1 Upton, NY 11973	Michael E. Wyllie MIC Micheal.Wyllie@noaa.gov	516-924-0517 516-924-0037 FAX: 516-924-0519
WAL (72402)	NWS/WSCMO[2,3] Building N162 Wallops Island, VA 23337	Sam West Chief, UA Section	757-824-1586 FAX: 757-824-2414
	Weather Office[3,4] Building E106 Wallops Island, VA 23337	Ted Wilz[5] MIC	757-824-1325 757-824-1638 FAX: 757-824-2410

1 Additional rawinsondes or radiosondes may be requested from the NWS/ER or NWS/SR stations listed in Tables C-4.2 and C-4.3: (a) via AFOS [contact NHC's Communications Unit personnel for assistance]; (b) through the duty Hurricane Specialist (NHC); or (c) directly by phone. Messages sent via AFOS should contain a statement asking that the appropriate NWS station(s) acknowledge and confirm each request. Remember to identify the program as "**HRD/Hurricane Field Program**" and follow instructions in Note 4, at the bottom of Table C-4.1.

2 Normal hours of operation: 0600-2230 EDT (or EST, when appropriate).

3 If you can't reach your party on any of the numbers shown, contact the NASA switchboard operator (757-824-1000) and ask to have your party paged.

4 Normal hours of operation: 0530-1600 EDT (or EST, when appropriate).

5 Home phone number is 410-860-2108.

Table C-4.3 NWS/Southern Region RAWIN/RAOB locations/contacts[1]

Station Identifier	Address/Location	MIC/OIC	Telephone Numbers
BMX (72230)	NWS/WSO, NOAA 465 Weathervane Road Calera, AL 35040-5079	Gary S. Petti MIC Gary.Petti@noaa.gov	205-621-5645 205-621-5646 205-621-5647 205-664-3010 FAX: 205-664-7821
BRO (72250)	NWS/WSO, NOAA 20 South Vermillion Road Brownsville, TX 78521-5798	Richard R. Hagan MIC Richard.Hagan@noaa.gov	956-504-3084 956-504-3354 956-504-1432 956-504-3184 956-504-1631 FAX: 956-982-1766
CRP (72251)	NWS/WSO, NOAA International Airport 300 Pinson Drive Corpus Christi, TX 78406-1803	Joe Arellano, Jr. MIC Joe.Arellano@noaa.gov	361-299-1353 361-299-1354 361-289-0959 FAX: 361-289-7823
EYW (72201)[3]	NWS/WSO, NOAA International Airport 3535 S. Roosevelt Blvd. Ste.105 Key West, FL 33040-5234	Bobby McDaniel MIC (Home: 305-872-7303) Bobby.McDaniel@ noaa.gov	305-295-1324 305-295-1316 FAX: 305-293-9987 *(call ahead)*
FFC (72215)	NWS/WSMO, NOAA 4 Falcon Drive Peachtree City, GA 30269	Carlos Garza MIC Carlos.Garza@noaa.gov	770-486-1133 770-486-1333 770-486-0026 770-486-0027 FAX: 770-486-9333
FWD (72249)	NWS/WSFO, NOAA 3401 Northern Cross Blvd. Forth Worth, TX 76137-3610	Gifford "Skip" Ely MIC Skip.Ely@noaa.gov	817-831-1581 817-831-1157 817-831-1574 817-831-1595 FAX: 817-831-3025
JAN (72235)	NWS/WSFO, NOAA 234 Weather Service Drive Jackson, MS 39208	Tice H. Wagner, III MIC Tice.Wagner@noaa.gov	601-965-4639 601-965-4638 601-939-2786 601-936-2189 FAX: 601-965-4028
JAX (72206)	NWS/WSO, NOAA 13701 Fang Drive Jacksonville, FL 32218	Stephen M. Letro MIC Steve.Letro@noaa.gov	904-741-4370 904-741-4411 904-741-5186 FAX: 904-741-0078

Table C-4.3 NWS/Southern Region RAWIN/RAOB locations/contacts[1] (continued)

Station Identifier	Address/Location	MIC/OIC	Telephone Numbers
LCH (72240)	NWS/WSO, NOAA 500 Airport Blvd., #115 Lake Charles, LA 70607-0668	Steve Rinard MIC Steve.Rinard@noaa.gov	318-477-3422 318-477-2495 318-477-0354 FAX: 318-474-8705
LZK (72340)	NWS/WSO, NOAA N. Little Rock Airport 8400 Remount Road N. Little Rock, AR 72118	Renee Fair MIC Renee.Fair@noaa.gov	501-834-9102 501-834-3955 501-834-0308 FAX: 501-834-0715
MFL (72203)	NWS/WSMO, NOAA 11691 S.W. 17th Street Miami, FL 33165-2149	Russell “Rusty” Pfost MIC Rusty.Pfost@noaa.gov	305-229-4500 305-229-4501 305-229-4523 305-229-4528 FAX: 305-229-4553 FAX: 305_559-4503
SHV (72248)	NWS/WSO, NOAA 5655 Hollywood Avenue Shreveport, LA 71109-7750	Lee Harrison MIC Lee.Harrison@noaa.gov	318-635-9398 318-636-7345 318-636-4594 318-635-8734 FAX: 318-636-9620
SIL (72233)	NWS/WSFO, NOAA 62300 Airport Road Slidell, LA 70460-5243	Paul S. Trotter MIC Paul.Trotter@noaa.gov	504-649-0429 504-589-2808 504-649-0357 504-645-0565 FAX: 504-649-2907
TBW (72210)	NWS/WSO, NOAA 2525 14th Avenue, S.E. Ruskin, FL 33570 [Tampa Bay Area]	Ira Brenner MIC Ira.Brenner@noaa.gov	813-641-2512 813-645-4111 813-641-1720 813-641-1807 FAX: 813-641-2441 FAX: 813-641-2619
SJU (78526)	NWS/WSFO, NOAA 4000 Carretera 190 Carolina, PR 00979	Israel Matos[5] MIC Israel.Matos@noaa.gov Rafael Mojica WCM	787-253-4501 787-253-4504 UA:[4] 787-253-4587 FAX: 787-253-7802
TLH (72214)	NWS/WSO, NOAA Regional Airport 3300 Capital Circle, S.W. Suite 227 Tallahassee, FL 32310-8723	Paul Duval MIC Paul.Duval@noaa.gov	850-942-8398 850-942-9394 FAX: 850-942-9396

1 See footnote 1 in Table C-4.2.

2 Hours: 0400-2000 CDT (or CST, when appropriate).

3 If unable to contact MIC, further information is available from the Miami WSFO.

4 UA: Upper air station.

5 Pager: 1-800-652-0608

Table C-4.4 NWS/Eastern Region coastal radar locations/contacts

Station Identifier/ Type Radar/ Lat./Lon.	Address/Location	MIC/OIC	Telephone Numbers
KAKQ (93773) WSR-88D 36.9839°N 77.0072°W	NWS/WSO, NOAA 1009 General Mahone Hwy. Wakefield, VA 23888	Anthony Siebres MIC Anthony.Siebres@noaa.gov	757-899-5734 757-899-5735 FAX: 757-899-3605
KCLX (53845) WSR-88D 32.6555°N 81.0422°W	NWS/WSO, NOAA 5777 S. Aviation Avenue Charleston, SC 29406	Stephen T. Rich MIC Stephen.Rich@noaa.gov	803-744-0303 803-744-0211 803-727-4395 FAX: 803-747-5405
KLTX (93774) WSR-88D 33.9894°N 78.4289°W	NWS/WSO, NOAA 2015 Gardner Drive Wilmington, NC 28405	Richard W. Anthony MIC Richard.Anthony@noaa.gov	910-763-8331 910-762-4289 910-762-9476 FAX: 910-762-1288
KLWX (93767) WSR-88D 38.9753°N 77.4778°W	NWS/WFO, NOAA 44087 Weather Service Rd Sterling, VA	Jim Travers MIC James.Travers@noaa.gov	703-260-0107 X222 Fax: (703) 260-0809
KMHX (93768) WSR-88D 34.7761°N 76.8761°W	NWS/WSO, NOAA 533 Roberts Road Newport, NC 28570	Thomas Kriehn MIC Thomas.Kriehn@noaa.gov	252-223-5122 253-223-5631 252-223-2328 FAX: 252-223-3673
KOKX (94703) WSR-88D 40.8656°N 72.8639°W	NWS/WSO, NOAA 175 Brookhaven Avenue Bldg #NWS 1. Upton, NY 11973	Michael E. Wyllie MIC Michael.Wyllie@noaa.gov	516-924-0517 516-924-0037 FAX: 516-924-0519
KRAX (93772) WSR-88D 35.6656°N 78.4897°W	NWS/WSO, NOAA Centennial Campus NCSU 1005 Capability Dr. Research Building III, Suite 300 Raleigh, NC 27606	Steve Harned MIC Steve.Harned@noaa.gov	919-515-8209

Note 1: NWS/ER point of contact for WSR-88D information is the Eastern Region Hurricane Watch Office (516-244-0172).

Table C-4.5 NWS/Southern Region coastal radar locations/contacts

Station Identifier/ Type Radar/ Lat./Lon.	Address/Location	MIC/OIC	Telephone Numbers
KBRO (12919) WSR-88D 25.9161°N 97.4189°W	NWS/WSO, NOAA 20 South Vermillion Road Brownsville, TX 78521-6851	Richard R. Hagan MIC Richard.Hagan@noaa.gov	956-504-3084 956-504-3354 956-504-3184 956-504-1631 FAX: 956-982-1766
KCRP (12924) WSR-88D 27.7842°N 97.5111°W	NWS/WSO, NOAA International Airport 300 Pinson Drive Corpus Christi, TX 78406	Joe Arellano, Jr. MIC Joe.Arellano@noaa.gov	361-289-1353 361-289-1354 361-289-1357 FAX: 361-289-7823
KBYX(92804) WSR-88D 24.5975°N 81.7031°W	NWS/WSO, NOAA Key West International Airport 3535 S. Roosevelt Blvd. Ste.105 Key West, FL 33040-5234	Bobby McDaniel MIC (Home: 305-872-7303) Bobby.McDaniel@ noaa.gov	305-295-1324 305-295-1316 FAX: 305-293-9987 *(call ahead)*
KHGX (03980) WSR-88D 29.4719°N 95.0792°W	NWS/WSO, NOAA 1620 Gill Road Dickinson, TX 77539	William "Bill" Read MIC Bill.Read@noaa.gov	281-337-5192 281-337-5285 281-534-2157 281-534-5625 FAX: 281-337-3798
KJAX (13889) WSR-88D 30.4847°N 81.7019°W	NWS/WSO, NOAA 13701 Fang Drive Jacksonville, FL 32218	Stephen M. Letro MIC Stephen.Letro@noaa.gov	904-741-4411 904-741-5186 FAX: 904-741-0078
KLCH (03937) WSR-88D 30.1253°N 93.2158°W	NWS/WSO, NOAA 500 Airport Boulevard, #115 Lake Charles, LA 70605	Steve Rinard MIC Steve.Rinard@noaa.gov	318-477-3422 318-477-2495 318-477-0354 FAX: 318-474-8705
KLIX (53813) WFSR-88D 30.3367°N 89.8256°W	NWS/WSFO, NOAA 62300 Airport Road Slidell, LA 70460	Paul S. Trotter MIC Paul.Trotter@noaa.gov	504-649-0984 504-649-0429 504-589-2808 504-649-0899 504-645-0565 FAX: 504-649-2907

Table C-4.5 NWS/Southern Region coastal radar locations/contacts (continued)

Station Identifier/ Type Radar/ Lat./Lon.	Address/Location	MIC/OIC	Telephone Numbers
KAMX (12899) WSR-88D 25.6111°N 80.4128°W	NWS/WSFO/NOAA 11691 S.W. 17th Street Miami, FL 33165-2149	Russell "Rusty" Pfost MIC Rusty.Pfost@noaa.gov	305-229-4500 305-229-4501 305-229-4520 305-229-4528 FAX: 305-229-4553 305-559-4503
KMLB (12838) WSR-88D 28.1133°N 80.6542°W	NWS/WSO, NOAA 421 Croton Road Melbourne, FL 32935	Bart Hagemeyer MIC Bart.Hagemeyer@noaa.gov	407-254-6083 407-254-6923 407-259-7589 407-259-7618 FAX: 407-255-0791
KMOB (13894) WSR-88D 30.6794°N 88.2397°W	NWS/WSO, NOAA 8400 Airport Boulevard Mobile, AL 36608	Randall McKee MIC Randall.McKee@noaa.gov	334-633-0921 334-633-7342 334-633-6443 334-633-2471 FAX: 334-607-9773
KTBW (92801) WSR-88D 27.7056°N 82.4022°W	NWS/WSO, NOAA 2525 14th Avenue, S.E. Ruskin, FL 33570 [Tampa Bay Area]	Ira Brenner MIC Ira.Brenner@noaa.gov	813-645-4111 813-641-2512 813-641-1720 FAX: 813-641-2619 813-641-2441
TJUA(11655) WSR-88D 18.1156°N 66.0781°W	NWS/WSFO, NOAA 4000 Carretera 190 Carolina, PR 00979	Israel Matos MIC Israel.Matos@noaa.gov Rafael Mojica WCM	787-253-4501 787-253-4504 787-253-4502 FAX: 787-253-7802
KTLH (93805) WSR-88D 30.3975°N 84.3289°W	NWS/WSO, NOAA Regional Airport 3300 Capital Circle, S.W. Suite 227 Tallahassee, FL 32310-8723	Paul Duval MIC Paul.Duval@noaa.gov	850-942-8398 850-942-9394 850-942-9395 FAX: 850-942-9396

Note 1: NWS/SR official contact for WSR-88D information is Victor Murphy (W/SR/SRH), WSR-88D Meteorologist (817-978-2367 ext. 130).

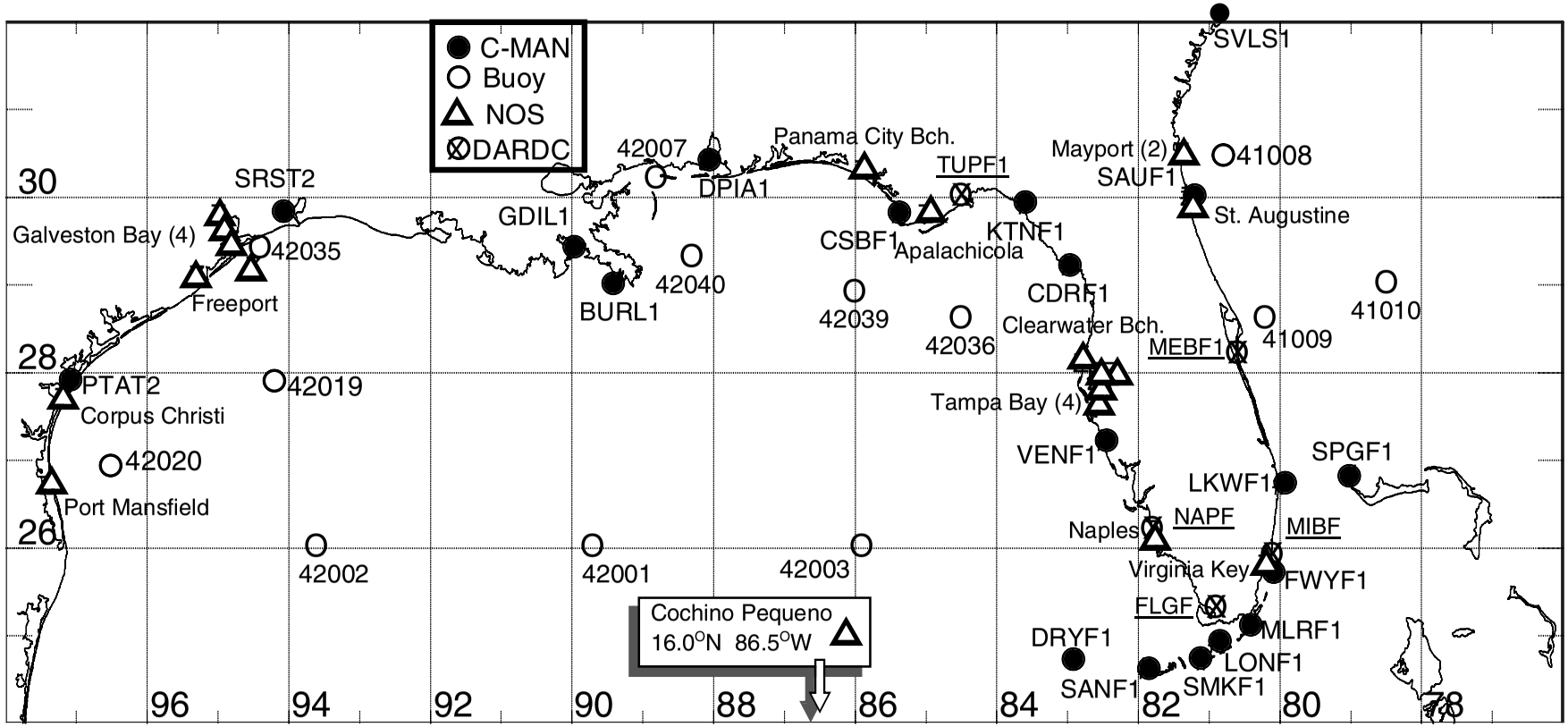

Fig. C-2. Marine buoy, C-MAN, NOS (lower case), and DARDC (underlined) locations in the Gulf of Mexico, Florida, and southern Georgia. See Tables C-3.1 -- C-3.5.

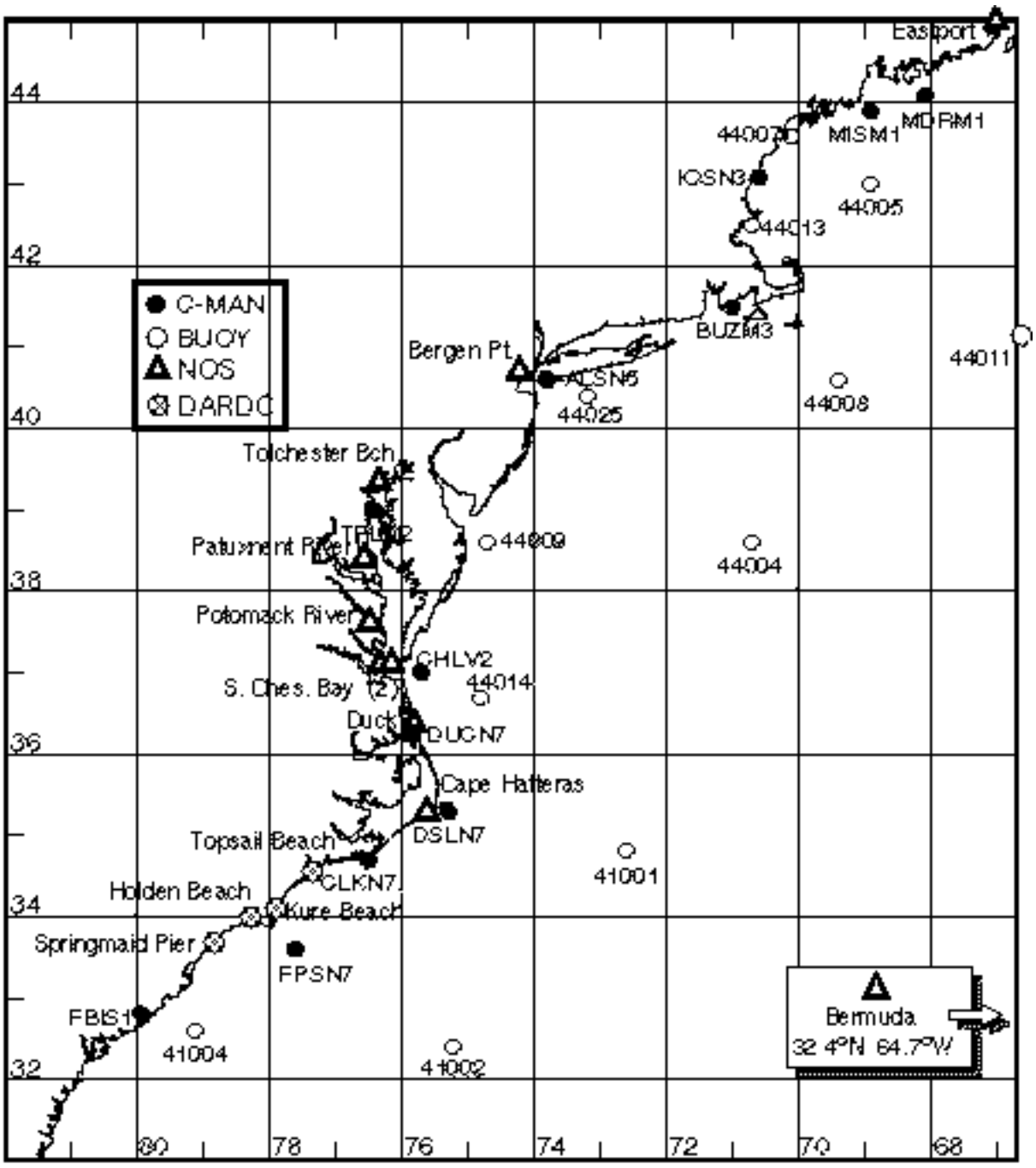

Fig C-3 Marine buoy, C-MAN, and NOS (lower case) locations for the U S. east coast. See Tables C-3.1 -- C-3.5.

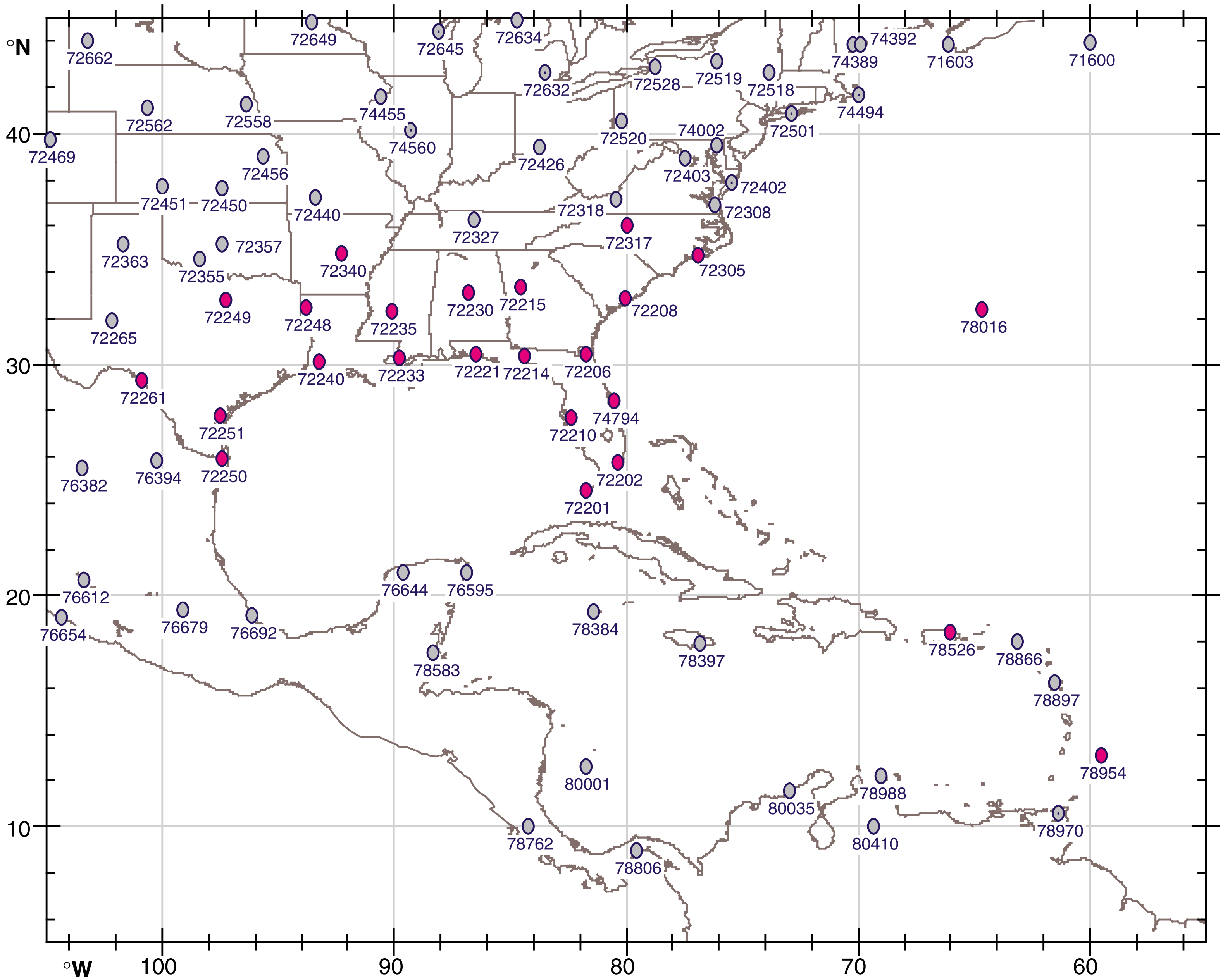

Fig. C-4. Locations of RAWIN/RAOB stations. See Tables C-4.1-C-4.5 for information about stations in red.

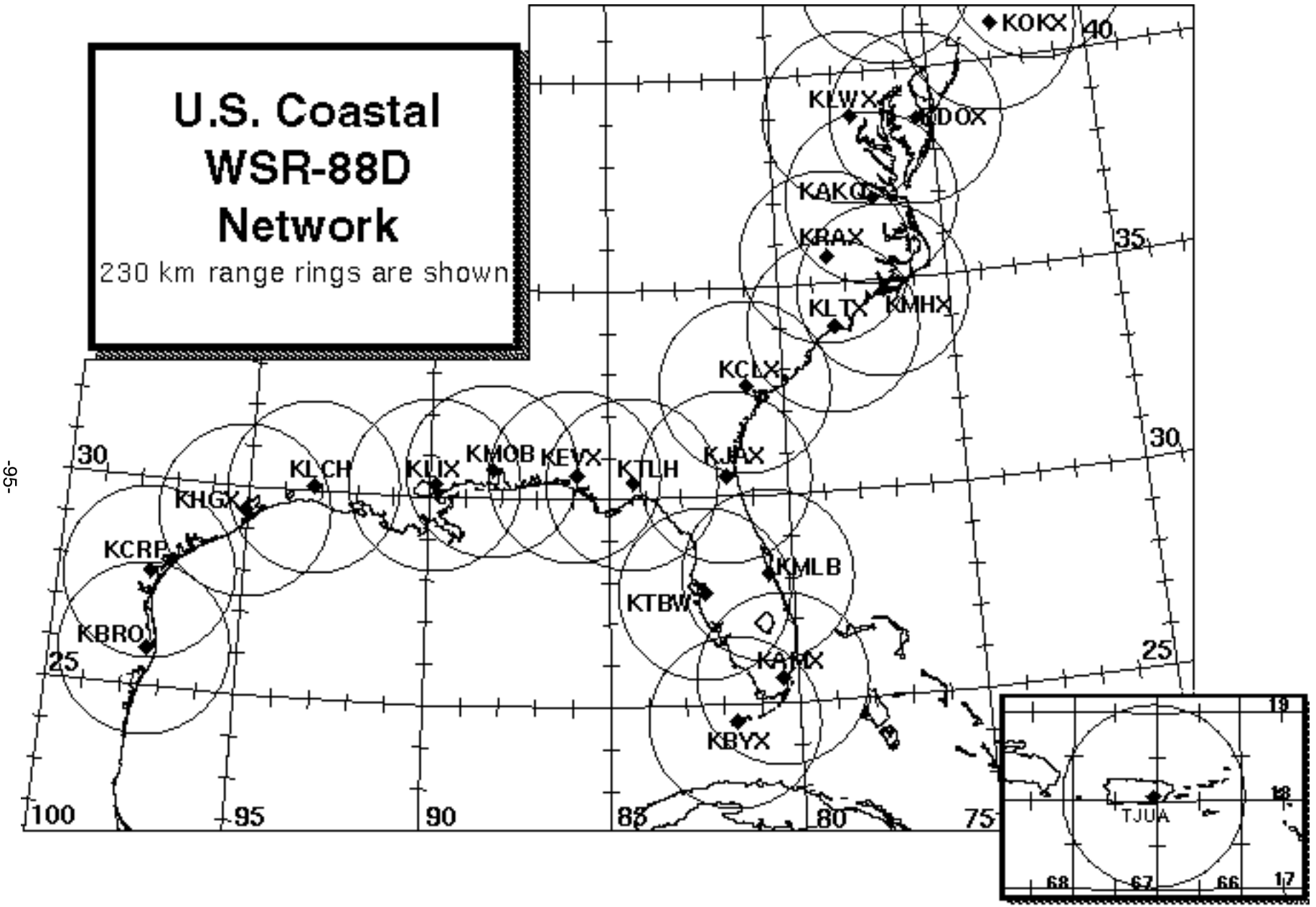

Fig. C-5. Locations of coastal WSR-88D stations. See tables C-4.1 -- C-4.5 for complete information.

APPENDIX D:

PRINCIPAL DUTIES OF THE NOAA SCIENTIFIC PERSONNEL

PRINCIPAL DUTIES OF THE NOAA SCIENTIFIC PERSONNEL

CAUTION

Flight operations are routinely conducted in turbulent conditions. Shock-mounted electronic and experimental racks surround most seat positions. Therefore, all personnel reporting for flight will wear closed-toe shoes. In addition, it is strongly recommended that "soft" or canvas type shoes not be worn and that personal clothing be selected for appearance, safety, coverage, and fit. A light jacket is advisable as the temperature within the aircraft is kept low to protect the data systems.

Smoking is prohibited within 50 ft of the aircraft while they are on the ground. No smoking is permitted on the aircraft at any time.

GENERAL INFORMATION FOR ALL SCIENTIFIC MISSION PARTICIPANTS

Mission participants are advised to carry the proper personal identification [i.e., travel orders, "shot" records (when appropriate), and passports (when required)]. Passports will be checked by AOC personnel prior to deployment to countries requiring same. All participants must provide their own meals for in-flight consumption. Utensils, condiments, ice, beverages, and cooking and storage facilities will be provided. There will be a $1.00 seat charge on each flight to defray galley expenses.

D.1 Field Program Director

(1) Responsible to the HRD director for the implementation of the Hurricane Field Program Plan.

(2) Only official communication link to AOC. Communicates flight requirements and changes in mission to AOC.

(3) Only formal communication link between AOML and CARCAH during operations. Coordinates scheduling of each day's operations with AOC only after all (POD) reconnaissance requirements are completed between CARCAH and AOC.

(4) Convenes the Hurricane Field Program Operations Advisory Panel. This panel selects missions to be flown in comparison with others as specified in sections 9-16 of this plan.

(5) Provides for pre-mission briefing of flight crews, scientists, and others (as required).

(6) Assigns duties of field project scientific personnel.

(7) Coordinates press statements with NOAA/Public Affairs.

D.2 Assistant Field Program Director

(1) Assumes the duties of the field program director in his absence.

D.3 Field Program Ground Team Manager

(1) Has overall responsibility for field operations ground support logistics and communications.

a. Provides arrangements and support for required supplies, expendables, accommodations, etc.
b. Maintains a current source of information regarding HRD operational, personnel, and equipment status for use as directed by the field program director.

(2) Responsible for coordination and communication of field program activities as required.

(3) Responsible for updating the Miami Ground Operations Center (MGOC) as required.

(4) Provides the ground supervision and acts as the reporting officer, subject to the field program director, for all HRD project personnel.

D.4 Miami Ground Operations Center: Senior Team Leader

(1) During operations, the MGOC senior team leader is responsible for liaison between HRD base and field personnel and other organizations as requested by the field program director, the director of HRD, or their designated representatives.

D.5 Named Experiment Lead Project Scientist

(1) Has overall responsibility for the experiment.

(2) Coordinates the project and sub-project requirements.

(3) Determines the primary modes of operation for appropriate instrumentation.

(4) Assists in the selection of the mission.

(5) Provides a written summary of the mission to the field program director (or his designee) at the experiment's debriefing.

D.6 Lead Project Scientist

(1) Has overall scientific responsibility for his/her aircraft.

(2) Makes in-flight decisions concerning alterations of: (a) specified flight patterns; (b) instrumentation operation; and (c) assignment of duties to on-board scientific project personnel.

(3) Acts as project supervisor on the aircraft and is the focal point for all interaction of project personnel with operational or visiting personnel.

(4) Conducts preflight and post flight briefings of the entire crew. Completes formal check lists of instrument operations, noting malfunctions, problems, etc.

(5) Provides a written report of each mission day's operations to the field program director at the mission debriefing.

D.7 Cloud Physics Scientist

(1) Has overall responsibility for the cloud physics project on the aircraft.

(2) Briefs the on-board lead project scientist on equipment status before takeoff.

(3) Determines the operational mode of the cloud physics sensors (i.e., where, when, and at what rate to sample).

(4) Operates and monitors the cloud physics sensors and data systems.

(5) Provides a written preflight and post flight status report and flight summary of each mission day's operations to the on-board lead project scientist at the post flight debriefing.

D.8 Boundary-Layer Scientist

(1) Insures that sufficient numbers of AXCPs, AXBTs, and buoys are on the aircraft for each mission as required.

(2) Operates the AXCP, AXBT, and buoy equipment (as required) on the aircraft.

(3) Briefs the on-board lead project scientist on equipment status before takeoff.

(4) Determines where and when to release the AXCPs, AXBTs, and buoys (as appropriate) subject to clearance by flight crew.

(5) Performs preflight, inflight, and post flight checks and calibrations.

(6) Provides a written preflight and post flight status report and a flight summary of each mission day's operations to the on-board lead project scientist at the post flight debriefing.

D.9 Airborne Radar Scientist

(1) Determines optimum meteorological target displays. Continuously monitors displays for performance and optimum mode of operations. Thoroughly documents modes and characteristics of the operations.

(2) Provides a summary of the radar display characteristics to the on-board lead project scientist at the post flight debriefing.

(3) Maintains tape logs and changes magnetic tape (as needed).

(4) On most missions, an on-board radar scientist will also function in the role of the on-board Doppler radar scientist. The individual who is designated as the mission's Doppler radar scientist will be responsible for the following: (a) operate and/or monitor the system; (b) document the modes and characteristics of the system's operation; (c) document all airborne Doppler radar data collected; and (d) provide a summary of the airborne Doppler radar system's operation to the on-board lead project scientist at the post flight debriefing.

(5) During the ferry to the storm the Doppler scientist should record a tape of the sea return on either side of the aircraft at elevation angles varying from -20° through +20°. This tape will allow correction of any antenna mounting biases or elevation angle corrections.

D.10 Dropwindsonde Scientist

(1) Examines dropwindsonde observations for accuracy.

(2) Determines the most likely values of temperature, dew-point depression, and horizontal wind at mandatory and significant (pressure) levels.

(3) Provides final code to the data system technician for ASDL, transmission or insures correct code in the event of automatic data transmission.

D.11 Workstation Scientist

(1) Operates HRD's workstation.

(2) Runs programs that determine wind center and radar center as a function of time, composite flight-level and radar reflectivity relative to storm center and that process and code dropwindsonde observations.

(3) Checks data for accuracy and sends appropriate data to ASDL computer.

(4) Maintains records of the performance of the workstation and possible software improvements.

APPENDIX E:

NOAA RESEARCH OPERATIONAL PROCEDURES AND CHECK LISTS

NOAA RESEARCH OPERATIONAL PROCEDURES AND CHECK LISTS

E.1 Procedures and Mission Directives: "Conditions-of-Flight" Commands

For safety onboard the aircraft smoking is prohibited and all personnel should wear long pants and closed toed shoes. For comfort personnel should bring a jacket or sweater as the cabin gets cold during flight. Personnel are responsible for their meals. AOC provides a refrigerator, microwave, coffee, water, and soft drinks for a mandatory $2.00 per flight "mess" fee.

Mission participants should be aware of the designated "conditions-of-flight."There are five designated basic conditions of readiness encountered during flight. The pilot will set a specific condition and announce it to all personnel over the aircraft's PA (public address) and ICS (interphone communications systems). All personnel are expected to take action in accordance with the instructions for the specific condition announced by the pilot. These conditions and appropriate actions are shown below.

CONDITION 1: TURBULENCE/PENETRATION. All personnel will stow loose equipment and fasten safety belts.

CONDITION 2: HIGH ALTITUDE TRANSIT/FERRY. There are no cabin station manning requirements.

CONDITION 3: NORMAL MISSION OPERATIONS. All scientific and flight crew stations are to be manned with equipment checked and operating as dictated by mission requirements. Personnel are free to leave their ditching stations.

CONDITION 4: AIRCRAFT INSPECTION. After take-off, crew members will perform a wings, engines, electronic bays, lower compartments, and aircraft systems check. All other personnel will remain seated with safety belts fastened and headsets on.

CONDITION 5: TAKE-OFF/LANDING. All personnel will stow or secure loose equipment, don headsets, and fasten safety belts/shoulder harnesses.

E.2 Lead Project Scientist

E.2.1 Preflight

_____ 1. Participate in general mission briefing.

_____ 2. Determine specific mission and flight requirements for assigned aircraft.

_____ 3. Determine from CARCAH or field program director whether aircraft has operational fix responsibility and discuss with AOC flight director/meteorologist and CARCAH unless briefed otherwise by field program director.

_____ 4. Contact HRD members of crew to:

a. Assure availability for mission.
b. Arrange ground transportation schedule when deployed.
c. Determine equipment status.

_____ 5. Meet with AOC flight crew at least 90 minutes before takeoff, provide copies of flight requirements, and provide a formal briefing for the flight director, navigator, and pilots.

_____ 6. Report status of aircraft, systems, necessary on-board supplies and crews to appropriate HRD operations center (MGOC in Miami).

E.2.2 In-Flight

_____ 1. Confirm from AOC flight director that satellite data link is operative (information).

_____ 2. Confirm camera mode of operation.

_____ 3. Confirm data recording rate.

_____ 4. Complete Form E-2.

E.2.3 Post flight

_____ 1. Debrief scientific crew.

_____ 2. Report landing time, aircraft, crew, and mission status along with supplies (tapes, *etc.*) remaining aboard the aircraft to MGOC.

_____ 3. Gather completed forms for mission and turn in at the appropriate operations center. [**Note**: all data removed from the aircraft by HRD personnel should be cleared with the AOC flight director.]

_____ 4. Obtain a copy of the 10-s flight listing from the AOC flight director. Turn in with completed forms.

_____ 5. Determine next mission status, if any, and brief crews as necessary.

_____ 6. Notify MGOC as to where you can be contacted and arrange for any further coordination required.

_____ 7. Prepare written mission summary using form E-2 p.3 (due to Field Program Director1 week after the flight).

Form E-2
Page 1 of 5

Lead Project Scientist Check List

Date _____ **Aircraft** _____ **Flight ID** _____

A. —Participants:

HRD		AOC	
Function	**Participant**	**Function**	**Participant**
Lead Project Scientist		Flight Director	
Cloud Physics		Pilots	
Radar		Navigator	
Workstation		Systems Engineer	
Photographer/Observer		Data Technician	
Dropwindsonde		Electronics Technician	
AXBT/AXCP/Guest		Other	

Take-Off: _____ Location: _____ Landing: _____ Location: _____

Number of Eye Penetrations: _____

B. —Past and Forecast Storm Locations:

Date/Time	Latitude	Longitude	MSLP	Maximum Wind

C. —Mission Briefing:

Form E-2
Page 2 of 5

D. —Equipment Status (Up ↑, Down ↓, Not Available **—**, Not Used **O**)

Equipment	Pre-Flight	In-Flight	Post-Flight	# of DATs or Expendables
Aircraft				
Radar/LF				
Radar/TA (Doppler)				
Cloud Physics				
Data System				
Dropwindsondes				
AXBT/AXCP				
Workstation				
Videography				

REMARKS:

Mission Summary
Storm name
YYMMDDA# Aircraft 4 RF

Scientific Crew (4 RF)	
Lead Project Scientist	_____
Radar Scientist	_____
Cloud Physics Scientist	_____
Dropwindsonde Scientist	_____
Boundary-Layer Scientist	_____
Workstation Scientist	_____
Observers	_____

Mission Briefing: (include sketch of proposed flight track or page #)

Mission Synopsis: (include plot of actual flight track)

Evaluation: (did the experiment meet the proposed objectives?)

Problems:(list all problems)

Page __of __

Observer's Flight Track Worksheet

Date _____ Flight _____ Observer _____

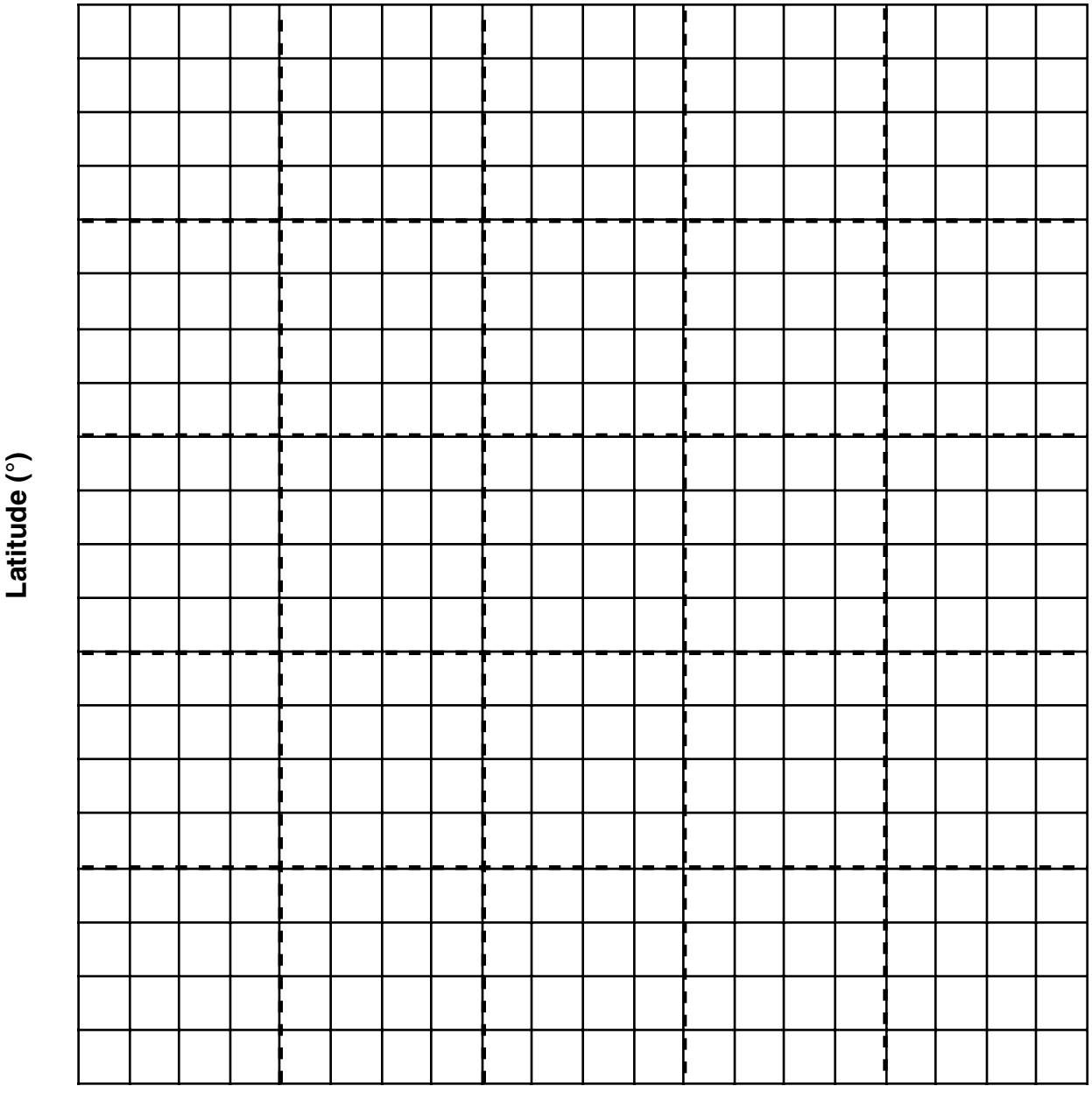

Lead Project Scientist Event Log

Date _____ Flight _____ LPS _____

Time	Event	Position	Comments

E.3 Cloud Physics Scientist

The on-board cloud physics scientist (CPS) is responsible for cloud physics data collection on his/her assigned aircraft. Detailed operational procedures are contained in the cloud physics kit supplied for each aircraft. General procedures follow. (Check off and initial.)

E.3.1 Preflight

_____ 1. Determine status of cloud physics instrumentation systems and report to the on-board lead project scientist (LPS).

_____ 2. Confirm mission and pattern selection from the on-board LPS.

_____ 3. Select mode of instrument operation.

_____ 4. Complete appropriate instrumentation preflight check lists as supplied in the cloud physics operator's kit.

E.3.2 In-Flight

_____ 1. Operate instruments as specified in the cloud physics operator's kit and as directed by the on-board LPS.

E.3.3 Post flight

_____ 1. Complete summary check list forms and all other appropriate forms.

_____ 2. Brief the on-board LPS on equipment status and turn in completed check sheets to the LPS.

_____ 3. Take cloud physics data tapes and other data forms and turn these data sets in as follows:

a. Outside of Miami - to the LPS.
b. In Miami - to AOML/HRD. [**Note**: all data removed from the aircraft by HRD personnel should be cleared with the AOC flight director.]

_____ 4. Debrief as necessary at MGOC or the hotel during a deployment.

_____ 5. Determine the status of future missions and notify MGOC as to where you can be contacted.

Form E-3
Page 1 of 3

Cloud Physics Scientist Check List

Date _____ Aircraft _____ Flight ID _____

A. —Instrument Status and Performance:

System	Pre-Flight	In-Flight	Downtime	# of Tapes
Johnson-Williams				
PMS Probes:				
—2D-P				
—2D-C				
—FSSP				
—Data System				
—Recorder				
FORMVAR				
DRI Charge Probe				
DRI Field Mills				
King Probe				

B. —Remarks:

Form E-3
Page 2 of 3

2-D Knollenberg Data Tape Log

Date _____ **Flight** _____ **Operator** _____

Tape #	EOF #	Time On	Time Off	Comments

FORMVAR Log

Date _____ Flight _____ Operator _____

Roll #	Time On	Time Off	Frame Count at Start	Comments

E.4 Boundary-Layer Scientist

The on-board boundary-layer scientist (BLS) is responsible for data collection from AXBTs, AXCPs, AXCTDs, BUOYs, and sea surface temperature radiometers (if these systems are used on the mission). Detailed calibration and instrument operation procedures are contained in the air-sea interaction (ASI) manual supplied to each operator. General supplementary procedures follow. (Check off and initial.)

E.4.1 Preflight

_____ 1. Determine the status of equipment and report results to the on-board lead project scientist (LPS).

_____ 2. Confirm mission and pattern selection from the on-board LPS.

_____ 3. Select the mode of operation for instruments after consultation with the HRD/BLS and the on-board LPS.

_____ 4. Complete appropriate preflight check lists as specified in the ASI manual and as directed from the on-board LPS.

E.4.2 In-Flight

_____ 1. Operate the instruments as specified in the ASI manual and as directed by the on-board LPS.

E.4.3 Post flight

_____ 1. Complete summary check list forms and all other appropriate check list forms.

_____ 2. Brief the on-board LPS on equipment status and turn in completed check lists to the LPS.

_____ 3. Debrief as necessary at MGOC or the hotel during a deployment.

_____ 4. Determine the status of future missions and notify MGOC as to where you can be contacted.

Form E-4
Page 1 of 3

AXBT/AXCP Check Sheet Summary

Flight _____ Aircraft _____ Operator _____

		Number
(1)	Probes dropped	_____
(2)	Failures	_____
(3)	Failures with no signal	_____
(4)	Failures with sea surface temperature, but terminated above thermocline	_____
(5)	Probes that terminated above 250 m, but below thermocline	_____
(6)	Probes used by channel number CH12	_____
	CH14	_____
	CH16	_____
	CH__	_____

NOTES:

Form E-4

AXBT and AXCP Check Sheet

Flight Number _____ AXBT/AXCP Contract Number _____

Take-Off Time _____ Landing Time _____

Storm _____ Storm Direction/Speed _____

AXCP/ AXBT #/Type	Channel Number	Lot Number	Drop Time (HHMMSS)	Lat. Deg. Min.		Long. Deg. Min.		Surface Temp. AXBT IRT		MLD (m)	Comments

Form E-4
Page 3 of 3

AXCP Log

Flight Number _____ AXBT/AXCP Contract Number _____

Take-Off Time _____ Landing Time _____

Storm _____ Storm Direction/Speed _____

Leg Number	Out/In	RA (m)	PMIN (mb)	VMAX (m/s)	RMAX (km)	Time PMIN	Time VMAX	Time End Pass

Leg/ Drop #	Tube #	Channel #	Probe Type		Ground Speed	Drop Time (HHMMSS)	Latitude (deg min)	Longitude (deg min)	Status		Comments
			Slow	Reg					Good	Bad	

E.5 Radar Scientist

The on-board Doppler radar scientist (DRS) is responsible for data collection from all radar systems on his/her assigned aircraft. Detailed operational procedures and check lists are contained in the operator's manual supplied to each operator. General supplementary procedures follow. (Check off and initial.)

E.5.1 Preflight

_____ 1. Determine the status of equipment and report results to the on-board lead project scientist (LPS).

_____ 2. Confirm mission and pattern selection from the on-board LPS.

_____ 3. Select the operational mode for radar system(s) after consultation with the on-board LPS.

_____ 4. Complete the appropriate preflight calibrations and check lists as specified in the radar operator's manual.

E.5.2 In-Flight

_____ 1. Operate the system(s) as specified in the operator's manual and as directed by the on-board LPS or as required for aircraft safety as determined by the AOC flight director or aircraft commander.

_____ 2. Maintain a written commentary in the radar logbook of tape and event times, such as the start and end times of F/AST legs. Also document any equipment problems or changes in R/T, INE, or signal status.

E.5.3 Post flight

_____ 1. Complete the summary check lists and all other appropriate check lists and forms.

_____ 2. Brief the on-board LPS on equipment status and turn in completed forms to the LPS.

_____ 3. Hand-carry all radar tapes and arrange delivery as follows:

a. Outside of Miami - to the LPS.
b. In Miami - to MGOC or to AOML/HRD. [**Note**: all data removed from the aircraft by HRD personnel should be cleared with the AOC flight director.]

_____ 4. Debrief at MGOC or the hotel during a deployment.

_____ 5. Determine the status of future missions and notify MGOC as to where you can be contacted.

Form E-5
Page 1 of 3

HRD Radar Scientist Check List

Flight ID: _____

Aircraft Number: _____

Doppler Radar Operators: _____

Radar Technician: _____

Number of digital magnetic tapes on board: _____

Component Systems Status:

MARS _____ Computer _____

DAT1_____ DAT2 _____

LF _____ R/T Serial # _____

TA _____ R/T Serial # _____

Time correction between radar time and digital time: _____

Radar Post flight Summary

Number of digital tapes used: DAT1 _____

DAT2 _____

Significant down time:

DAT1 _____ Radar LF _____

DAT2 _____ Radar TA _____

Other Problems:

HRD Radar Tape Log

Flight ___________ **Aircraft** ______ **Operator** ___________ Sheet ____ of ____

LF RPM _______________ TA RPM ______________

(Include start and end times of DATs, as well as times of F/AST legs and any changes of radar equipment status)

Tape #	F/AST On?	Event Time (HHMMSS)	Event

HRD Radar Down-Time Log

Flight _____ **Aircraft** _____ **Operator** _____ Sheet ____ of ____

Item	Time Down (HHMMSS)	Time Up (HHMMSS)	Problem

Item List: DAT1, DAT2, COMP, MARS, LF, TA.

Include serial numbers of any new R/Ts.

E.6 Dropwindsonde Scientist

The on-board lead project scientist (LPS) on each aircraft is responsible for determining the distribution patterns for dropwindsonde releases. Predetermined desired data collection patterns are illustrated on the flight patterns. However, these patterns often are required to be altered because of clearance problems, etc. Operational procedures are contained in the operator's manual. The following list contains more general supplementary procedures to be followed. (Check off and initial.)

E.6.1 Preflight

_____ 1. Determine the status of equipment and report results to the on-board LPS.

_____ 2. Confirm the mission and pattern selection from the LPS and assure that the proper number and distribution (frequency) of dropwindsonde s are on board the aircraft.

_____ 3. Complete the appropriate preflight calibrations and check lists.

E.6.2 In-Flight

_____ 1. Operate the system as specified in the operator's manual.

_____ 2. Obtain drop release approval (for each drop) from the AOC flight director or navigator for each specific time and location of drop.

_____ 3. Report to the LPS as soon as it is determined that the dropwindsonde is (or is not) transmitting a good signal.

_____ 4. Report completion of each drop and readiness for the next drop.

_____ 5. Complete Form E-6.

E.6.3 Post flight

_____ 1. Complete the summary form for dropwindsondes.

_____ 2. Brief the on-board LPS on equipment status and turn in reports and completed forms to the LPS.

_____ 3. Hand-carry all dropwindsonde data tapes and printouts and inform the AOC flight director that you are arranging delivery as follows:

a. Outside of Miami - to the LPS.
b. In Miami - to AOML/HRD (temporarily), either directly or via MGOC, for conversion to 9-track magnetic tapes.

_____ 4. Debrief at the MGOC or the hotel during a deployment.

_____ 5. Determine the status of future missions and notify MGOC as to where you can be contacted.

HRD GPS Dropwindsonde Scientist Log (Revised 6/1999)

Storm _____ Flight Director _____ Page ___ of ___

Flight ID _____ Dropwindsonde Scientists _____ Takeof _____ UTC

Mission ID _____ AVAPS Operators _____ Landing _____ UTC

Drop #	Sonde ID #	Time(UTC)	Lat (°N)	Lon (°W)	Surface Pressure (mb)	10m wind (knt)	MBL wind (knt)	XBT SST (°C)	Location Comment	Comments	Ob #

APPENDIX F:

GROUND OPERATION

GROUND OPERATION

In support of each field operation, a ground coordination team will serve on the staff of the HRD director. The ground coordination team will consist of the Miami Ground Operations Center (MGOC).

(1) Staff:

H. Friedman (senior team leader)
R. Jones (team leader)
J. Berkeley (meteorological technical support)

(2) Operational Scheduling:

During research missions the MGOC staff will form three teams as follows: one team leader and, when necessary and available, one meteorological technician support person. Each team will work an (approximately) 8-h shift; shifts will continue for the duration of operations or until MGOC personnel are released by the field program director or his designee.

(3) General Duties:

During operations, the MGOC acts as the liaison between HRD and other organizations as required by the field program director, the HRD director, or their designated representatives. Duties of the MGOC include the following:

a. Collect, plot, and file data from NHC.

b. Update messages on the auto-phone tape at MGOC (NHC).

c. Coordinate the acquisition of satellite photos for operational and research purposes.

d. Make motel/hotel reservations at alternate recovery sites as requested by field operations personnel.

e. Handle press affairs in Miami as follows:

- Refer press inquiries to J. Goldman, OAR/PA.
- Refer forecast inquiries to NHC.

f. Communicate with AOC ground coordinator, as required.

g. Make requests for special radar and/or rawinsonde (upper air) observations, subject to approval by the HRD director.

h. Maintain a crew status report of HRD participants for current and proposed missions. When missions are being conducted away from Miami, crew status information will be reported to MGOC by the field program director or his designee.

(4) Phone numbers:

NHC Public Affairs/F. Lepore	(305)-229-4404
AOC	(813)-828-3310
AOC (FAX, J. McFadden)	(813)-828-6881
AOC (auto line)	(813)-828-3310 —— (ext. 3128)
HRD (auto line at MGOC/TPC/NHC)	(305)-221-3679
HRD (voice line at MGOC/TPC/NHC)	(305)-221-4381
HRD FAX number	(305)-361-4402
AOC's long distance auto announce phone number	(800)-729-6622 —— (ext. 3128)
OAR/PA (J. Goldman)	(301)-713-2483
TPC/NHC (WFO)	(305)-229-4528
Miami Ground Operations Center (MGOC) at NHC	(305)-229-4407
Miami Ground Operations Center (MGOC) at HRD/AOML	(305)-361-4400
Zephyr/WIS Center at HRD/AOML	(305)-361-4368
TRDIS Operations at NHC	(305)-229-4429
Storm Surge Group at NHC	(305)-229-4456
WWV (for time check)	(303)-499-7111
Telepager (beeper) numbers for MGOC team leaders, H. Willoughby and F. Marks (HRD), and J. McFadden (AOC)	—— TBA

(5) Supplies:

a. Up-to-date phone list

b. Current copies of the following:

- HRD Hurricane Field Program Plan
- AOC Hurricane Operations Plan (if available)
- MGOC Manual (black, loose-leaf book)

(6) Information Pool:

Interface with NHC and others as required, and at appropriate times, obtain:

a. Satellite fixes at forecast times and 3-hourly intermediate fixes.

b. NHC official releases:

- Storm position and current strength and movement (including maximum wind and minimum—pressure).
- Forecast storm position and strength (wind and pressure) for 12, 24, 48, and 72 h.
- 0400, 1000, 1600, 2200 UTC and all intermediate advisories (based on synoptic 0000, 0600, 1200, and 1800 UTC).
- Public advisories.

c. NHC supplied additional data:

- 3-hourly storm positions.
- Aircraft reconnaissance reports (request extra copy from NHC Communications Unit).
- HURCAS computer product (request extra copy from NHC/Tropical Satellite and Analysis Center: 2130, 0330, 0930, 1530 EDT availability).

APPENDIX G:

NOAA EXPENDABLES AND SUPPLIES

Table G-1. DAT Tape, GPS-sonde, AXBT/AXCP/AXCTD Requirements Per Experiment[1]

Experiment	DAT Tapes Cloud Physics	Slow/Fast/Radar	DW[2] OP[2]
Hurricane Synoptic-Flow Experiment (single-option, dual-aircraft mission)	02	01 / 00 / 04	65 00
Extended Cyclone Dynamics Experiment (single-option, two-aircraft mission)	01	01 / 00 / 04	30 00
Vortex Motion and Evolution Experiment (single-option, dual-aircraft mission)			
High-level aircraft.	03	01/ 00 / 04	44 00
Low-level aircraft.	03	01 / 00 / 04	15 10
Tropical Cyclogenesis Experiment (single-option, dual-aircraft mission)			
High-level aircraft.	03	01 / 00 / 04	30 00
Low-level aircraft.	03	01 / 02 / 04	10 10
Tropical Cyclone Wind fields at Landfall (dual-option, single-aircraft mission)	01	01 / 02 / 04	25 00
Tropical Cyclone Air-sea Interaction Experiment (multi-option, single-aircraft mission)			
Option 1: Early-Season Option (two single-aircraft mission)	01	01 / 02 / 01	17 85
Option 1: Pre-Storm Option (single-aircraft mission)	01	01 / 02 / 01	17 44
Option 2: Near-Strom Option (dual-aircraft mission)	01	01 / 02 / 04	40 56
Option 3: Post-Storm Option (single-aircraft mission)	01	01 / 02 / 04	17 44

Experiment (continued)	DAT Tapes Cloud Physics	Slow/Fast/Radar	DW[2] OP[2]
Rainband Structure Experiment (multi-option, multi-aircraft mission)			
Option 1: Rainband Option (dual-aircraft mission)	01	01 / 02 / 04	25 00
Option 2: Concentric Eyewall Option (dual-aircraft mission)	01	01 / 02 / 04	25 00
Electrification of Tropical Cyclone Convection Experiment (single-option, single-aircraft mission)	03	01 / 02 / 04	20 00
Structure of Eyewall Convection Experiment (single-option dual-aircraft mission)			
High-level aircraft	03	01 / 02 / 05	36 00
Low-level aircraft.	03	01 / 02 / 05	36 00
Clouds and Climate Study (single-option dual-aircraft mission)	03	01 / 02 / 05	15 00

1 A mission is defined as one launch and recovery for research purposes. Entries shown for dual-aircraft (nonsequential mode) missions are for the total number of DAT tapes, GPS-sondes, AXBT's, AXCPs, and AXCTDs required for each experimental day's operation. Entries shown for two-aircraft, sequential mode operation missions are the requirements for each aircraft participating on each experimental day's operation.

2 DW: GPS-sondes; OP: AXBT, AXCP, and AXCTD probes.

APPENDIX H:

SYSTEMS OF MEASURE AND UNIT CONVERSION FACTORS

SYSTEMS OF MEASURE AND UNIT CONVERSION FACTORS

Table H-1 Systems of measure: Units, symbols, and definitions

Quantity	SI Unit	Early Metric	Maritime	English
length	meter (m)	centimeter (cm)	foot (ft)	foot (ft)
distance	meter (m)	kilometer (km)	nautical mile (nmi)	mile (mi)
depth	meter (m)	meter (m)	fathom (fa)	foot (ft)
mass	kilogram (kg)	gram (g)		
time	second (s)	second (s)	second (s)	second (s)
speed	meter per second (mps)	centimeter per second (cm s^{-1}) kilometers per hour (km h^{-1})	knot (kt) (nmi h^{-1})	miles per hour (mph)
temperature *-sensible*	degree Celsius (°C)	degree Celsius (°C)	-----	degree Fahrenheit (°F)
-potential	Kelvin (K)	Kelvin (K)	-----	Kelvin (K)
force	Newton (N) (kg m s^{-2})	dyne (dy) (g cm s^{-2})	poundal (pl)	poundal (pl)
pressure	Pascal (Pa) (N m^{-2})	millibar (mb) (10^3 dy cm^{-2})	inches (in) mercury (Hg)	inches (in) mercury (Hg)

Table H-2. Unit conversion factors

Parameter	Unit	Conversions
length	1 in	2.540 cm
	1 ft	30.480 cm
	1 m	3.281 ft
distance	1 nmi (nautical mile)	1.151 mi
		1.852 km
		6080 ft
	1 mi (statute mile)	1.609 km
		5280 ft
	1° latitude	59.996 nmi
		69.055 mi
		111.136 km
depth	1 fa	6 ft
		1.829 m
mass	1 kg	2.2 lb
force	1 N	10^5 dy
pressure	1 mb	10^2 Pa
		0.0295 in Hg
	1 lb ft^{-2}	4.88 kg m^{-2}
speed	1 m s^{-1}	1.94 kt
		3.59 kph
	1° lat. 6 h^{-1}	10 kt

ACRONYMS AND ABBREVIATIONS

θ_e	equivalent potential temperature
ABL	atmospheric boundary-layer
A/C	aircraft
AFRES	Air Force Reserve
AOC	Aircraft Operations Center
AOML	Atlantic Oceanographic and Meteorological Laboratory
ASDL	aircraft-satellite data link
ATOLL	Atlantic Tropical Oceanic Lower Layer
AXBT	airborne expendable bathythermograph
AXCP	airborne expendable current probe
AXCTD	airborne expendable conductivity, temperature, and depth probe
BLS	boundary layer scientist
CARCAH	Chief, Aerial Reconnaissance Coordinator, All Hurricanes
CDO	central dense overcast
CG	cloud-to-ground (lightning)
CIRA	Cooperative Institute for Research in the Atmosphere
C-MAN	Coastal-Marine Automated Network
COARE	Coupled Ocean-Atmosphere Response Experiment
CP	coordination point
CRT	cathode-ray tube
C-SCAT	C-band scatterometer
CVA	cyclonic vorticity advection
CW	cross wind
DLM	deep-layer mean
DOD	Department of Defense
DOW	Doppler on Wheels
DRI	Desert Research Institute (at Reno)
E	vector electric field
EPAC	Eastern Pacific
ERL	Environmental Research Laboratories
ETL	Environmental Technology Laboratory
EVTD	extended velocity track display
FAA	Federal Aviation Administration
F/AST	fore and aft scanning technique
FEMA	Federal Emergency Management Agency
FL	flight level
FP	final point
FSSP	forward scattering spectrometer probe
GFDL	Geophysical Fluid Dynamics Laboratory
G-IV	Gulfstream IV-SP aircraft
GOMWE	Gulf of Mexico Warm Eddy
GPS	global positioning system
HRD	Hurricane Research Division
HaL	Hurricanes at Landfall
INE	inertial navigation equipment
IP	initial point (or initial position)
IWRS	Improved Weather Reconnaissance System
JW	Johnson-Williams
K-SCAT	Ku-band scatterometer
LF	lower fuselage (radar)

LPS	Lead Project Scientist
MCS	mesoscale convective systems
MGOC	Miami Ground Operations Center
MLD	Mixed Layer Depth
MPO	Meteorology and Physical Oceanography
NCAR	National Center for Atmospheric Research
NCEP	National Centers for Environmental Prediction
NDBC	NOAA Data Buoy Center
NESDIS	National Environmental Satellite, Data and Information Service
NHC	National Hurricane Center
NLDN	National Lightning Detection Network
NOAA	National Oceanic and Atmospheric Administration
NWS	National Weather Service
ODW	Omega-based generation of dropwindsonde
OML	oceanic mixed-layer
PDD	pseudo-dual Doppler
PMS	Particle Measuring Systems
POD	Plan of the Day
PPI	plan position indicator
PV	potential vorticity
RA	radar altitude
RAOB	radiosonde (upper-air observation)
RAWIN	rawinsonde (upper-air observation)
RECCO	reconnaissance observation
RHI	range height indicator
RSMAS	Rosenstiel School of Marine and Atmospheric Science
SAL	Saharan air layer
SECE	Structure of Eyewall Convection Experiment
SFMR	Stepped-Frequency Microwave Radiometer
SLOSH	sea, lake, and overland surge from hurricanes (operational storm surge model)
SRSO	super rapid scan operations
SRA	Scanning Radar Altimeter
SST	sea-surface temperature
TA	tail (radar)
TAS	true airspeed
TC	tropical cyclone
TOGA	Tropical Oceans-Global Atmosphere
TOPEX	The Ocean Topography Experiment
TPC	Tropical Prediction Center (at NHC)
TRMM	Tropical Rainfall Measuring Mission
UMASS	University of Massachusetts (at Amherst)
USACE	United States Army Corps of Engineers
USAF	United States Air Force
UTC	universal coordinated time (U.S. usage; same as “GMT” and "Zulu" time)
VICBAR	name for a barotropic hurricane track prediction model (not an acronym)
VME	Vortex Motion and Evolution (Experiment)
VSDR	Vertically Scanning Doppler Radar
VTD	velocity-track display
XCDX	Extended Cyclone Dynamics Experiment

HURRICANE FIELD PROGRAM PLAN DISTRIBUTION—1999

Bureau of Meteorology, Research Center, Victoria, Australia
G. Holland

Department of Commerce/National Oceanic and Atmospheric Administration

Aircraft Operations Center
J. McFadden, AOC1
CAPT D. Winter, AOC
Staff, AOC (20 copies)

Atlantic Oceanographic and Meteorological Laboratory (R/E/AO)
K. Katsaros, OD
H. Friedman, HRD
S. Garzoli, PHOD
J. Gray, OD.
P. Ortner, OCD
J. Proni, OAD
C. Stewart, OD
H. Willoughby,HRD
Library, AOML
Staff, HRD/AOML (20 copies)

Environmental Research Laboratories
J. Calder, R/E
K. Groninger, R/Ex1

Geophysical Fluid Dynamics Laboratory (R/E/GF)
M. Bender
J. Mahlman
R. Tuleya

National Center for Environmental Prediction
S. Lord, W/NP2
L. Uccellini, W/NP

National Data Buoy Center
M. Burdette, W/DB2
E. Meindl, W/DB4

National Environmental Satellite, Data, and Information Service
D. Clark, E/SP3
N. Everson, E/RA22
A. Gruber, E/RA2
J. Wilkerson, E/RA3

National Ocean Service
S. Gill, N/OS4

National Severe Storm Laboratory
J. Kimpel, R/E/NS

National Weather Service
R. Dumont, FC
P. Hirschberg, W/OMx2
J. Kelly, W
N. Surgi, W/NP8
D. Wernly, W/OM11

NWS/Eastern Region
J. Forsing, W/ER (2 copies)

NWS/Pacific Region
R. Hagemeyer, W/PR

NWS/Southern Region
X.W. Proenza, W/SR
R. Pfost, W/WSFO - Miami
B. Hagemeyer, W/SR49

NWS Training Center
Director, WTC

NOAA Corps
E. Fields, NC
Office of Global Programs
M. Hall, GP
Office of Oceanic and Atmospheric Research
D. Evans, R (2 copies)
J. Gaynor, R/E
J. Golden, R/PDC
K. Groninger, R/Ex1
L. Koch, R
M. Langlais, R
Office of Systems Operations
R. Racer, W/OSO1x3
W. Telesetsky, W/OSO
T. Trunk, W/OSO14
Public Affairs
Barbara Semedo, PA
J. Goldman, PA (OAR) (2 copies)
Techniques Development Laboratory
W. Shaffer, W/OSD22
Tropical Prediction Center/National Hurricane Center (W/NP8)
L. Avila
R. Burpee (ret.)
C.Burr
J. Franklin
J. Gross
J. Guiney
F. Horsfall
J. Jarrell (2 copies)
B. Jarvinen
M. Lawrence
F. Lepore
M. Mayfield
C. McAdie
R. Pasch
E. Rappaport
Weather Research Program
W. Hooke, R
WSR-88D Operational Support Facility
E. Berkowitz, W/OSO42
D. Burgess, W/OSO45
T. Crum, W/OSO41
M. Fresch, W/OSO441
R. Reed, W/OSO43
S. Stewart, W/OSO452
A. White, W/OSO44

Department of Defense
U.S. Air Force
D. Harmes, Patrick AFB
J. Kerwin, Eglin AFB
R. Lafbare, Eglin AFB
J. Pavone, CARCAH
D. Urbanski, Patrick AFB
USAFETAC/DOL, Scott AFB
53rd WRS, Keesler AFB (12 copies)
U.S. Army
OJCS/J3/ESD
U.S. Army Corps of Engineers
R. Jensen, WES

U.S. Navy

Chairman, Dept. of Meteorology, NPS
Commander in Chief, U.S. Atlantic Command, Code J37
Commander, Atlantic Missile Range
R. Abbey, ONR
T. Bosse, NAVLANTMETOCFAC JAC/NAS, Jacksonville
R. Elsberry, NPS (2 copies)
L. Ritchie, Code 63ES
K. St. Germain, Code 7223

Department of Transportation/Federal Aviation Administration

Federal Aviation Administration, ATR-150

National Aeronautics and Space Administration

D. Atlas, Code 610
R. Hood, ES-43
R. Kakar, Code SEP
M. Karyampudi, Code 912
J. Rothermel, ES-43
J. Simpson, Code 612
O. Vaughan, ES-43
J. Wang, Code 675

National Center for Atmospheric Research

R. Carbone
A. Heymsfield
P. Hildebrand
W.-C. Lee
M. LeMone
L. Radke
R. Serafin

National Research Council

F. White

National Science Foundation

R. Greenfield
S. Nelson
P. Stephens

NTTC/NTIS Projects

National Technology Transfer Center

Private Sector

C. Neumann, SAIC
I. Popstefanija, Quadrant Engineering
C. Samsury, TWC
R. Williams, St. Georges, Bermuda
S. Yueh, JPL

University Corporation for Atmospheric Research

R. Anthes

University Scientists

B. Albrecht, U. of Miami/RSMAS
G. Barnes, U. of Hawaii
C. Bishop, PSU
H. Bluestein, U. of Oklahoma
L. Bosart, SUNY/Albany
S. Chen, U. of Miami/RSMAS

H.-R. Cho, U. of Toronto
K. Emanuel, MIT
S. Esbensen, Oregon State U.
L. Fedor, U. of Colorado
W. Frank, PSU
M. Fritsch, PSU
S. Gedzelman, CCNY
W. Gray, CSU
J. Hallett, DRI/U. of Nevada
R. Houze, Jr., U. of Washington
R. Johnson, CSU
K. Knupp, U. of Alabama/Huntsville
T. Krishnamurti, FSU
J. Lawrence, U. of Houston
S. Leatherman, IHC
E.W. McCaul, U. of Alabama/Huntsville
J. Molinari, SUNY/Albany
M. Montgomery, CSU
R. Pfeffer, FSU
J. Prospero, U. of Miami, CIMAS
P. Ray, FSU
D. Raymond, NM Institute for Mines and Technology
C. Rooth, U. of Miami/RSMAS
F. Roux, Laboratorie D'Aerologie
S. Rutledge, CSU
F. Sanders, MIT (ret.)
W. Schubert, CSU
L. Shapiro, U. of Munich
R. Smith, U. of Munich
R. Smith, Yale U.
W. Smith, NASA/Langley Research Center
S. Stage, FSU
J. Straka, U. of Oklahoma
C. Swift, U. of Massachusetts/Amherst (3 copies)
G. Tripoli, U. of Wisconsin
C. Velden, U. of Wisconsin
T. Wilheit, Texas A&M U.
J. Wurman, U. of Oklahoma
E. Zipser, U. of Utah

U.S. Coast Guard
Commandant, G-OIO

U.S. Nuclear Regulatory Commission
R. Kornasiewicz, NL-007

World Meteorological Organization, Geneva, Switzerland
K. Abe
G.O.P. Obasi
WMO Library

Acknowledgment

The preparation of HRD's **1999 Hurricane Field Program Plan** was a team effort. The authors would like to express their appreciation to: the HRD scientists that contributed information on specific experiments; Shirley Murillo and Joyce Berkeley, for their efforts on updating the information in Appendix C.